1-1-1965

Excitation transfer between the 4(2)P levels in potassium, induced by inelastic collisions.

George D. Chapman
University of Windsor

EXCITATION TRANSFER BETWEEN THE 4^2P LEVELS IN POTASSIUM, INDUCED BY INELASTIC COLLISIONS

By

George D. Chapman

A Thesis
Submitted to the Faculty of Graduate Studies through the
Department of Physics in Partial Fulfillment of
the Requirements for the Degree of Doctor
of Philosophy at the University
of Windsor.

Windsor, Ontario

1965

HEX 6/30

APPROVED:

Approved by letter of December 1, 1965

Professor P. Franken
University of Michigan

Professor E.E. Habib

Professor N.E. Hedgecock

Professor L. Krause (Supervisor)

ABSTRACT

Sensitized fluorescence in potassium vapour and its mixtures with inert gases was investigated in order to determine cross sections for the inelastic collisions leading to excitation transfer between the $4^2P_{1/2}$ and $4^2P_{3/2}$ states in potassium. The study was carried out at potassium vapour pressures of about 10^{-6} torr, which were not previously accessible to such experiments. At these low densities it was possible to determine the cross sections under single-collision conditions and in the absence of radiation trapping. The following are the values of the cross sections Q_{12} ($4^2P_{1/2} \rightarrow 4^2P_{3/2}$) and Q_{21} ($4^2P_{1/2} \leftarrow 4^2P_{3/2}$). For K-K collisions: 370 and 250 $\mathring{A}^2$; for K-He: 60 and 41 $\mathring{A}^2$; for K-Ne: 14 and 9.5 $\mathring{A}^2$; for K-A: 37 and 22 $\mathring{A}^2$; for K-Kr: 61 and 41 $\mathring{A}^2$; for K-Xe: 104 and 72 $\mathring{A}^2$. The cross sections for potassium-inert gas collisions do not increase monotonically with the polarizabilities of the inert gas atoms but show a close similarity to the electron-inert gas elastic scattering cross sections. This behaviour is interpreted on the basis of a semi-classical model for the interaction, which involves overlap forces. At somewhat higher inert gas pressures, where single-collision conditions no longer prevailed, the collision numbers were found to vary non-linearly with inert gas pressure and reached saturation values at pressures much lower than expected from a theoretical

analysis. These effects are tentatively attributed to changes in the collision mechanism and in the lifetimes of the potassium resonance states caused by the increasing inert gas pressures.

ACKNOWLEDGEMENTS

I am most grateful to Dr. L. Krause, under whose supervision this research was conducted, for years of advice and constructive criticism and in particular for his tireless reading of this dissertation in manuscript. I should also like to express my gratitude to Dr. M. Czajkowski with whom I have enjoyed many stimulating and enlightening discussions over the past two years.

I should like to acknowledge the assistance of Dr. Ross Pottie (Division of Applied Chemistry, National Research Council of Canada), who undertook the spectrographic analysis of the chemical deposit formed in our spectral lamps and fluorescence cells by the corrosive action of potassium on pyrex.

The success of the experimental work owes a great deal to the expertise of Master Glassblower W. Eberhart, who manufactured the fluorescence cells, and Mr. W. Grewe who constructed the photomultiplier cryostat and many other pieces of apparatus.

I should like to thank the National Research Council of Canada for the scholarships which were awarded to me during 1962-66.

TABLE OF CONTENTS

LIST OF TABLES

LIST OF FIGURES

LIST OF FIGURES (cont'd)

I. INTRODUCTION

The study of inelastic collisions between heavy, low velocity particles has been a subject of interest for many years. The investigation of such phenomena has gained impetus from the current interest in energy transfer processes in the ionosphere and stellar atmospheres. Experiments involving inelastic atomic collisions are, in addition, well suited to the purpose of checking the validity of the theoretical approaches to atomic collisions by providing information regarding the nature and magnitude of the inter-atomic forces involved.

From a theoretical point of view, the most thoroughly documented of the inelastic collision processes are those that take place between the alkali metals and alkali metal and inert gas atoms. Almost all of the current theoretical treatments of the subject[1,2,3] predict cross sections for a given pair of atoms of about the same order of magnitude. It therefore becomes necessary to experimentally determine accurate values of cross sections for collisions of each alkali metal with its own ground state and with the complete set of inert gases. Only by determining the exact relationships between the various cross sections will a choice of the "correct" theoretical approach be possible. We rely, therefore, on the fine structure of a spectrum of inelastic

cross sections to provide the criterion for such a choice.

The present investigation concerns itself with the determination of the cross sections for radiationless energy transfer between the first excited fine structure states in potassium ($4^2P_{1/2}$ and $4^2P_{3/2}$) induced by collisions with ground state potassium atoms ($4^2S_{1/2}$) and inert gas atoms in their ground states (n^1S_0). Such transitions may be described by the following equation:

$$K(4^2P_{3/2}) + X \underset{k_2}{\overset{k_1}{\rightleftharpoons}} K(4^2P_{1/2}) + X + \Delta E \,, \qquad (1)$$

where X may be either a potassium or inert gas atom in the ground state, and k_1 and k_2 are rate constants which are proportional to the cross sections for the two processes. The energy defect between the ^2P states (57 cm^{-1} or 0.007 eV) is absorbed from or given up to the kinetic energy of relative motion of the colliding partners. A process of this type was first observed by Cario and Franck[4] in experiments on mercury fluorescence sensitized by thallium. According to Franck[5], the cross sections for the energy transfer process should vary inversely with the energy defect between the states. Beutler and Josephy[6] demonstrated this principle in experiments with sensitized fluorescence in sodium.

Collisions of this type are often referred to as "collisions of the second kind" after Franck's extension of the terminology of Klein and Rosseland[7]. However, there seems to be some ambiguity in this term, as applied to the processes described by equation (1), as only the $^2P_{1/2} \longleftarrow {}^2P_{3/2}$

transition proceeds by means of a true collision of the second kind.

If an ensemble of potassium atoms is irradiated with photons corresponding to either the transition $4^2S_{1/2} \longleftarrow 4^2P_{1/2}$ (7699 Å) or $4^2S_{1/2} \longleftarrow 4^2P_{3/2}$ (7665 Å), both wavelengths will appear in the fluorescent spectrum because of inelastic collisions of the type described by equation (1). The fluorescence which is of the same wavelength as the light exciting the sample is called resonance fluorescence, a term coined by R.W. Wood[8] to describe transitions due to excited states from which there is but one allowed return path to the ground state. The fluorescent component of that wavelength, which is not present in the exciting beam, is called sensitized fluorescence.

Wood[8] studied resonance fluorescence in sodium and defined the process of radiation imprisonment or multiple scattering of resonance radiation. A cone of incident resonance radiation was found to be well defined by fluorescent light in sodium vapour at low density. As the vapour density was increased, fluorescence first filled the entire fluorescence vessel (volume fluorescence) and, in the high pressure limit, was eventually confined to a thin layer adjacent to the entrance window (surface fluorescence). This phenomenon, which gives rise to considerable difficulty in experiments such as the present one, is caused by multiple absorptions and reemissions of the photons emitted by the primary excited atoms. The effects of the diffusion process will be discussed

in greater detail in the following sections.

Several attempts have been made to account theoretically for the process, such as those of Compton[9], Milne[10] and Holstein[11]. Barrat[12] investigated both theoretically and experimentally the diffusion of mercury resonance radiation. Some authors have used these theories to compensate for imprisonment effects in the study of sensitized fluorescence in the alkalis, but their use necessitates assumptions regarding the geometry of the system that may be difficult to justify.

Wood[13,14] carried out the first study of sensitized fluorescence in sodium; investigations of the sodium-inert gas systems were conducted by Wood and Mohler[15] and were followed by the sodium-inert gas experiments of Lochte-Holtgreven[16]. Seiwert[17] worked with sodium and sodium-argon mixtures, and sensitized fluorescence in potassium was studied by Thangaraj[18] and by Hoffmann and Seiwert[19]. The latter authors adopted the theory of Holstein (Seiwert[20,21]) to correct for radiation diffusion. Chapman, Krause and Brockman[22] worked with pure potassium vapour at reduced vapour pressures, while Chapman and Krause[23] studied sensitized fluorescence in the potassium-argon system. Jordan[1] studied mixtures of sodium with all the inert gases and of potassium with helium, neon and argon.

Sensitized fluorescence in cesium was investigated by Bunke and Seiwert[24] and, more recently, by Czajkowski and Krause[25]. Czajkowski, McGillis and Krause[26] determined the cesium-inert gas cross sections at very low cesium metal vapour densities. The most recent publications of experimental

work in this area are those of Rae and Krause[27] who determined the inelastic cross sections for rubidium-rubidium collisions, and of Pitre, Rae and Krause[28] who measured the cross sections for collisions between rubidium and the inert gas atoms.

The present experiment was carried out at very low potassium vapour pressures to avoid theoretical corrections for the effects of radiation diffusion. It was also possible to measure potassium-inert gas collisions at gas pressures low enough to ensure single-collision conditions. Since the energy defect between the ^2P states of potassium is small with respect to those of the heavier alkali metals, the results of this experiment may serve as a valid check on the various theories, which usually assume a small energy gap between the relevant states.

II. THEORETICAL

A. The Macroscopic Theory

(i) The Rate Processes of Sensitized Fluorescence

In order to measure the cross sections for inelastic collisions, it is necessary to consider the factors involved in the maintenance of steady state conditions in a three level atomic system. Figure 1 shows the $^2P_{1/2}$ and $^2P_{3/2}$ fine structure levels of potassium as well as the $^2S_{1/2}$ ground level.

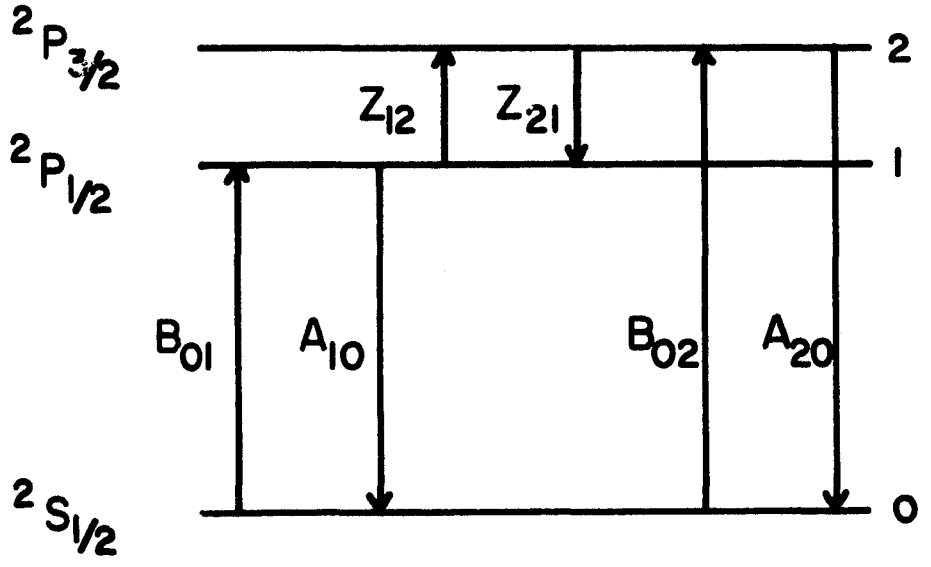

Figure 1. Energy Level Diagram of Potassium.
The B coefficients correspond to excitation by absorption of photons, the A coefficients refer to spontaneous radiative decay, and the Z coefficients to radiationless energy transfer due to inelastic collisions.

The coefficients B_{01} and B_{02} determine the populations of the $^2P_{1/2}$ and $^2P_{3/2}$ states respectively, achieved by irradiation of ground state atoms by photons of the appropriate energy. A_{10} and A_{20} are the spontaneous radiative decay coefficients, and are equal to the inverse of the mean lifetimes of the two states.

The coefficients Z_{12} and Z_{21} correspond to radiationless energy transfers between the two excited states, induced by inelastic collisions with ground state atoms. These coefficients are density dependent and represent the number of collisions per atom and per second leading to the radiationless energy transfer.

If it is assumed that only the processes of excitation, spontaneous decay and collisional energy transfer take place in the vapour, it is possible to set up two coupled differential rate equations describing the state of the system:

$$\dot{N}_1 = -(1/\gamma_1 + Z_{12})N_1 + B_{01}N_0 + Z_{21}N_2 , \qquad (2)$$

$$\dot{N}_2 = -(1/\gamma_2 + Z_{21})N_2 + B_{02}N_0 + Z_{12}N_1 , \qquad (3)$$

where $N_{0,1,2}$ are the occupation numbers of the various states. It is assumed that $\gamma_1 = \gamma_2 = \gamma$, where γ is the mean lifetime of the two resonance states.

If only one of the two resonance states is populated, equations (2) and (3) yield a set of four equations, two of which do not contain B_{01} or B_{02}:

$$\dot{N}_1 = -(1/\gamma + Z_{12})N_1 + Z_{21}N_2 , \qquad (4)$$

$$\dot{N}_2 = -(1/\gamma + Z_{21})N_2 + Z_{12}N_1 . \qquad (5)$$

Under steady state conditions, $\dot{N}_1 = \dot{N}_2 = 0$. Dividing equation (4) by N_2 and equation (5) by N_1 yields

$$Z_{21} = (1/\tau + Z_{12})\eta_1 \quad , \tag{6}$$

and

$$Z_{12} = (1/\tau + Z_{21})\eta_2 \quad , \tag{7}$$

where $\eta_1 = N_1/N_2$ when state $^2P_{3/2}$ is excited, and $\eta_2 = N_2/N_1$ when state $^2P_{1/2}$ is excited.

Since the difference between the energies of the two resonance states in potassium is small, the ratio of the population densities of the two states is the same as the ratio of the intensities of the lines emitted by the two states.

Solving equations (6) and (7) for Z_{12} and Z_{21}, we obtain

$$Z_{12} = \frac{1}{\tau}\left[\frac{\eta_2 + \eta_1\eta_2}{1 - \eta_1\eta_2}\right], \tag{8}$$

and

$$Z_{21} = \frac{1}{\tau}\left[\frac{\eta_1 + \eta_1\eta_2}{1 - \eta_1\eta_2}\right]. \tag{9}$$

Both Z_{12} and Z_{21} are functions of the relative velocity of the colliding partners and of the density of atoms in the ground state, N_0.

By analogy with the classical kinetic theory of gases, the average cross section for radiationless energy transfer between the two levels is defined as follows:

$$Q_{12} = \frac{Z_{12}}{N_0 v_r} \quad . \tag{10}$$

Q is the total cross section in cm^2, N_0 is the number of ground state atoms per cm^3 and v_r is the mean relative velocity of the colliding atoms, given by

$$v_r = \sqrt{\frac{8kT}{\pi\mu}} \quad , \tag{11}$$

where k is the Boltzmann coefficient, T is the absolute temperature and μ is the reduced mass of the colliding atoms. The total collision cross section may be represented as follows, in terms of the differential cross section q(v):

$$v_r Q = \int f(v)\, v\, q(v)\, d^3v \quad . \tag{12}$$

This thermal averaging is carried out over the Maxwell-Boltzmann velocity distribution function, f(v).

It is expected from the principle of detailed balancing that the ratio of Z_{12}/Z_{21} should be given by

$$\frac{Z_{12}}{Z_{21}} = \frac{g_2}{g_1} e^{-\Delta E/kT} \quad , \tag{13}$$

where g_1 and g_2 are the statistical weights of the $^2P_{1/2}$ and $^2P_{3/2}$ states ($g_1 = 2$; $g_2 = 4$) and ΔE is the energy defect between them. The exponential term is the Boltzmann factor which determines the probability that the kinetic energy of relative motion will be greater than ΔE.

(ii) Imprisonment of Resonance Radiation and Quenching of Fluorescence

When a potassium atom is excited to one of the resonance levels by absorption of a photon, it will, on the average, remain in the excited state for a time equal to the

mean lifetime of the state, τ. If, during that time, an inelastic collision takes place, the excitation energy may be transferred to the other resonance state which also has a lifetime τ.

If the atomic density of the system is high, or if the path of the photon through the metal vapour is appreciable, then this "primary" photon may be reabsorbed by a potassium atom in the ground state. This absorption and reemission process may occur many times before a photon is registered by the recording system. The process is called imprisonment or diffusion of resonance radiation.

The imprisonment process artificially lengthens the lifetimes of the excited states, depending on the average number of reabsorptions per photon; this gives rise to spurious values of the cross sections. Since the oscillator strength for the $4^2S_{1/2} \longleftarrow 4^2P_{3/2}$ transition is twice that for the $4^2S_{1/2} \longleftarrow 4^2P_{1/2}$ transition, the probability of a transition from the $^2P_{1/2}$ to the $^2P_{3/2}$ level will appear smaller compared with the reverse transition, than would otherwise be the case. Thus the effective ratio of the two cross sections will be smaller than that predicted by equation (13).

There is a second process which has not been taken into consideration in equations (2) and (3)--the quenching of resonance fluorescence by inert gases.

If a potassium atom in one of the excited ^2P states interacts with a foreign gas atom in such a way that the

entire excitation energy is converted into the kinetic energy of relative motion of the colliding pair, or into internal energy of the foreign atom, fluorescence is said to be quenched.[29] Quenching is most probable if the foreign gas is composed of polyatomic molecules whose closely spaced vibrational and rotational energy levels easily absorb a wide band of energies.

Since the energy difference between the fine structure resonance states of potassium is small, the quenching cross sections for the two levels with a given foreign gas atom should be the same. For this reason, if quenching occurs, it should not alter the ratio of the cross sections for inelastic collisions, but it may lower the absolute magnitude of both cross sections by artificially shortening the lifetimes of the resonance states.

Because the inert gases possess no electronic states whose energies are close to those of the ^2P states in potassium, the quenching cross sections of these gases with potassium are expected to be much smaller than those for excitation transfer among the potassium ^2P levels.

B. The Microscopic Theory of Inelastic Atomic Collisions

(i) General Statement of the Problem

In general, when a potassium atom in one of the resonance states is perturbed by either a ground state potassium atom or an inert gas atom in its ground state in such a way as to cause radiationless energy transfer, there will

exist for a short time a quasi-molecule which may or may not be in a bound state. During the time of interaction, that is, the duration of the two body system, the colliding pair may be described by a wave function involving the electronic states of both atoms. The following paragraphs present a general conceptual approach to the solution of the two body problem, which will be useful in the discussion of the various theories which have been proposed for the energy transfer process.

Let us define the two eigenstates of the diatomic system as functions of the atomic eigenstates at infinite separations:

$$\begin{aligned} \Psi_1 &= f(K\,^2P_{1/2}, X) \\ \Psi_2 &= f(K\,^2P_{3/2}, X) \end{aligned} \quad . \tag{14}$$

X represents the wave function of a potassium or inert gas atom in the gound state, while the excited potassium atomic wave functions contain the degenerate Zeeman substates (4 for $^2P_{3/2}$ and 2 for $^2P_{1/2}$). It is expected that the functions given by equation (14) will go over smoothly into the eigenfunction of the two body system upon close approach since the potassium collisions take place under adiabatic conditions.[3] This wave function will be some linear combination of the functions (14).

$$\Psi = C_1(t)\Psi_1 + C_2(t)\Psi_2 \ ,$$

where $C_1(t)$ and $C_2(t)$ are time dependent Fourier expansion coefficients representing the amplitudes of the probability

that at a time t the system will be found in the state ψ_1 or ψ_2.

It is assumed that the initial state is a pure state with $C_1(t)$ or $C_2(t) = 0$ at $t = 0$. The solution to the problem should yield the probability per unit time that a transition will take place between ψ_1 and ψ_2. The time dependence of $C_2(t)$ is given by

$$\dot{C}_2^{(r+1)}(t) = \frac{-i}{\hbar} \sum_k C_k^{(r)}(t)\, H_{2k}(t)\, e^{i\omega_{2k}t} , \qquad (16)$$

where r+1 is the order of approximation, and H_{2k} is the matrix element of the Hamiltonian, H. The Hamiltonian is defined in terms of the forces assumed to be operating in the interaction and the matrix element connects the states 2 and k. ω_{2k} is the Bohr angular frequency, given by

$$\omega_{2k} = \frac{1}{\hbar}(E_2 - E_k) . \qquad (17)$$

For the sake of simplicity, only the first order perturbation will be considered, with the assumption that only one other state (or group of substates) is involved. Starting with a pure state, ψ_1, $C_k^{(0)}(t) \equiv C_1^{(0)}(t) = 1$, and equation (16) becomes

$$C_2^{(1)}(t) = \frac{-i}{\hbar} \int_{-\infty}^{\infty} H_{21}(t)\, e^{i\omega_{21}t}\, dt . \qquad (18)$$

If the interaction forces are applied for only a short time, the amplitude of the state ψ_2 will be proportional to the time dependent Fourier component of the matrix element H_{21} which connects the two states.

From equation (18), the probability amplitude of finding the system in state ψ_2 at a time τ' (or at any later time) will be

$$c_2^{(1)}(\tau') = -\frac{H_{21}}{\hbar}\frac{e^{i\omega_{21}\tau'}-1}{\omega_{21}} , \qquad (19)$$

where it has been assumed that H_{21} is time independent (slowly varying with time) except for being turned on at $t = 0$ and off at $t = \tau'$.[30] The probability of finding the system in state ψ_2 at any time t is

$$P_{12} = \left|c_2^{(1)}(t)\right|^2 . \qquad (20)$$

Therefore, from equation (19),

$$P_{12} = \frac{4\left|H_{21}\right|^2 \sin^2\frac{1}{2}\omega_{21}}{\hbar^2\omega_{21}^2} . \qquad (21)$$

If, as previously pointed out, the final state ψ_2 is composed of a number of substates of equal energy which do not greatly differ in energy from the original state of the system, then the density of final states, ρ_2, may be defined so that $\rho_2\, dE_2$ is the number of states in the energy range dE_2. Then the transition probability per unit time from the substates of ψ_1 to the substates of ψ_2 will be given by

$$P'_{12} = \frac{1}{t}\frac{4\left|H_{21}\right|^2}{\hbar}\rho_2\int_{-\infty}^{+\infty}\frac{\sin^2\frac{1}{2}\omega_{21}t}{\omega_{21}^2}\,d\omega_{21} , \qquad (22)$$

where the angular frequency has replaced the energy term. After integration, equation (22) becomes

$$P'_{12} = \frac{2\pi}{\hbar}\rho_2\left|H_{21}\right|^2 . \qquad (23)$$

Equation (23) represents the probability per unit time of a transition from state ψ_1 to state ψ_2. The probability of the reverse transition is obtained in the same way and has the same form as equation (23), with the indices interchanged. Since the interaction Hamiltonian is hermitian,

$$\frac{P'_{12}}{P'_{21}} = \frac{\rho_2}{\rho_1} = \frac{4}{2} \quad , \tag{24}$$

which agrees with the probability ratios obtained from the principle of detailed balancing (equation (17)). These transition probabilities provide the point of contact between the statistical sample which must be employed in an experiment and the microscopic system composed of a colliding pair of atoms which should, at least in principle, be treated quantum mechanically.

The above treatment oversimplifies the problems involved in assuming that there are matrix elements connecting all the degenerate substates of one fine structure state with all the degenerate substates of the other fine structure state, and that a simple first order approximation to the perturbation is sufficient. Neither of these assumptions is necessarily true, but the formalized solution of the problem (equation (23)) is sufficient for the discussion of most of the theories proposed in recent years.

It is immediately apparent that the probabilities P' are proportional to the collision numbers derived from the statistical model and presented as equations (8) and (9) and

are, therefore, proportional to the collision cross sections. In order to predict these cross sections theoretically and, thus, to evaluate the matrix elements connecting the various substates, both the interaction Hamiltonian and the wave functions ψ_1 and ψ_2 must be known. If, upon selection of a Hamiltonian and of the appropriate wave functions, the matrix elements connecting a given pair of substates are found to be zero, selection rules for the particular model may then be formulated in the given order of approximation.

There have been many attempts to interpret the processes involved in inelastic atomic collisions. Some of these have been undertaken from a classical or semi-classical viewpoint and others are based on quantum mechanical models. Of the latter, the most recent theories have employed time dependent perturbation theories of transition probabilities with the associated choices of interaction Hamiltonian and atomic wave functions. The following section gives a review of several theories which are of interest to the present investigation.

(ii) A Review of the Theories of Inelastic Atomic Collisions

One of the earliest quantitative treatments of energy transfer in atomic collisions was developed by Kallmann and London.[31] They gave a precise quantum mechanical treatment of the collision process assuming a dipole-dipole interaction. This theory was based on the assumption that the energy defect of the colliding atoms is small. The authors considered that adiabatic systems are not likely to lead to excitation transfer

and that as the energy defect, ΔE, increased, the system should become progressively more adiabatic.

Since the exchange forces between atoms of the same species were not included in the development of the theory, it might be expected that the experimental values of the inelastic cross sections would be larger than those predicted by Kallmann and London. Kallman and London also predicted that the cross sections should not depend on the sign of ΔE and that for inexact resonance ($\Delta E \neq 0$) the cross sections for inelastic collisions should vary as $(\Delta E)^{-2/3}$. These two stipulations can be easily verified in this and other experiments involving the alkali metals.

One of the major difficulties arising in a purely quantum mechanical treatment of atomic interactions occurs in operations involving the relative coordinates of the centres of mass of the colliding systems. In order to avoid such problems, Zener[32] presented a treatment of low velocity atomic collisions on the basis of classical concepts. He replaced atoms with sets of linear oscillators in the manner of the classical dispersion theory. His final expressions included the formulae of Kallmann and London[31] and of Rice[33] as special cases; they are, however, tractable only in the case of head-on collisions and are not directly applicable to the case of potassium.

Zener derived, from general considerations, those factors which he considered most important in atomic collision processes. They were the relative velocity and the sharpness

of the potential of the colliding pair (which together determine the interaction time), the energy defect, and the interaction energy between the initial and final states of the system. His conclusions indicate that the lower limit for the interaction time in collisions involving potassium is about 10^{-13} seconds.

A more sophisticated treatment of atomic collisions was developed by Stueckelberg.[34] It referred to collisions between atoms of the same species and was based on a partial wave analysis of the colliding systems. His treatment included a resonance curve (similar to that of Bates[35]) which indicated the variation of the inelastic cross sections with the energy defect of the colliding atoms.

Like Kallmann and London, Stueckelberg did not include exchange forces in his treatment. His most useful theoretical prediction is, that cross sections involving dipole-dipole interactions should vary as $(\Delta E)^{-2/3}$, if variations in relative velocities and dipole strengths between systems with different energy defects are ignored.

A return to the classical description of atomic collisions has recently been proposed by Jefimenko.[36] His model is a simplified version of a quantum mechanical model; the arrangement of the electrons about the nucleus of an atom is determined by quantum mechanical requirements, but the inter atomic forces are attributed to electrostatic interactions between the known charge distributions. The model includes the possibility of overlap forces, based upon the concept of

the excited electron of one of the colliding atoms existing as a free particle. A similar idea was used previously by Fermi[37] in his treatment of the broadening and shift of high order spectral lines.

Potential curves derived from this theory were used by Jefimenko in his studies of the dissociation energies of homonuclear molecules[36] and of the satellite bands in the spectra of cesium[38], rubidium[39] and potassium[40]. The applicability of Jefimenko's theory to the present experiment will be examined in section IV.

Time dependent perturbation theory was recently employed by Jordan[1] in a theoretical study of the mixing of the resonance states in the alkali metals by collisions with inert gas atoms. Jordan used modified hydrogenic wave functions and derived the Hamiltonian of the interaction from both van der Waals and quadrupole-induced dipole (QID) forces. He obtained the selection rules $m = 0$ for the van der Waal interaction and $m = 0, \pm 2$ for the QID interaction. Bender[41], using Hartree-Fock wave functions, derived the same selection rule for van der Waals interactions. (m is the projection of the total angular momentum, $\mathbf{J}$, of the alkali metal atom on the inter-nuclear axis of the collision partners.)

Jordan found that the two types of interaction were of comparable strength and defined the weighted average of the two collision cross sections as the effective cross section. The cross sections were found to increase with the polarizabilities of the inert gas atoms. Experimental determinations of the mixing cross sections for collisions between

sodium and all the inert gas atoms and for potassium with helium, neon and argon were made by the same author and the results were compared with those predicted by his theory.

More recently, J. Callaway and E. Bauer[2] developed a general method for the study of inelastic collisions of heavy particles founded on the possibility of obtaining a complete solution to the time-dependent perturbation theory. The wave functions used were Slater determinants and the interaction was reduced to the one-electron case. The treatment was restricted to the long range interactions dominated by the smallest negative power of the inter-nuclear separation appearing in the effective potential. Cross sections were calculated for the systems Na-He, Na-A, K-He and K-A, and were found to be in moderate agreement with experimental values.

W. R. Thorson[42] presented a theory involving stationary states and partial wave analysis to account for the zero-order elastic and first order inelastic scattering in slow atomic collisions between H atoms and H^+ ions. Unfortunately, the analysis is not easily applied to the atomic systems which are the subject of the present investigation.

It is unfortunate that most of the existing theories of excitation transfer are based upon non-adiabatic interactions of systems with a very small energy defect, ΔE. These assumptions of near-resonance conditions limit the applicability of the theories to the case of sodium; the departure from this theoretical basis becomes greater as the energy defect increases for the heavier alkali metals.

The existence of exchange forces in collisions between atoms of the same species has also been generally ignored and it is unlikely that cross sections calculated from such theories will be in close agreement with experimental results.

III. EXPERIMENTAL

A. Description of the Apparatus

A typical arrangement of the apparatus used to study potassium-potassium and potassium-inert gas collisions is shown in figure 2. A radio frequency alkali vapour lamp, which is described in Appendix A[43], was used as a source of resonance radiation. The potassium resonance lines emitted by the lamp were separated by a grating monochromator and then passed, if necessary, through one or more Spectrolab interference filters. They were then brought to a focus in the fluorescence cell situated in an oven whose temperature was accurately controlled. The cell could be evacuated to about 10^{-7} torr and could be filled with inert gases at pressures up to one atmosphere.

The fluorescence spectrum was, in general, passed through a second set of interference and neutral density filters, scanned with a recording spectrometer, and registered by means of an electrometer amplifier and strip chart recorder or by means of a counting train.

(i) The Spectral Lamp

The radio frequency light source, whose detailed description is given in Appendix A, consisted of a cylindrical pyrex tube which contained about 0.5 gm of potassium in

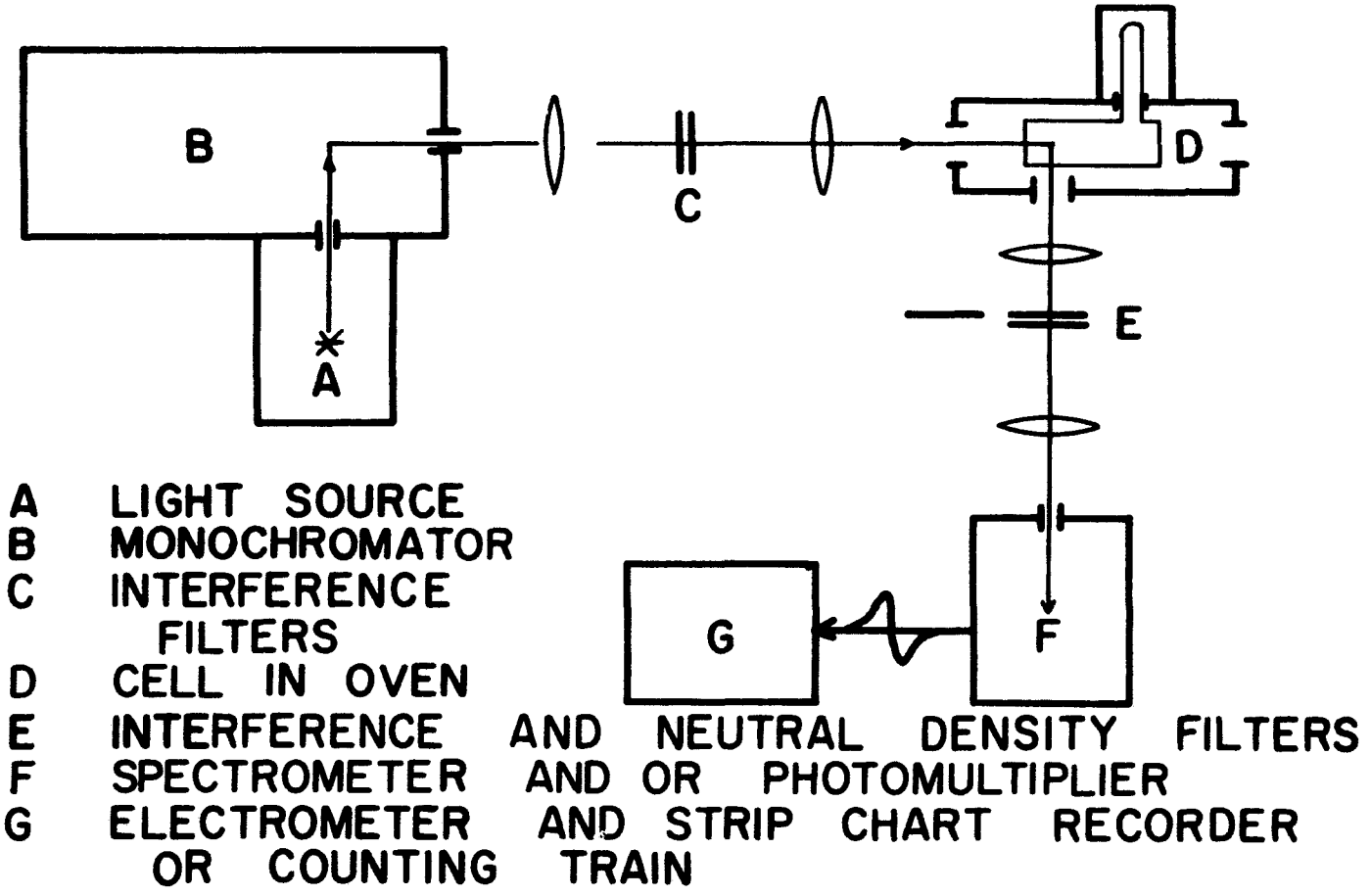

Fig. 2. Arrangement of the Apparatus

a reservoir and about 2 torr of argon as a buffer gas. The tube was placed in the tank coil of a push-pull power oscillator operated at 40 mc/sec. The base of the lamp, which contained the potassium, was temperature controlled to establish the desired potassium vapour pressure. The lamp emitted potassium resonance lines of high intensity, small half-width, and little self-reversal.

(ii) The Monochromator and Interference Filters

A Bausch and Lomb grating monochromator was used, jointly with Spectrolab interference filters, to resolve the potassium resonance lines. The monochromator was fitted with a 1200 line/mm grating blazed at 7500 $\mathring{A}$ in the first order, which gave a reciprocal dispersion of 16 $\mathring{A}$/mm. The focal length of the instrument was 500 mm and the aperture was f/4.4.

The transmitted intensity of the monochromator varied linearly with slit width; for all experimental runs a width of 1.50 mm was used, giving a spectral purity of one part in 2000.

The Spectrolab interference filters were used both singly and in pairs to improve the spectral purity of the incident beam and to aid in the resolution of the fluorescent resonance lines. The filters would accept an incident light cone of half-angle 6^{o} before serious losses in spectral purity set in. The filters used in the experiments are tabulated below, with transmissions of the two resonance lines as specified by the manufacturer.

Serial Number	Transmission of 7665 Å	Transmission of 7699 Å
10885	0.625	0.0015
10975	0.650	~0.001
10897	0.0015	0.590
10972	~0.001	0.710

The transmissions of all the filters were measured in situ for each of the experiments since the tolerance for non-parallel light was very low.

(iii) The Fluorescence Cell

The design of the fluorescence cell, shown in figure 3, was dictated by the desire to keep reabsorption of resonance fluorescence to an absolute minimum and thus to limit the distance through which the exciting and the fluorescent light had to travel through the absorbing vapour. In the present arrangement, the light from the monochromator was focussed in the corner formed by the front and side, or observation, windows which were made of pyrex filter glass. As a result, the maximum distance between either window and the observed region did not exceed one millimeter. The internal filter, whose transmission in the infrared was 2%, was included to restrict the optical depth at which fluorescence was observed. Two models of the cell, one with and one without the filter, were used and gave indistinguishable experimental results.

The side arm, which contained the liquid potassium, was about 40 mm in length and 12 mm in diameter. This short, wide reservoir ensured that the vapour density in the cell

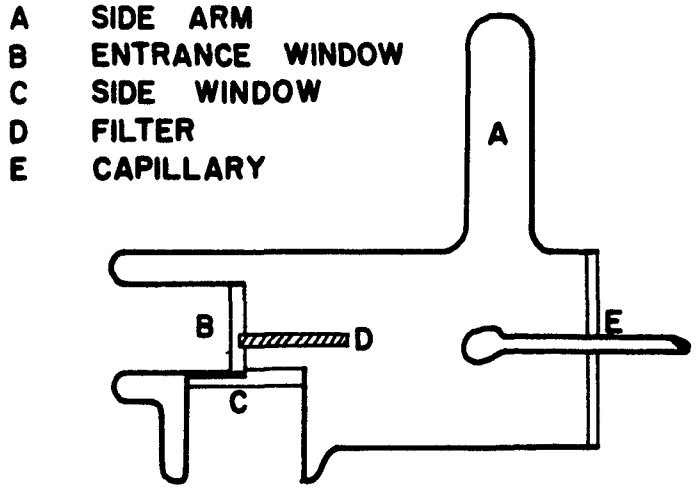

Fig. 3. The Fluorescence Cell

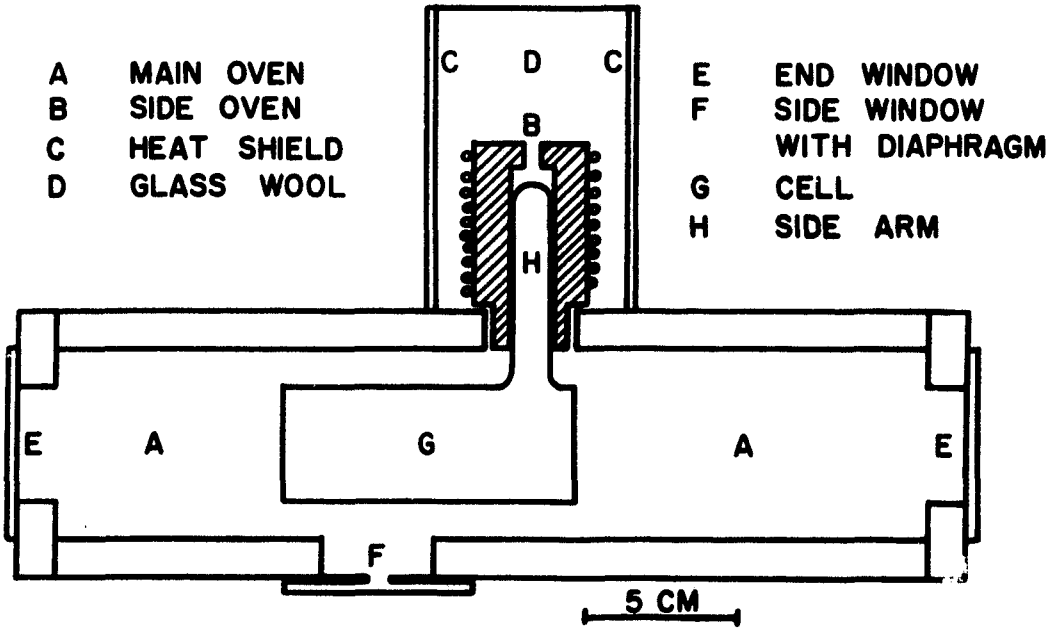

Fig. 4. Detail of the Oven

would be determined by the temperature of the side arm and would not be altered by molecular diffusion effects.[44]

The cell was coupled to the evacuating and filling system by a length of capillary tubing which successfully prevented migration of the potassium out of the cell over hundreds of hours of operation at 370°K.

(iv) The Ovens and Temperature Controller

The detail of the oven is shown in figure 4. It was essentially a rectangular box fabricated of transite board and fitted with two banks of Chromel A heating wire (#26) with a parallel resistance of 20 ohms. Windows for the incident light were provided at each end of the oven, coaxial with the cell which was mounted at the geometric centre of the oven. An exit window was provided for the observation of the fluorescent spectrum.

The side arm of the cell protruded from the back wall of the main oven into the side oven, which consisted of a cylindrical brass tube machined to fit the side arm snugly with the aid of spring bronze spacers. The high thermal capacity and conductivity of the brass ensured a uniform and stable temperature along the length of the side arm.

It was essential that the temperatures of the two ovens remain stable over long periods of time, especially in the case of the side oven, whose temperature determined the potassium vapour pressure. Some available temperature controllers of the cycling type were tested and proved unsatisfactory. For these reasons, a sensitive proportional

temperature controller was developed.

This controller, whose operation is depicted schematically in figure 5, is essentially a magnetic amplifier which incorporates a thermistor as a temperature-sensing element in a negative feed back loop. As the thermistor resistance varies with temperature, there is a proportional variation in the voltage drop across it. This voltage variation is applied to the base of a grounded emitter amplifier to produce an amplified out-of-phase signal which is fed into a current gain stage. The current output of the final stage is fed into the D.C. coils of a saturable core reactor whose A.C. current output serves to heat the ovens.

Figure 6 is a circuit diagram of one of the control amplifiers while figure 7 shows the complete circuit of the controller. If the sensitivity of the control circuit at constant gain is defined as dV'/dT where V' is the voltage on the base of TR_1 and T is the temperature in degrees Celsius, and if we assume that the resistance $R_1 + P_1$ is so small that the voltage V_0 does not change, then:

$$\frac{dV'}{dT} = \frac{V_0 r}{(r + R_T(T))^2} \frac{dR_T(T)}{dT} , \qquad (25)$$

where r is the resistance of P_2. Equation (25) may be rewritten as follows in terms of the temperature coefficient of resistance, α, of the thermistor:

$$\frac{dV'}{dT} = \frac{\alpha V_0 r R_T(T)}{(R_T(T) + r)^2} , \qquad (26)$$

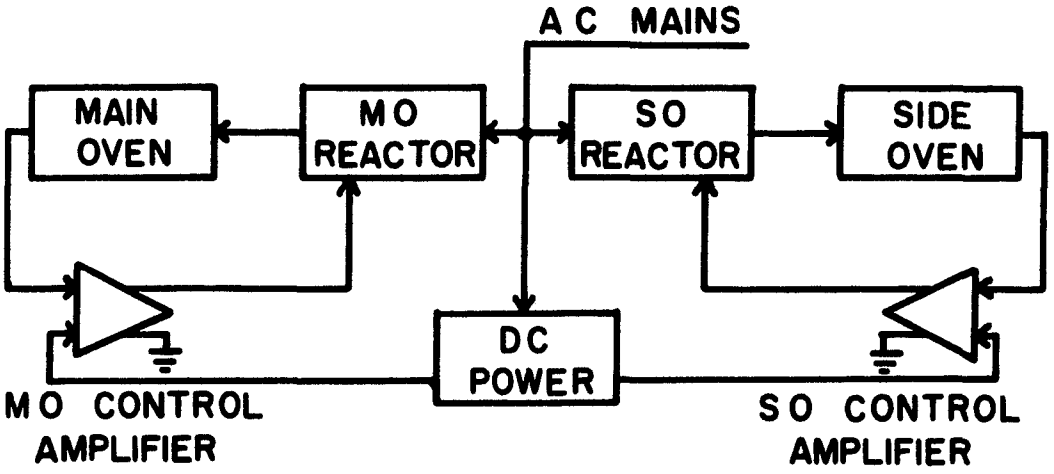

Fig. 5. Block Diagram of the Proportional Temperature Controller

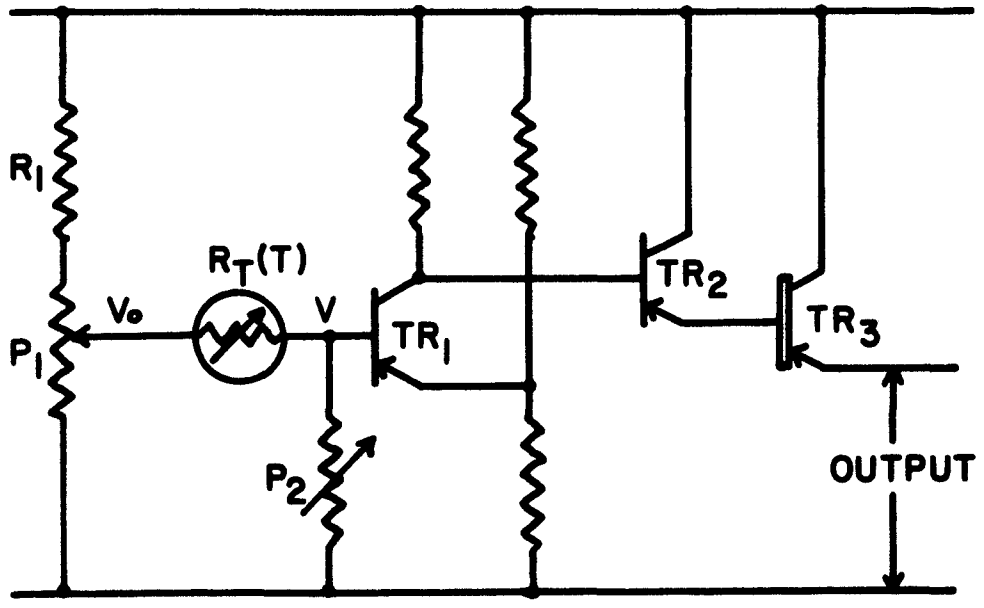

Fig. 6. Circuit Diagram of an Oven Control Amplifier

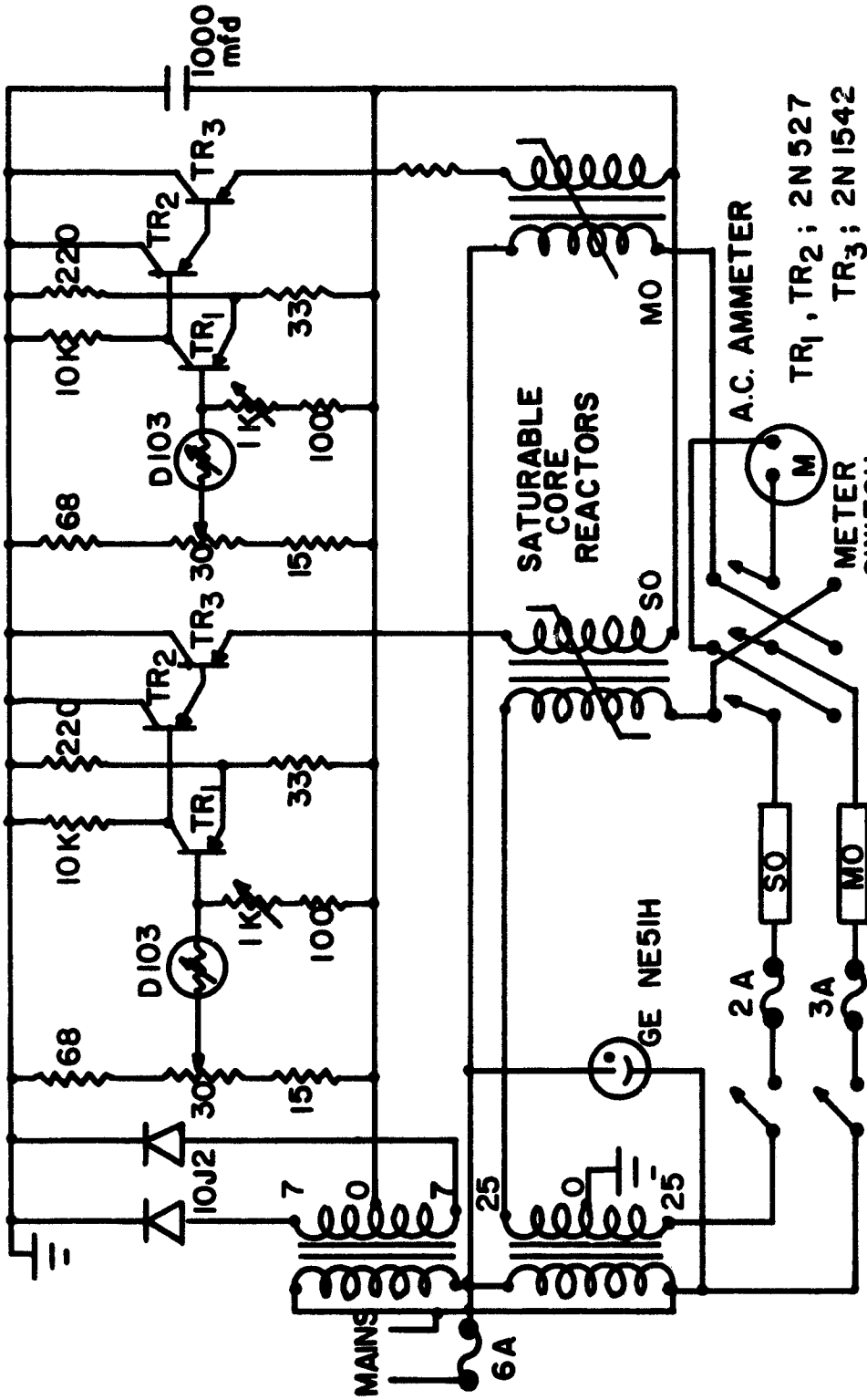

Fig. 7. Circuit Diagram of the Proportional Temperature Controller

where $\alpha = \frac{1}{R_T(T)} \frac{dR_T(T)}{dT}$. Equation (26) may be regarded as the basic design equation for the control amplifier.

For optimum stability and protection from thermal drift, the amplifier components were mounted on a water-cooled heat fin and the current through the thermistors was kept low to eliminate self-heating. The units which were used had an overall power gain of 10^6: the power gain of the reactors was about 30, for a maximum controlled output of 200 watts.

Throughout the experiments, the controller maintained the side oven within $\pm 0.1^{\circ}C$ and the main oven, which was not as well insulated, within $\pm 1.0^{\circ}C$. The temperature controller was insensitive to line voltage fluctuations of up to 20%.

(v) The Evacuating and Filling System

The vacuum system was constructed of pyrex glass and contained no metal sections with which the inert gases might come into contact. Vacuum was attained by means of an Edwards model 1SC50B rotary pump fitted with a 2A non-return valve and an Edwards model EO-2 diffusion pump operated with Dow Corning 704 Silicone pumping fluid. This combination was capable of vacua of the order of 10^{-7} torr or better. The pumps were protected from cooling water and power failures by a relay system built around an FSM-1 Flowtrol unit.

The pressure measuring devices used with this system are tabulated below, along with their approximate useful pressure ranges.

Device	Lower Pressure (torr)	Upper Pressure (torr)
Mercury Manometer	10	500
Oil Manometer (704 Silicone)	0.5	30
LKB Autovac Gauge (Type 3294B)	10^{-3}	2.0
Edwards Pirani Gauge Model 8/2	10^{-4}	0.1
CVC Ionization Gauge Type GIC-110A (with Bayard-Alpert head)	10^{-9}	10^{-3}

For work at very low pressures, the Edwards gauge was considered more precise than the LKB gauge, since it employed a measuring head consisting of four Pirani units in a Wheatstone bridge circuit. Two of these heads were sealed off at high vacuum to provide a stable zero pressure reference which was not sensitive to fluctuations in ambient temperature. The Edwards gauge was calibrated with a CVC McLeod gauge type GM-100A. It was found that the calibration curves supplied by the Edwards Company were accurate within the experimental error for all the inert gases with the exception of helium pressures which showed a constant difference of 10%. The McLeod gauge was not used during the experiments to prevent the possible contamination of the vacuum system with mercury.

(vi) The Spectrometer and Recording Systems

During the experiments with inert gases, a modified Perkin-Elmer model 112 spectrometer was employed. The instrument was fitted with a Bausch and Lomb 1200 lines/mm plane

replica grating blazed at 7500 Å. This arrangement, which had an aperture of f/4, produced a reciprocal dispersion of 13 Å/mm. The entrance and exit slits of the instrument were maintained at 0.80 mm, which gave sufficient resolution consistent with transmitted intensities adequate for experiments with inert gas pressures above a few tenths of a torr. At lower gas pressures, Spectrolab interference filters were placed in series with the spectrometer, resulting in a total spectral purity of the potassium resonance lines of one part in 10^6 or better.

An external detection system was fitted to the spectrometer, consisting of an I.T.T. FW118 photomultiplier tube housed in a liquid air cooled cryostat, described by Krause and Neville[45]. The phototube was a 16-stage device with an S-1 (Ag— O— Cs) photocathode 3 mm in diameter, which had a peak sensitivity centred around 8000 Å. The tube was operated at 1.8 kilovolts, supplied by a Fluke 413C power supply, during all experimental runs.

In the experiments involving pure potassium vapour, the spectrometer was eliminated because of its relatively low transmission. An improved version of the cryostat-phototube combination was used in conjunction with two Spectrolab interference filters in series with one another.

The signal from the photomultiplier was fed into a Victoreen VTE-2 electrometer or a Keithley 603 electrometer amplifier. The amplified D.C. output was then recorded by a Philips strip chart recorder. Alternatively, for weak signals,

the phototube output was fed directly into a Philips counting train which included a power supply, a threshold discriminator, and a seven-decade visual read out scaler.

B. Experimental Procedure

Each fluorescence cell was thoroughly cleaned before use with a potassium dichromate cleaning solution followed by distilled water. The cell was then painted with aquadag, positioned in the oven, and sealed to the vacuum system at the capillary and side arm. The side arm contained a sealed pyrex ampoule of 99.95% pure potassium (0.5 to 1.0 gm) which was obtained, sealed under vacuum in glass containers, from the A.D. Mackay Company of New York.

The cell was outgassed for several days at 200°C and at a pressure not higher than 10^{-7} torr. After outgassing, the ampoule was broken and the potassium was distilled into the cell; the side arm was then sealed and cut off at about 4 cm from the cell.

Once potassium was admitted to the cell, temperatures in the main oven were kept below 150°C to limit the corrosive action of the potassium on the pyrex[22], which seems to consist of a simple replacement of sodium in the glass by potassium and results in an opaque brown deposit. An analysis of the deposit showed that it consisted largely of silicon and potassium. There were also small quantities of iron, aluminum, boron and sodium, which are constituents of the glass. On

exposure to air, the deposit turned white, suggesting air oxidation or hydration of unstable compounds. The deposit was not formed at temperatures below 150°C.

The image of the exit slit of the monochromator was focussed close to the exit window of the cell in such a way that no reflections occurred. The side oven was placed over the side arm of the cell and was enclosed by an aluminum heat shield packed with glass wool. Thermistors were fastened with asbestos cement to the main body of the cell and to the side arm.

Chromel-alumel thermocouples were attached to the cell close to the thermistors. These were used, in conjunction with a Leeds and Northrup 8686 millivolt potentiometer to measure the temperatures.

The vapour pressure of the potassium was obtained from the temperature of the side oven by using the empirical formula of Ditchburn and Gilmour[46]:

$$\log_{10} P\,(\text{torr}) = \frac{-4552}{T\,(^{\circ}K)} - 0.5 \log_{10} T\,(^{\circ}K) + 8.793 \quad . \quad (27)$$

The pressure of both potassium vapour and of inert gases was related to the number of atoms per cm^3 by the following equation which follows from kinetic theory:

$$N\,(\text{atoms/cc}) = \frac{P\,(\text{torr})}{T\,(^{\circ}K)} \times 9.656 \times 10^{18} \quad . \quad (28)$$

In the case where the side arm of the cell is long and narrow, the ratio of the vapour pressure in the main body of the cell, P', to the vapour pressure in the side arm, P,

is given by

$$\frac{P'}{P} = \sqrt{\frac{T}{T'}} \ ,$$

where T and T′ are the corresponding absolute temperatures of the two sections of the cell. If, however, the mean free path of the potassium atoms is greater than the diameter of the side arm, the two pressures will be equal. It can be shown that with the present diameter of the side arm (12 mm) the pressures P and P′ are equal up to about 2×10^{-3} torr. In addition, T and T′ differed by only $20^{\circ}K$, so that the maximum error in vapour pressure above 2×10^{-3} torr will only be two or three percent.

The spectroscopically pure inert gases used in these experiments were obtained in one litre pyrex bulbs from the Linde Company, Tonawanda , N.Y. The gases were admitted to the cell and to the manometric sections of the vacuum system by means of a stopcock fitted with an extremely fine glass orifice. The pressures of krypton and xenon were more easily controlled by evaporating them from a liquid air trap attached to the supply bulbs.

Whenever the mercury manometer was used, it was opened to the vacuum system only when a few torr of gas were present in the system. It was always exhausted with the cell cut off from the system; the system was then cleaned of any contaminating mercury vapour by pumping it down to very low pressures for several hours before the cell was reopened. In this way, mercury contamination of the potassium was avoided.

Throughout the inert gas experiments, the main oven was maintained at $95 \pm 1^{o}C$ and the side oven at $75.0 \pm 0.1^{o}C$. The desired amount of gas was admitted to the cell and sufficient time was allowed for equilibrium to be established. One of the resonance lines was then made incident on the metal-gas mixture, and the fluorescence spectrum was scanned by the Perkin-Elmer spectrometer. The other resonance line was then made incident, and the procedure was repeated at least four times. The average intensity ratios η_1 and η_2 were obtained from the peak heights registered by the strip chart recorder. These values, later used in equations (8) and (9) together with the lifetime (2.6×10^{-8} sec - Landolt-Bornstein[47]) to calculate collision numbers, represent the basic experimental results.

At low gas pressures (below 0.2 torr), Spectrolab interference filters were used in series with the spectrometer to increase the resolution of the resonance lines. In this case the spectrum was not scanned, but the wavelength drive of the spectrometer was set on the peaks of the two resonance lines in turn; the output of the photomultiplier was recorded with the Philips counting train. Intensity profiles were plotted as a function of wavelength drive position, both with and without the interference filters. This was done to ensure that the wavelength drive could be positioned exactly on the peaks of the resonance lines and that no shift of the peaks would occur because of the insertion of the filters.

The ratio of the transmissions of the two filters was measured in preference to measuring their individual transmissions. At a high gas pressure (5-10 torr) the true η values were measured without filters, then the measurements were repeated with the filters in place. The normalizing factor used to bring the η values measured using filters into agreement with the true η values was taken to be the ratio of filter transmissions. This technique was less liable to systematic errors than the measurement of the separate transmissions.

In the experiments with pure potassium, the spectrometer was replaced by a cryostat containing an I.T.T. FW118 photomultiplier in order to increase the intensity of the fluorescent light signals: the η values were expected to be small in the vapour pressure region which was of interest. Two Spectrolab interference filters were placed in series with the monochromator to give a spectral purity in the incident beam of one part in 10^9.

The fluorescence spectrum was analyzed by means of another pair of interference filters which transmitted only sensitized fluorescence. The intensity of the latter was registered by the Philips counting train and the background noise was monitored with the incident beam of resonance radiation cut off. The total fluorescent intensity was then measured using a neutral density filter in the fluorescent beam to avoid overloading the scaler, whose dead time was about one microsecond. The transmissions of the interference filters and neutral density filters were measured in situ, using potassium fluorescent light at very low vapour pressures.

IV. RESULTS AND DISCUSSION

A. Investigation of Effects Due to the Imprisonment of Radiation

When resonance radiation is made incident on a sample of potassium vapour, the intensity of resonance fluorescence should increase linearly with the density of the vapour. This behaviour would be expected at very low vapour densities, at which the mean free path of a photon is greater than the distance of the fluorescing vapour element from the window. Any deviation from linearity will be due to reabsorption, provided that no complicating processes, such as quenching, take place.

If only one component of the resonance doublet at a time is used to irradiate the vapour, the onset of radiation trapping will occur at different vapour densities for the two components. These densities will, in fact, be in the reciprocal ratio of the respective oscillator strengths, as may be shown by the following argument.

Let I_1 and I_2 be the observed intensities of the 7699 $\mathring{A}$ and 7665 $\mathring{A}$ fluorescent components, respectively, and I_1^0 and I_2^0 the fluorescent intensities emitted by a volume element in the vapour at a depth x, which would be observed if no reabsorption were taking place. The intensities of both lines are attenuated exponentially according to the

following equations:

$$I_1 = I_1^0 \; e^{-xk_1} \; , \tag{29}$$

and

$$I_2 = I_2^0 \; e^{-xk_2} \; , \tag{30}$$

where k_1 and k_2 are the integrated absorption coefficients:

$$k_{1,2} = \int k(\nu_{1,2}) \, d\nu_{1,2} = \frac{\pi e^2}{mc} \, N f_{1,2} \; . \tag{31}$$

N is the vapour density in atoms/cm^3 and f_1 and f_2 are the oscillator strengths for the relevant transitions.

Since we are interested only in the first observable effect of radiation diffusion, the exponential terms in equations (29) and (30) may be expanded in a Taylor series with the retention of only the two leading terms.

$$I_1 = I_1^0 \, (1 - xk_1) \tag{32}$$

$$I_2 = I_2^0 \, (1 - xk_2) \tag{33}$$

If we define the deviation from linearity (or the absorption) by

$$\Delta I_{1,2} = I_{1,2} - I_{1,2}^0 \; ,$$

then, from equations (32) and (33), we obtain

$$\Delta I_1 = - I_1^0 \, x \, k_1 \; , \tag{34}$$

and

$$\Delta I_2 = - I_2^0 \, x \, k_2 \; . \tag{35}$$

If the relative deviations, $\Delta I_1 / I_1^0$ and $\Delta I_2 / I_2^0$, are assigned equal and arbitrarily small values (of the order of the error in measuring the intensities) then, from equations

(34) and (35),

$$k_1(N_1) = k_2(N_2) \quad (N_1 \neq N_2) \ . \tag{36}$$

Using the definition of these coefficients given in equation (31), equation (36) becomes

$$N_1 f_1 = N_2 f_2 \ . \tag{37}$$

Equation (37) states that the ratio of the pressures, at which absorption is first detectable for the two resonance lines, should be equal to the inverse ratio of the two oscillator strengths. The ratio of $f_2/f_1 = 2$ for potassium, so that the intensity curve for I_2 should begin to drop (equations (32) and (33)) at half the pressure at which the curve for I_1 begins to drop.

Since the depth of the fluorescing element, x, is not contained in equation (37), the above argument holds for the entire fluorescing volume. At low densities, error in this ratio induced by differences in the resonance line shapes should be negligible, since the absorption takes place mainly at the centres of the lines.

Figure 8 is a plot of the resonance fluorescent intensities as a function of vapour pressure. In the pressure range shown, the contribution of sensitized fluorescence to the total was about one part in 10^5. The fluorescent intensities were about equal to one another, but are scaled differently for the sake of clarity.

It may be seen that the curve for the 7665 Å fluorescence becomes non-linear at about 3.5×10^{-6} torr, and that

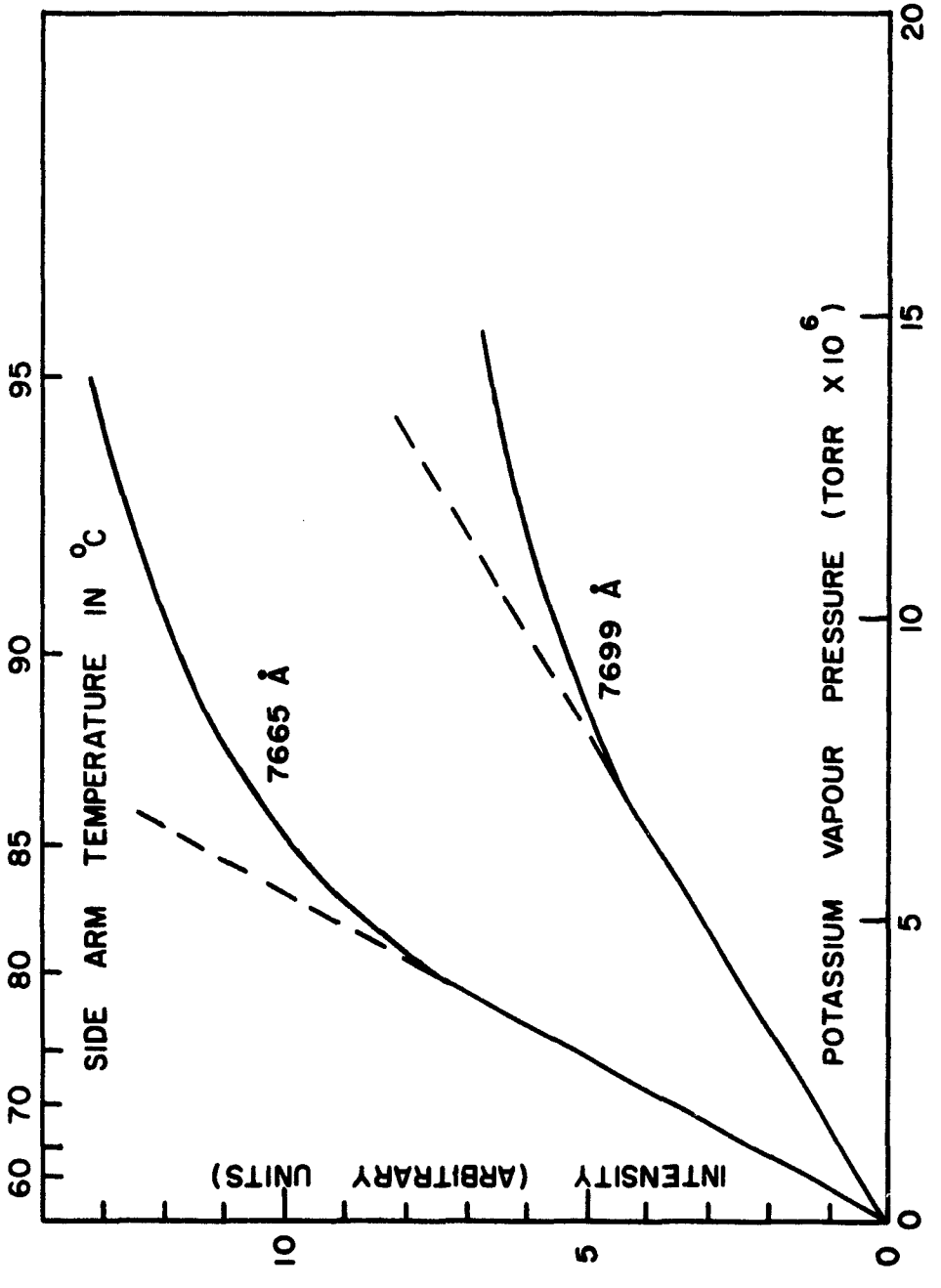

Fig. 8. A Plot of the Fluorescent Intensities Against the Potassium Vapour Pressure

for the 7699 Å component at about 7.0×10^{-6} torr, in good agreement with equation (37). The same behaviour has been observed in cesium[25] and in rubidium vapour[27]. This result clearly shows that radiation diffusion sets in at much lower potassium vapour pressures than had previously been supposed.[22]

An additional check was made of the vapour pressure at which radiation imprisonment first appears in the vapour, by monitoring the relationship between the vapour pressure and the η values. Since the intensity ratios are difficult to measure at low vapour pressures (10^{-7} to 10^{-5} torr), the potassium was sensitized by a fixed amount of inert gas while its vapour density was varied. Before each change in vapour pressure, the fluorescence cell was evacuated. Any change observed in the η values was interpreted as being due to radiation diffusion.

This experiment was first conducted using a fixed pressure of 20 torr of argon,[23] and led to a choice of 75°C as the optimum side arm temperature for the inert gas experiments. More recently, fluorescence was sensitized with 10 torr of helium; the results of this experiment are shown in figure 9. Again the optimum temperature, at which high intensity is consistent with the absence of radiation trapping, appears to be 75°C.

Because of these preliminary results, it was decided to carry out the experiments with inert gases at a side oven temperature of 75°C. The main oven was kept at 95°C in order to prevent condensation of potassium on the cell windows.

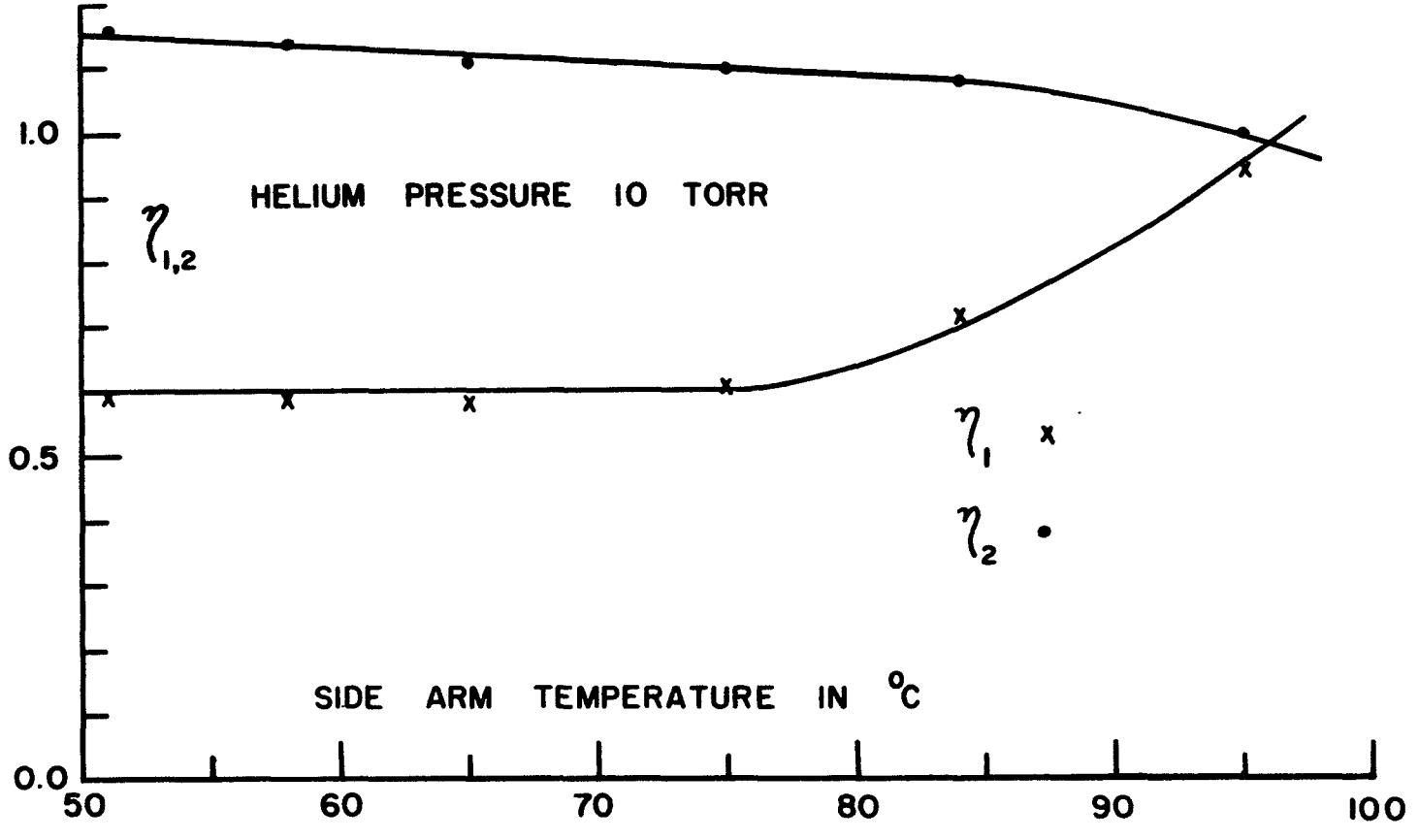

Fig. 9. Intensity Ratios in a Potassium-Helium Mixture at Various Temperatures

B. The Total Cross Sections for Inelastic Collisions between Potassium and Inert Gas Atoms

(i) The Experimental Results

The experimental values of fluorescent intensity ratios, η, obtained in mixtures of potassium with helium, neon, argon, krypton and xenon, are shown in tables 1-5 respectively. Each table includes values obtained with at least two different samples of potassium in fluorescence cells with and without an internal opaque filter.

Figure 10 is a graph of the intensity ratios, induced by potassium-inert gas collisions, as functions of inert gas pressure. No experimental points are shown because their very large number would cause confusion in the high and low pressure regions of the curves. It may be seen that the intensity ratios never reach the expected values of $\eta_1 = 0.625$ and $\eta_2 = 1.60$ in the pressure range in which the η values become independent of pressure. These theoretical limits have not been reached in any experiments with alkali metals or alkali metal-inert gas mixtures.[1,16,19,22,23]

The collision numbers Z_{12} and Z_{21} were obtained by substituting values of η_1 and η_2, taken from the smoothed curves, into equations (8) and (9). A typical plot of Z_{12} and Z_{21} as functions of krypton pressure is shown in figure 11. The corresponding curves obtained with the other inert gases all exhibit a linear section between about 20 and 150 torr which, when extrapolated to zero pressure, does not pass through the origin.

TABLE 1

Fluorescent Intensity Ratios Induced by Potassium-Helium Collisions

Helium Pressure (torr)	η_1 I_1/I_2	η_2 I_2/I_1	Helium Pressure (torr)	η_1 I_1/I_2	η_2 I_2/I_1
4.1×10^{-3}	1.89×10^{-3}	3.22×10^{-3}	5.8	4.89×10^{-1}	1.02
6.9×10^{-3}	3.01×10^{-3}	4.25×10^{-3}	7.0	5.05×10^{-1}	1.03
1.1×10^{-2}	4.64×10^{-3}	5.96×10^{-3}	8.0	5.43×10^{-1}	1.08
1.2×10^{-2}	4.11×10^{-3}	7.00×10^{-3}	1.01×10	5.52×10^{-1}	1.14
1.5×10^{-2}	6.13×10^{-3}	8.82×10^{-3}	1.18×10	5.89×10^{-1}	1.14
1.6×10^{-2}	6.20×10^{-3}	1.01×10^{-2}	1.37×10	5.71×10^{-1}	1.21
1.9×10^{-2}	7.70×10^{-3}	1.15×10^{-2}	1.94×10	6.08×10^{-1}	1.25
2.1×10^{-2}	8.27×10^{-3}	1.24×10^{-2}	2.50×10	6.22×10^{-1}	1.30
2.5×10^{-2}	1.03×10^{-2}	1.49×10^{-2}	2.55×10	5.55×10^{-1}	1.32
4.3×10^{-2}	1.80×10^{-2}	2.82×10^{-2}	2.95×10	6.01×10^{-1}	1.40
5.6×10^{-2}	2.14×10^{-2}	3.26×10^{-2}	4.0×10	6.04×10^{-1}	1.40
1.1×10^{-1}	3.57×10^{-2}	5.50×10^{-2}	4.3×10	6.31×10^{-1}	1.40
1.6×10^{-1}	4.64×10^{-2}	6.88×10^{-2}	5.0×10	5.99×10^{-1}	1.43
1.6×10^{-1}	4.80×10^{-2}	7.70×10^{-2}	6.3×10	5.88×10^{-1}	1.50
1.9×10^{-1}	6.14×10^{-2}	8.10×10^{-2}	6.3×10	6.04×10^{-1}	1.47
3.2×10^{-1}	9.02×10^{-2}	1.53×10^{-1}	7.8×10	6.05×10^{-1}	1.46
5.2×10^{-1}	1.39×10^{-1}	2.38×10^{-1}	8.1×10	5.96×10^{-1}	1.51
7.3×10^{-1}	1.94×10^{-1}	3.39×10^{-1}	1.01×10^{2}	6.09×10^{-1}	1.53
9.5×10^{-1}	2.51×10^{-1}	4.09×10^{-1}	1.03×10^{2}	6.07×10^{-1}	1.52
1.1	2.33×10^{-1}	4.03×10^{-1}	1.27×10^{2}	5.96×10^{-1}	1.56
1.4	2.73×10^{-1}	5.62×10^{-1}	1.65×10^{2}	6.04×10^{-1}	1.53
2.1	3.77×10^{-1}	6.62×10^{-1}	2.04×10^{2}	6.31×10^{-1}	1.54
3.2	4.43×10^{-1}	8.12×10^{-1}	2.52×10^{2}	5.80×10^{-1}	1.53
3.5	4.25×10^{-1}	7.81×10^{-1}	2.90×10^{2}	6.09×10^{-1}	1.53
4.3	4.86×10^{-1}	8.85×10^{-1}			

TABLE 2

Fluorescent Intensity Ratios Induced by Potassium-Neon Collisions

Neon Pressure (torr)	η_1 I_1/I_2	η_2 I_2/I_1	Neon Pressure (torr)	η_1 I_1/I_2	η_2 I_2/I_1
1.2×10^{-2}	8.79×10^{-4}	1.60×10^{-3}	4.3	1.32×10^{-1}	2.29×10^{-1}
4.0×10^{-2}	1.77×10^{-3}	3.82×10^{-3}	4.7	1.52×10^{-1}	2.62×10^{-1}
5.0×10^{-2}	3.18×10^{-3}	4.88×10^{-3}	7.5	2.04×10^{-1}	3.88×10^{-1}
7.8×10^{-2}	4.83×10^{-3}	6.28×10^{-3}	1.0×10	2.39×10^{-1}	4.48×10^{-1}
1.0×10^{-1}	5.10×10^{-3}	8.19×10^{-3}	1.4×10	2.92×10^{-1}	5.77×10^{-1}
1.04×10^{-1}	5.06×10^{-3}	8.02×10^{-3}	1.7×10	3.13×10^{-1}	6.33×10^{-1}
1.32×10^{-1}	6.28×10^{-3}	8.89×10^{-3}	2.6×10	3.74×10^{-1}	7.73×10^{-1}
1.60×10^{-1}	8.38×10^{-3}	1.08×10^{-2}	3.4×10	4.12×10^{-1}	8.54×10^{-1}
1.75×10^{-1}	8.57×10^{-3}	1.37×10^{-2}	4.3×10	4.21×10^{-1}	9.71×10^{-1}
2.05×10^{-1}	9.28×10^{-3}	1.38×10^{-2}	5.5×10	4.51×10^{-1}	1.00
2.40×10^{-1}	1.18×10^{-2}	1.68×10^{-2}	6.3×10	4.64×10^{-1}	1.05
2.50×10^{-1}	1.27×10^{-2}	1.84×10^{-2}	9.1×10	4.86×10^{-1}	1.13
2.60×10^{-1}	1.27×10^{-2}	1.75×10^{-2}	1.23×10^{2}	5.08×10^{-1}	1.23
2.7×10^{-1}	1.13×10^{-2}	1.96×10^{-2}	1.56×10^{2}	5.49×10^{-1}	1.27
3.0×10^{-1}	1.31×10^{-2}	1.90×10^{-2}	1.92×10^{2}	5.25×10^{-1}	1.32
3.2×10^{-1}	1.37×10^{-2}	2.12×10^{-2}	2.24×10^{2}	5.50×10^{-1}	1.36
3.6×10^{-1}	1.66×10^{-2}	2.17×10^{-2}	2.54×10^{2}	5.40×10^{-1}	1.32
4.0×10^{-1}	1.98×10^{-2}	3.08×10^{-2}	2.90×10^{2}	5.58×10^{-1}	1.39
1.1	4.45×10^{-2}	8.00×10^{-2}	3.23×10^{2}	5.62×10^{-1}	1.40
1.9	7.78×10^{-2}	1.26×10^{-1}	3.65×10^{2}	6.00×10^{-1}	1.41

TABLE 3

Fluorescent Intensity Ratios Induced by Potassium-Argon Collisions

Argon Pressure (torr)	η_1 I_1/I_2	η_2 I_2/I_1	Argon Pressure (torr)	η_1 I_1/I_2	η_2 I_2/I_1
3.35×10^{-2}	3.78×10^{-3}	5.63×10^{-3}	2.08×10	4.08×10^{-1}	8.33×10^{-1}
5.80×10^{-2}	6.65×10^{-3}	9.69×10^{-3}	2.46×10	4.34×10^{-1}	8.87×10^{-1}
7.20×10^{-2}	6.74×10^{-3}	1.21×10^{-2}	3.00×10	4.49×10^{-1}	1.00
1.07×10^{-1}	1.06×10^{-2}	1.65×10^{-2}	4.2×10	4.92×10^{-1}	1.10
1.3×10^{-1}	1.24×10^{-2}	2.02×10^{-2}	5.5×10	5.00×10^{-1}	1.18
1.6×10^{-1}	1.52×10^{-2}	2.42×10^{-2}	6.1×10	5.22×10^{-1}	1.20
1.6×10^{-1}	1.38×10^{-2}	2.42×10^{-2}	7.1×10	5.15×10^{-1}	1.28
1.9×10^{-1}	1.57×10^{-2}	2.78×10^{-2}	9.6×10	5.30×10^{-1}	1.33
2.1×10^{-1}	1.94×10^{-2}	3.08×10^{-2}	1.25×10^{2}	5.69×10^{-1}	1.37
2.4×10^{-1}	2.04×10^{-2}	3.80×10^{-2}	1.44×10^{2}	5.53×10^{-1}	1.39
5.7×10^{-1}	6.05×10^{-2}	1.03×10^{-1}	1.50×10^{2}	5.86×10^{-1}	1.39
1.0	7.87×10^{-2}	1.26×10^{-1}	1.77×10^{2}	5.77×10^{-1}	1.44
2.1	1.40×10^{-1}	2.55×10^{-1}	1.88×10^{2}	5.61×10^{-1}	1.37
3.2	1.83×10^{-1}	3.18×10^{-1}	2.00×10^{2}	6.04×10^{-1}	1.51
4.6	2.36×10^{-1}	4.15×10^{-1}	2.30×10^{2}	5.70×10^{-1}	1.44
5.5	2.53×10^{-1}	4.47×10^{-1}	2.50×10^{2}	5.87×10^{-1}	1.47
8.0	3.07×10^{-1}	6.00×10^{-1}	2.53×10^{2}	5.85×10^{-1}	1.40
9.6	3.27×10^{-1}	6.56×10^{-1}	2.94×10^{2}	5.96×10^{-1}	1.50
1.11×10	3.54×10^{-1}	7.33×10^{-1}	3.00×10^{2}	5.87×10^{-1}	1.48
1.30×10	3.78×10^{-1}	7.51×10^{-1}	3.44×10^{2}	5.86×10^{-1}	1.45
1.50×10	3.80×10^{-1}	7.96×10^{-1}	3.50×10^{2}	5.93×10^{-1}	1.46
1.80×10	4.45×10^{-1}	8.89×10^{-1}			

TABLE 4

Fluorescent Intensity Ratios Induced by Potassium-Krypton Collisions

Krypton Pressure (torr)	η_1 I_1/I_2	η_2 I_2/I_1	Krypton Pressure (torr)	η_1 I_1/I_2	η_2 I_2/I_1
0.00	1.21×10^{-3}	1.13×10^{-3}	1.43×10	4.30×10^{-1}	9.01×10^{-1}
1.0×10^{-2}	2.63×10^{-3}	3.48×10^{-3}	2.0×10	4.62×10^{-1}	9.69×10^{-1}
2.5×10^{-2}	4.95×10^{-3}	7.19×10^{-3}	2.8×10	4.76×10^{-1}	1.08
3.4×10^{-2}	6.05×10^{-3}	9.35×10^{-3}	3.6×10	5.30×10^{-1}	1.15
3.8×10^{-2}	7.66×10^{-3}	1.05×10^{-2}	5.1×10	5.54×10^{-1}	1.23
5.0×10^{-2}	---	1.32×10^{-2}	6.1×10	5.53×10^{-1}	1.26
6.0×10^{-2}	1.07×10^{-2}	1.47×10^{-2}	7.3×10	5.62×10^{-1}	1.32
7.8×10^{-2}	1.18×10^{-2}	1.90×10^{-2}	8.5×10	5.56×10^{-1}	1.29
8.0×10^{-2}	1.41×10^{-2}	1.76×10^{-2}	9.1×10	5.60×10^{-1}	1.30
9.0×10^{-2}	1.37×10^{-2}	2.24×10^{-2}	9.5×10	5.65×10^{-1}	1.39
1.1×10^{-1}	1.73×10^{-2}	2.45×10^{-2}	1.12×10^{2}	5.72×10^{-1}	1.39
1.35×10^{-1}	2.17×10^{-2}	3.08×10^{-2}	1.31×10^{2}	5.75×10^{-1}	1.41
1.4×10^{-1}	2.12×10^{-2}	3.19×10^{-2}	1.53×10^{2}	5.69×10^{-1}	1.45
1.6×10^{-1}	2.46×10^{-2}	3.70×10^{-2}	1.88×10^{2}	5.90×10^{-1}	1.47
1.9×10^{-1}	3.11×10^{-2}	4.03×10^{-2}	2.06×10^{2}	5.82×10^{-1}	1.45
1.9	1.58×10^{-1}	2.86×10^{-1}	2.27×10^{2}	5.76×10^{-1}	1.48
4.5	2.61×10^{-1}	4.86×10^{-1}	2.62×10^{2}	5.60×10^{-1}	1.48
7.5	3.38×10^{-1}	6.41×10^{-1}	3.00×10^{2}	5.79×10^{-1}	1.45
9.9	3.57×10^{-1}	7.39×10^{-1}	3.33×10^{2}	5.77×10^{-1}	1.50

TABLE 5

Fluorescent Intensity Ratios Induced by Potassium-Xenon Collisions

Xenon Pressure (torr)	η_1 I_1/I_2	η_2 I_2/I_1	Xenon Pressure (torr)	η_1 I_1/I_2	η_2 I_2/I_1
1.95×10^{-2}	5.45×10^{-3}	8.13×10^{-3}	2.4	2.76×10^{-1}	5.23×10^{-1}
3.4×10^{-2}	8.85×10^{-3}	1.26×10^{-2}	3.3	3.18×10^{-1}	5.37×10^{-1}
4.6×10^{-2}	1.26×10^{-2}	1.69×10^{-2}	3.8	3.23×10^{-1}	6.32×10^{-1}
6.1×10^{-2}	1.55×10^{-2}	2.21×10^{-2}	5.4	4.02×10^{-1}	7.06×10^{-1}
8.2×10^{-2}	1.93×10^{-2}	2.82×10^{-2}	5.9	4.00×10^{-1}	7.68×10^{-1}
1.0×10^{-1}	2.51×10^{-2}	3.65×10^{-2}	5.9	4.03×10^{-1}	6.72×10^{-1}
1.08×10^{-1}	2.75×10^{-2}	3.93×10^{-2}	9.0	4.37×10^{-1}	9.08×10^{-1}
1.1×10^{-1}	2.33×10^{-2}	4.00×10^{-2}	1.06×10	4.77×10^{-1}	7.32×10^{-1}
1.15×10^{-1}	2.83×10^{-2}	4.09×10^{-2}	1.08×10	4.31×10^{-1}	9.09×10^{-1}
1.2×10^{-1}	2.96×10^{-2}	4.25×10^{-2}	1.25×10	4.81×10^{-1}	9.82×10^{-1}
1.35×10^{-1}	3.22×10^{-2}	4.80×10^{-2}	1.55×10	5.21×10^{-1}	1.05
1.5×10^{-1}	3.67×10^{-2}	5.27×10^{-2}	1.62×10	5.00×10^{-1}	1.07
1.7×10^{-1}	4.22×10^{-2}	6.04×10^{-2}	1.81×10	4.92×10^{-1}	1.09
2.55×10^{-1}	5.82×10^{-2}	8.40×10^{-2}	2.46×10	5.51×10^{-1}	1.16
3.7×10^{-1}	5.88×10^{-2}	9.63×10^{-2}	2.53×10	5.26×10^{-1}	1.22
5.2×10^{-1}	9.29×10^{-2}	1.45×10^{-1}	3.0×10	5.23×10^{-1}	1.25
5.5×10^{-1}	9.36×10^{-2}	1.43×10^{-1}	3.1×10	5.71×10^{-1}	1.20
7.5×10^{-1}	1.41×10^{-1}	2.03×10^{-1}	4.1×10	5.63×10^{-1}	1.36
7.5×10^{-1}	1.12×10^{-1}	1.96×10^{-1}	4.2×10	5.84×10^{-1}	1.27
8.5×10^{-1}	1.31×10^{-1}	2.25×10^{-1}	4.8×10	5.55×10^{-1}	1.35
9.0×10^{-1}	1.54×10^{-1}	2.44×10^{-1}	6.1×10	5.98×10^{-1}	1.35
1.3	1.81×10^{-1}	3.08×10^{-1}	6.2×10	5.64×10^{-1}	1.38
1.8	2.30×10^{-1}	4.18×10^{-1}	7.4×10	6.02×10^{-1}	1.36

. . . continued

Table 5 - Potassium-Xenon Collisions (cont'd)

Xenon Pressure (torr)	η_1 I_1/I_2	η_2 I_2/I_1	Xenon Pressure (torr)	η_1 I_1/I_2	η_2 I_2/I_1
8.3×10	5.79×10^{-1}	1.50	1.56×10^{2}	6.00×10^{-1}	1.45
8.4×10	6.04×10^{-1}	1.38	1.72×10^{2}	5.89×10^{-1}	1.45
9.7×10	6.01×10^{-1}	1.40	1.82×10^{2}	5.80×10^{-1}	1.52
1.03×10^{2}	5.64×10^{-1}	1.43	1.91×10^{2}	5.99×10^{-1}	1.46
1.19×10^{2}	6.02×10^{-1}	1.41	2.16×10^{2}	5.93×10^{-1}	1.48
1.27×10^{2}	6.00×10^{-1}	1.46	2.21×10^{2}	5.73×10^{-1}	1.44
1.40×10^{2}	5.95×10^{-1}	1.46	2.43×10^{2}	5.76×10^{-1}	1.42
1.40×10^{2}	5.89×10^{-1}	1.50			

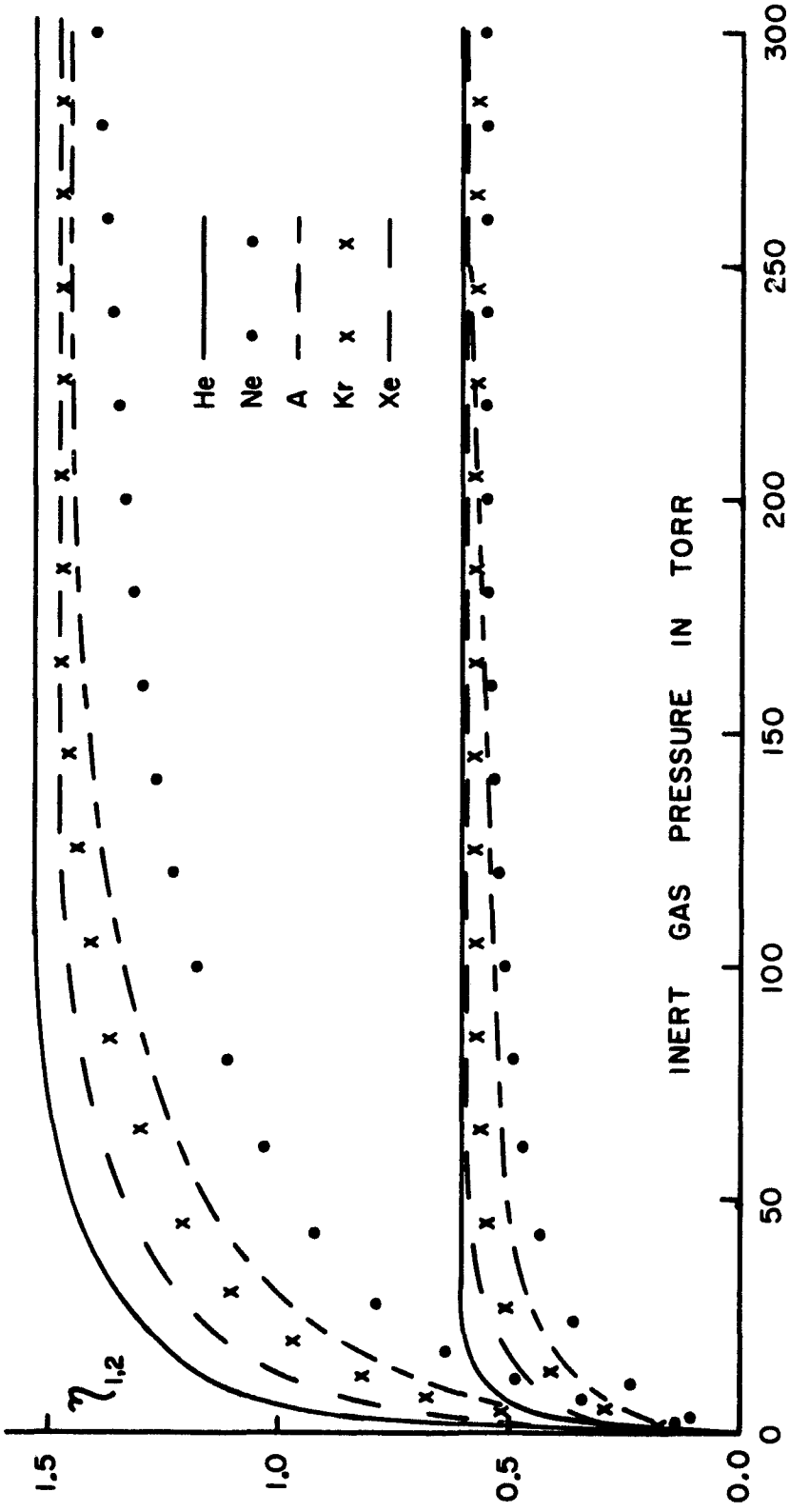

Fig. 10. Intensity Ratios in Potassium-Inert Gas Mixtures

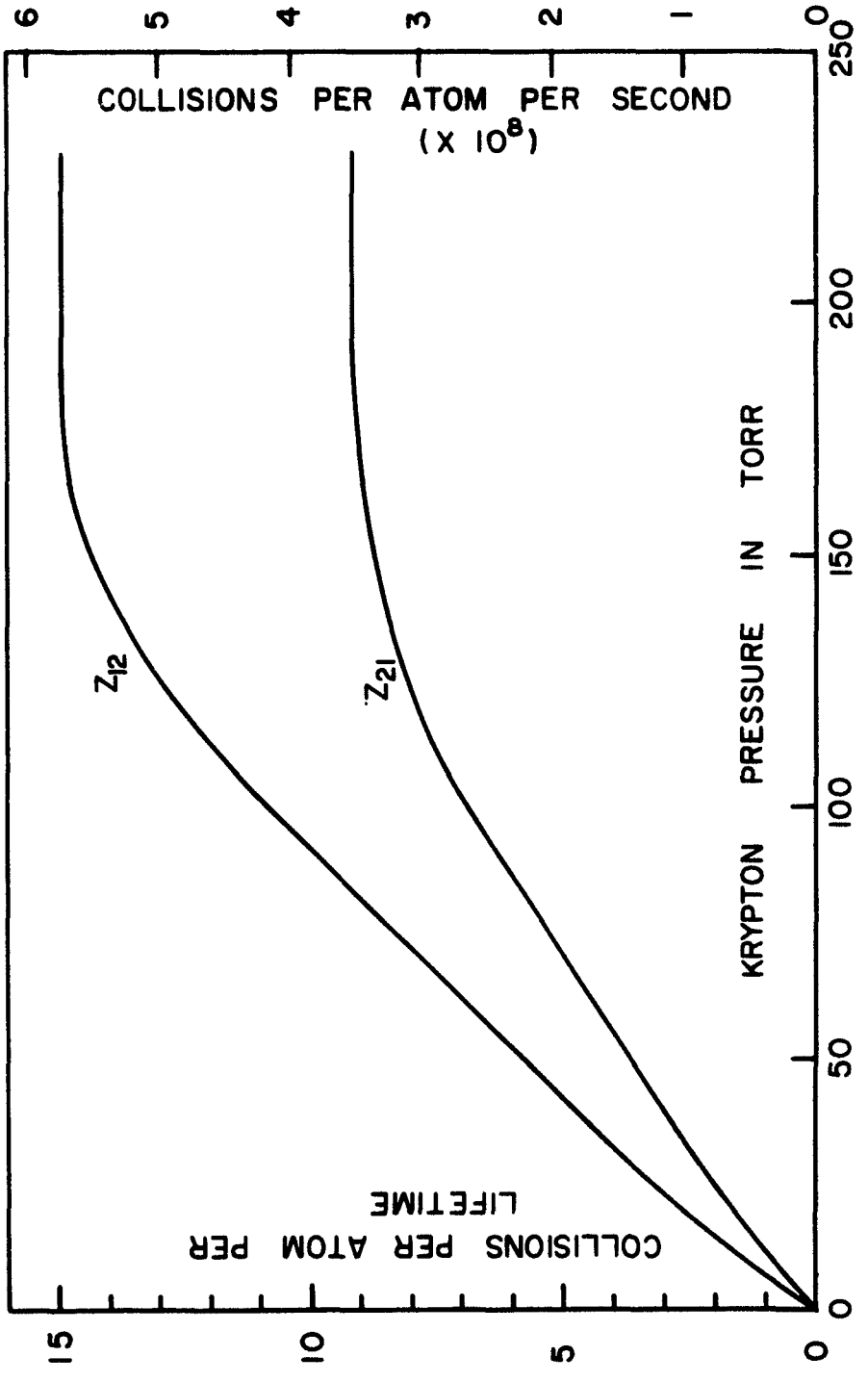

Fig. 11. The Variation of Potassium-Krypton Collision Numbers with Krypton Pressure

η values obtained at very low gas pressures, and under single-collision conditions, are shown in figures 12-16. When $\eta \ll 1$, equations (8) and (9) reduce to the form $Z = \eta/\gamma$. As expected, the plots in this region are linear and pass through the origin; their slopes, substituted into equation (10), yielded the collision cross sections which are listed in table 6 along with their ratios Q_{12}/Q_{21} which, according to equation (13), should equal 1.60. The tabulated cross sections and experimental errors were obtained from least-squares analyses of the collision number curves in the low pressure regions. The values obtained in this way agree with the cross sections and errors obtained in a point-by-point calculation based on the individual values of η_1 and η_2.

The cross sections measured under single collision conditions are considered to be more reliable than those obtained at higher gas pressures. Other processes, such as quenching, collisional stimulation of emission and pressure broadening may compete with the inelastic collision processes. The effective cross sections for these competing processes are expected to be smaller than the inelastic cross section, but their exact values are unknown. By measuring the inelastic cross sections under single collision conditions (usually less than one interaction per hundred mean lifetimes), it becomes extremely unlikely that any atom which has engaged in an inelastic collision will have also undergone any other type of collisional process during the lifetime of the excited state.

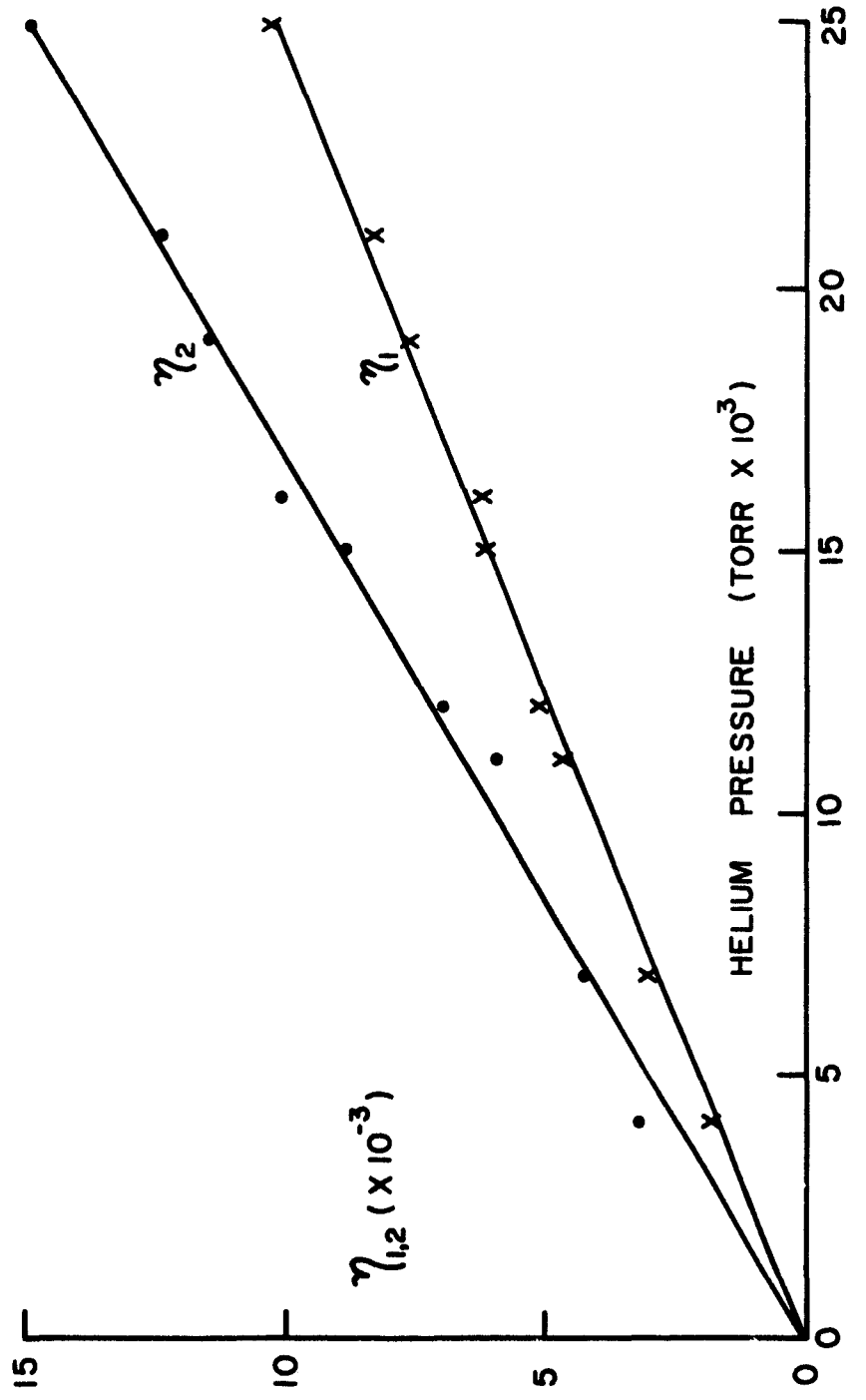

Fig. 12. Intensity Ratios in a Potassium-Helium Mixture Under Single Collision Conditions

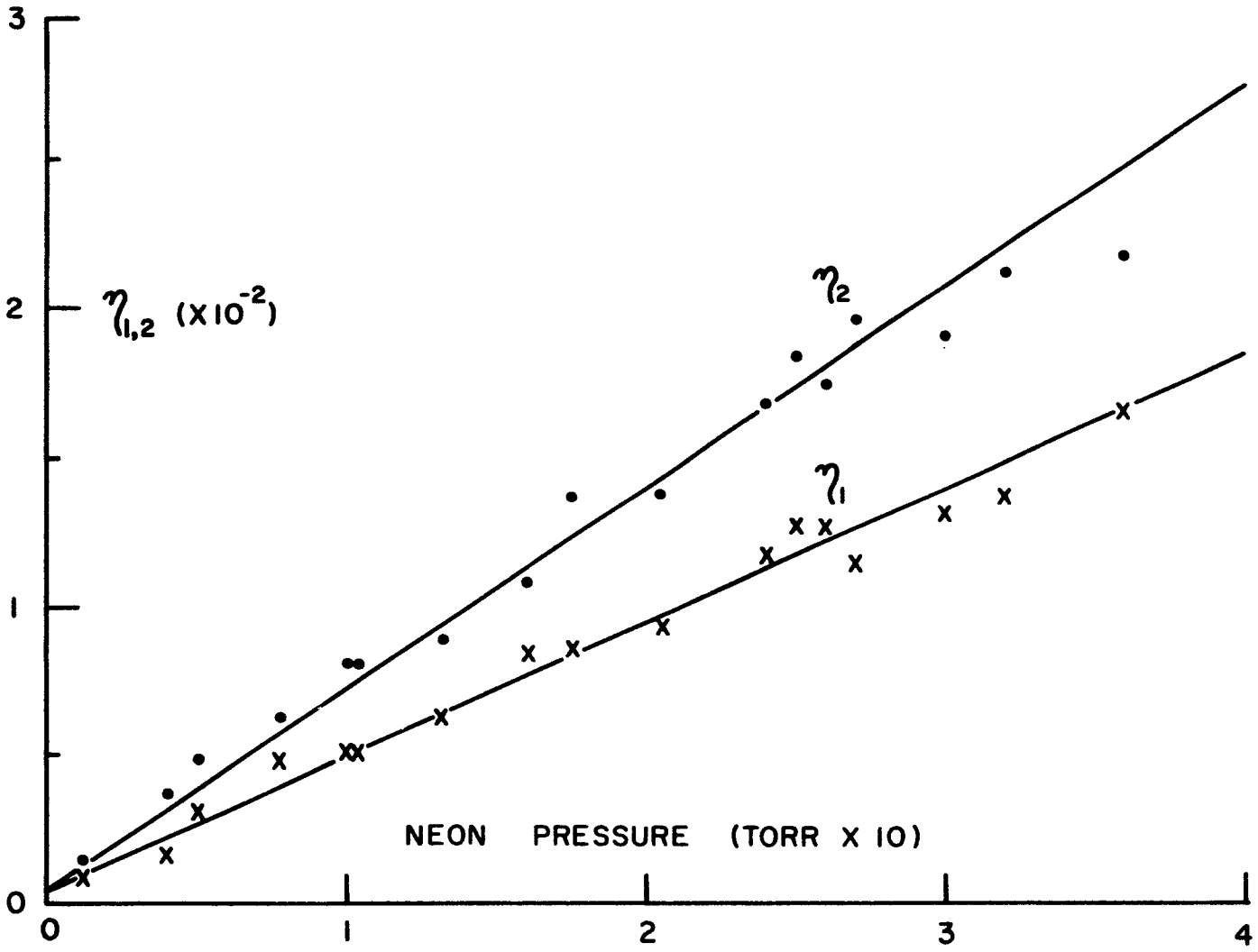

Fig. 13. Intensity Ratios in a Potassium-Neon Mixture Under Single Collision Conditions

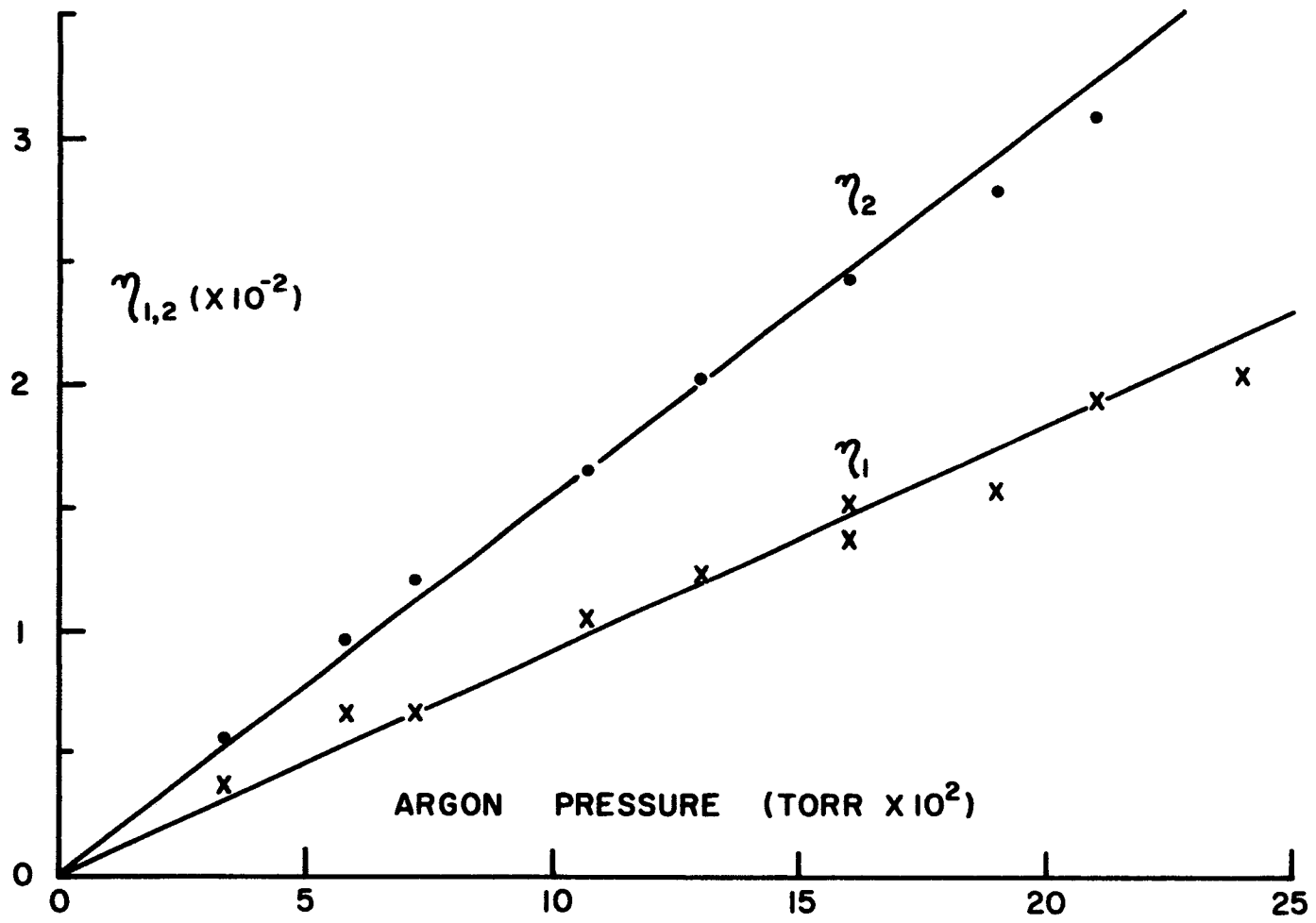

Fig. 14. Intensity Ratios in a Potassium-Argon Mixture Under Single Collision Conditions

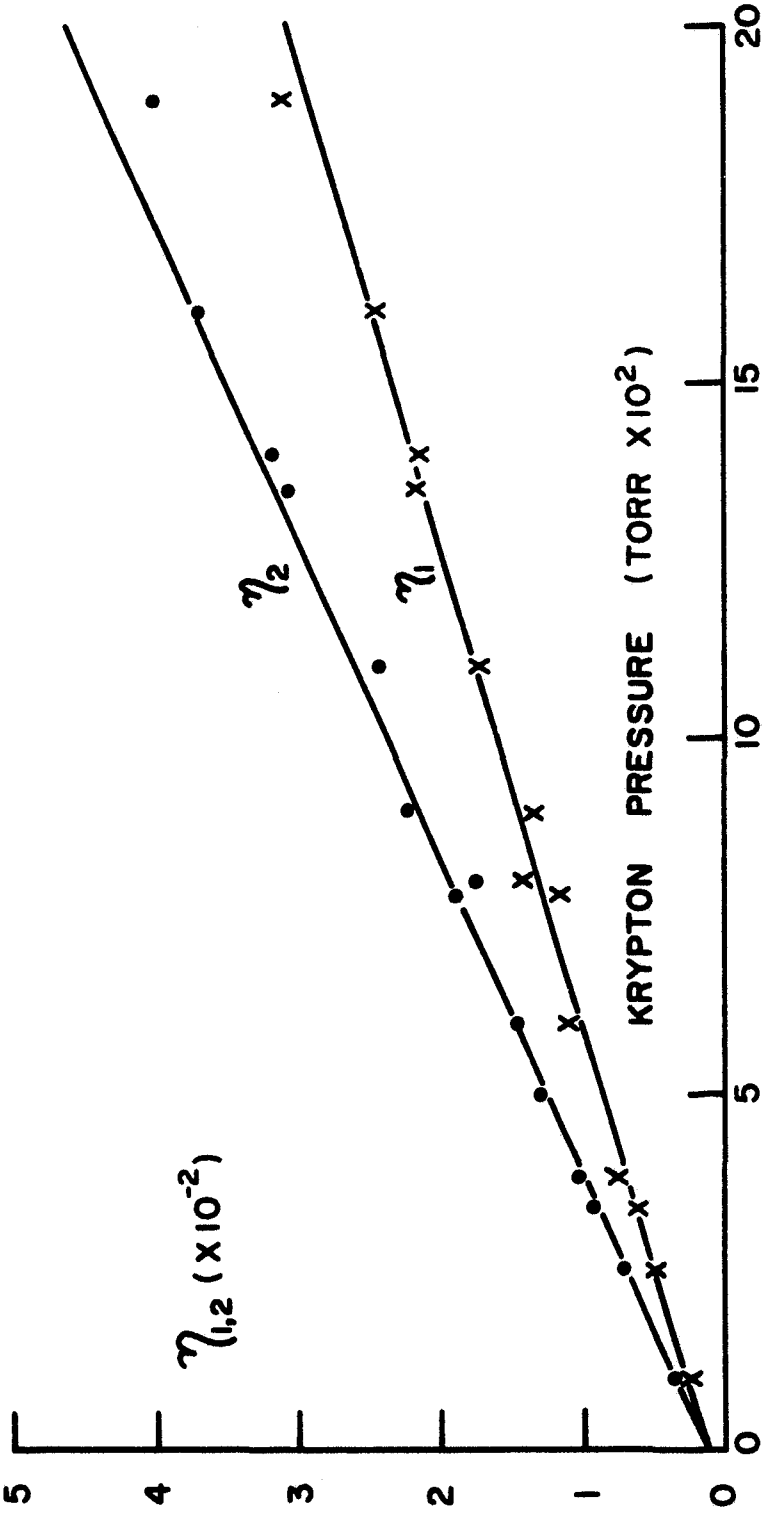

Fig. 15. Intensity Ratios in a Potassium-Krypton Mixture Under Single Collision Conditions

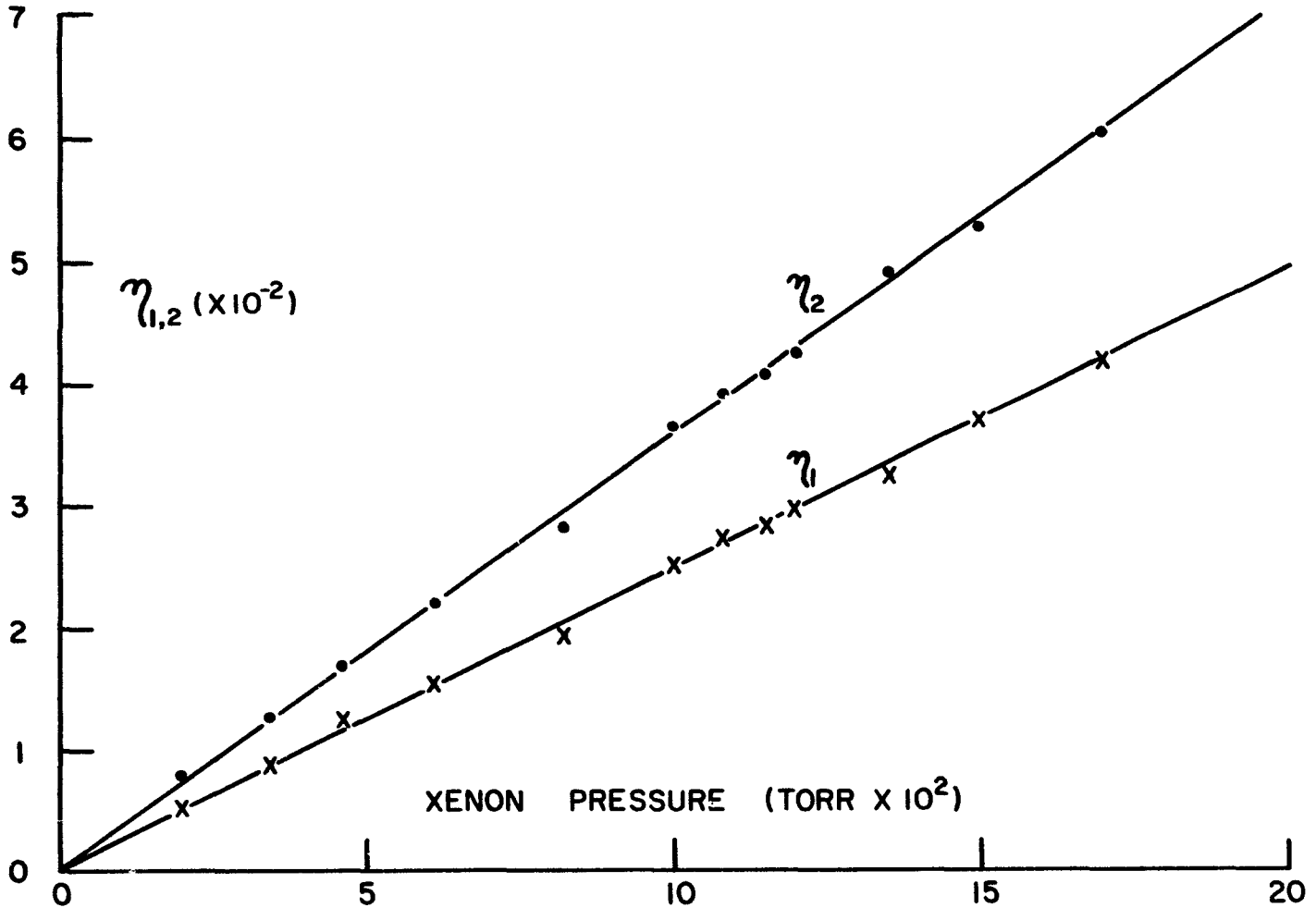

Fig. 16. Intensity Ratios in a Potassium-Xenon Mixture Under Single Collision Conditions

TABLE 6

Cross Sections for Potassium-Inert Gas Collisions from Various Sources

Collision Partners	Polarizability of Inert Gas Å^3	Source	Q_{12} $^2P_{1/2} \rightarrow {}^2P_{3/2}$ Å^2	Q_{21} $^2P_{1/2} \leftarrow {}^2P_{3/2}$ Å^2	Q_{12}/Q_{21}
K-He	0.206	This investigation	59.5 ± 1.5	40.8 ± 2.1	1.46 ± 0.12
		Jordan (exp)		52.8 ± 5.8	
		Jordan (theo)		36.2 ± 9.0	
		Callaway (theo)	49	25	
K-Ne	0.408	This investigation	14.3 ± 1.3	9.45 ± 0.68	1.51 ± 0.25
		Jordan (exp)		14.0 ± 1.2	
		Jordan (theo)		40.5 ± 10.0	
K-A	1.64	This investigation	36.7 ± 1.4	22.4 ± 1.6	1.64 ± 0.18
		Jordan (exp)		34.0 ± 3.1	
		Jordan (theo)		91.0 ± 40.0	
		Callaway (theo)	78	78	
K-Kr	2.48	This investigation	61.4 ± 2.6	40.7 ± 1.8	1.51 ± 0.12
K-Xe	4.02	This investigation	104 ± 2	72.3 ± 2.2	1.44 ± 0.07

It may be seen that the cross sections for collisions of potassium with helium, neon and argon are about 30% lower than those quoted by Jordan and that the agreement with Callaway and Bauer's calculations for helium and argon is not particularly good. The ratio of the cross sections Q_{21}/Q_{12} is in good agreement with that predicted by the principle of detailed balancing (equation (13)) for all the potassium-inert gas mixtures with the exception of potassium-xenon, where it is about 6% low.

The relatively high value for the potassium-helium cross section is not expected on the basis of most current theories[1,2]; the cross sections should increase monotonically from helium to xenon as the polarizability increases. The shapes of the collision number curves also do not conform to expectations. These two features as well as the low Z_{12}/Z_{21} ratio in the case of xenon are sufficiently important to warrant more detailed discussion.

(ii) The Variation of the Cross Sections from K-He to K-Xe

The magnitudes of the inelastic cross sections given in table 6 do not increase monotonically with polarizability from helium to xenon, as would be expected if the atomic interactions were attributable solely to van der Waals or quadrupole-induced dipole forces[1]: there is, instead, a pronounced minimum at neon. Similar behaviour has been observed in the metal-inert gas systems of caesium[26] and rubidium[28].

It may be argued that since we are observing an effective or average cross section, the high value for the

potassium-helium cross section may be due to the magnitude of the helium thermal velocity; the velocities of the remaining four inert gases do not differ radically from one another. If, however, we use the v^2 velocity dependence of the cross sections quoted by Callaway and Bauer[2] as the most probable, and carry out the thermal averaging given by equation (12), the differential cross sections q(v) still exhibit a pronounced minimum at neon. This is also true of an assumed linear dependence on velocity and of v^3 dependence. It would seem, then, that the large helium cross section is not entirely due to the velocity dependence of the interaction, or that the velocity dependence is much stronger than has been assumed.

Jefimenko[36] recently proposed a semi-classical theory of atomic interactions which he applied to the study of satellite bands in mixtures of alkali metals with inert gases or hydrocarbons[39,40]. The interaction is considered to be taking place between the valence electron of the alkali metal, which acts as a free particle moving with its orbital velocity, and the inert gas atom. If the electron penetrates the outer electron shell of the inert gas atom, overlap forces come into play. If the foreign gas atom is small enough to be completely contained within the orbital radius of the alkali valence electron, an inclusion molecule may be formed for a short period of time. The approach of Jefimenko parallels that employed by Fermi[37] in his treatment of high order spectral line broadening and shift.

The connection between the inelastic cross sections given in table 6 and the overlap forces may be determined by

comparing these cross sections with the total scattering cross sections for electrons with inert gases, where the electrons are assigned velocities equal to that of the $4^2P_{3/2}$ orbital electron in potassium. After the method of Jefimenko, using the ground state radius of the potassium atom given by Whalley and Schneider[48], this velocity was found to have the value of 0.64 $(eV)^{1/2}$, at which the Ramsauer-Townsend effect is observed in argon, krypton and xenon; at velocities corresponding to about 1 eV these gases are very transparent to electrons. The average electron scattering cross sections obtained by several observers may be found in Massey and Burhop.[49] These cross sections are plotted, together with the inelastic c oss sections from table 6, in figure 17 against the atomic numbers of the inert gases, which serve as a convenient index. The similarity between the two curves is unmistakeable. For all of the inert gases, the inelastic cross section is just one order of magnitude larger than the total cross section for electrons.

On the basis of this semi-classical model it is expected that, as the diameter of the gas atoms decreases from xenon to helium, the influence of the overlap forces will increase. This is due to the fact that deeper penetration of the outer electron shells of the inert gas atoms by the potassium valence electron is possible. If the outer shell of the gas atom is penetrated, the shielding of the nuclear field will decrease as the number of the remaining electrons in deeper lying shells decreases. In the case of

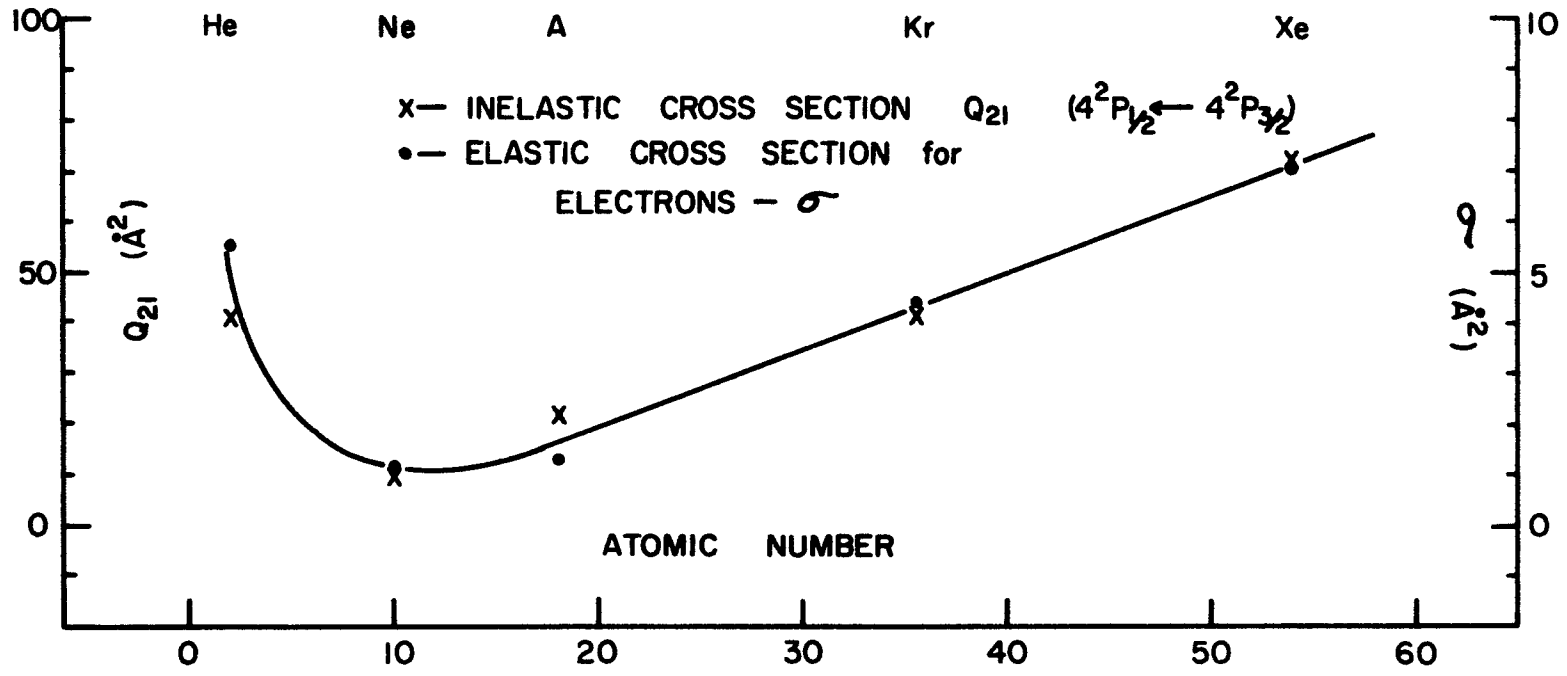

Fig. 17. A Comparative Plot of Q_{21} $(^2P_{1/2} \leftarrow {}^2P_{3/2})$ and the Elastic Cross Sections for Electrons Whose Velocities Equal that of the $4^2P_{3/2}$ Valence Electron

helium, the potassium electron is exposed to the coulomb field of the nucleus, not shielded by any complete electron shell. According to Jefimenko, point charge-induced dipole forces may be important in this case.

The evidence of figure 17 indicates that the effect of the free electron interaction or overlap forces must be taken into account in order to explain the progression of cross sections. Since however the inelastic cross sections are an order of magnitude larger than the total cross sections for electrons, overlap forces must be only partly responsible for the interaction. The remaining interaction energy may be ascribed to van der Waals or other atomic interaction forces. Similar agreement has been demonstrated between the electron scattering cross sections and the inelastic atomic cross sections in mixtures of rubidium[28] and cesium[26] with the inert gases.

(iii) Effects Contributing to the Behaviour of the Z-P Curves

The Z-P curves for all the inert gases at low pressures are linear and pass through the origin. However, as the gas pressure is increased to about one torr, they acquire a negative curvature and, in all cases, again become linear between about 20 and 150 torr. As may be seen in figure 11, the curves then flatten out and the systems saturate as the collision numbers become independent of the inert gas pressures.

Throughout the experimental range of pressures, the ratio of the collision numbers Z_{12}/Z_{21} has the value predicted by the principle of detailed balancing, with the exception of xenon for which the ratio is slightly low. It should also be

noted that, with all the gases, saturation occurs at pressures at which the potassium is undergoing at most 33 collisions per lifetime, (γZ), which is a value much lower than should be expected. Table 7 shows the saturation values of η_1, η_2, Z_{12} and Z_{21} for all the inert gases. The ratios Z_{12}/Z_{21} were obtained from a point-by-point calculation based on all the η values (40 to 60 points for each gas).

It is usually assumed that the duration, t_o, of the collision complex is of the order of one molecular vibration period, about 10^{-12} seconds.[3] Using the values of the cross sections listed in table 6 in the following classical relationship,

$$t_o = \frac{2}{v_r}\left(\frac{Q}{\pi}\right)^{1/2},$$

the average value of t_o for all inelastic collisions is found to be 1.7×10^{-12} seconds, in good agreement with the above assumption. The systems should begin to saturate when the time between the collisions is about as long as the duration of a collision and three body collisions become probable. This should occur, on the basis of the experimental estimate of t_o quoted above, when γZ reaches the value of about 10^3. Using this value in equations (8) and (9) clearly shows that at this point $\eta_1 = 1/\eta_2$. This conclusion, which follows directly from the experimental values of the collision cross sections, is consistent with the theoretical limits for the intensity ratios. The values for η and γZ listed in table 7 fulfill neither of these predictions.

TABLE 7

Saturation Parameters for the Mixing of the $4^2P_{1/2}$ and $4^2P_{3/2}$ States in Potassium

Collision Partners	Saturation Pressure (torr)	η_1	η_2	γz_{12} Collisions per Lifetime	γz_{21} Collisions per Lifetime	z_{12}/z_{21}
K-He	100	0.605	1.53	33	21	1.53 ± 0.07
K-Ne	380	0.600	1.41	15	9.4	1.56 ± 0.07
K-A	230	0.590	1.45	16	10	1.60 ± 0.04
K-Kr	170	0.575	1.47	15	9.2	1.56 ± 0.06
K-Xe	120	0.590	1.47	18	11	1.53 ± 0.06
Theoretical For All Mixtures		0.625	1.60			1.60

There are several possible mechanisms which might explain the behaviour of the collision numbers: these include possible changes in the lifetime, t_o, of the quasi-molecular state, alteration in the interaction mechanism, changes in the velocity distribution of the colliding atoms and shortening of the lifetimes of the ^2P states in potassium. These various possibilities merit further discussion.

(a) Changes in the lifetime of the collision complex

If it is assumed that the lifetime, t_o, of the quasi-molecule increases with inert gas pressure or that there is a minimum time after one inelastic collision before the potassium atom can engage in a second such collision, then the phenomenon of saturation will occur at a lower pressure than that predicted above. Thus the maximum possible number of inelastic collisions per average lifetime of the excited potassium atoms will be decreased. If such were the case, then on the basis of the saturation $\tilde{\sigma}Z$ values given in table 7, the lifetime of the diatomic state would have to be about 10^{-9} seconds. This is roughly equal to the lifetime of a metastable molecule and is much too large to be consistent with the strength of the interatomic forces involved in these collisions; it is also clearly at variance with the interaction times obtained from the cross sections under single collision conditions. If the duration of the collisions were the problem, the true collision number Z' should be related to the observed collision numbers, Z, by an equation of the following form:

$$Z' = \frac{Z}{1 - t_o Z} \quad .$$

In no case do the observed data yield to such an analysis.

The formation of potassium-inert gas molecules independently of the inelastic collision process might also cause a decrease in the number of collisions per lifetime. However, this effect would also change the ratio Z_{12}/Z_{21} since the molecular dissociation energy would be absorbed from the kinetic energy continuum. No such change in the Boltzmann factor has been observed.

(b) Changes in the mechanism of interaction

As the inert gas pressure is raised, changes may occur in the mechanism of the inelastic collisions. Less efficient processes may dominate the collision number curves at higher pressures, as the selection rules for the various types of interactions (van der Waals, QID, etc.) become smeared out.[50] If cross sections are calculated from the slopes of the linear sections of the Z-P curves above 20 torr, they are found to be about 55% lower than the values obtained under single collision conditions for all the inert gases; this tends to support the change of mechanism hypothesis. Changes of mechanism with pressure, with any accompanying changes in the selection rules, are not expected to change the ratio of Z_{12}/Z_{21}, in agreement with the observed behaviour of the collision numbers. The possible effects of changes in the interaction mechanism must not be overlooked, but at the same time they cannot be entirely responsible for the observed behaviour of the

collision numbers.

(c) Changes in the velocity distribution function

The collision frequencies in the potassium-inert gas mixtures may also be changed by variations in the atomic velocity distributions. The velocity distribution may be changed by the inelastic collisions themselves. A collision which induces a $^2P_{1/2} \longrightarrow {}^2P_{3/2}$ transition at a temperature of 368^oK ($kT = 256\ cm^{-1}$) leaves the colliding pair of atoms with their kinetic energy of relative motion reduced by 22%; similarly, the reverse transition adds to the relative kinetic energy. Thus, immediately after an inelastic collision, the velocities of the colliding atoms are quite different from those predicted by Maxwell-Boltzmann statistics. However, the relaxation time for the restoration of equilibrium velocities is of the order of the elastic collision interval[51], and the elastic collision cross sections have been shown by Rothe and Bernstein[52] to be at least an order of magnitude larger than the inelastic cross sections given in table 6. In addition, the ratio Z_{12}/Z_{21} would be drastically altered by such large changes in kinetic energy; no significant deviation of this ratio from that predicted theoretically has been observed.

It has been demonstrated by Kummler and McCarty[53] that the variation of the intensity of the exciting line across the absorption line in a fluorescence spectrum will result in a non-Maxwellian velocity distribution of the excited atoms or molecules. If the centre of the absorption

line is appreciably displaced from the centre of the exciting line, or if the exciting line is strongly self reversed, then either fast or slow atoms may be selectively excited, leading to a non-equilibrium velocity distribution of the excited atoms. An exact analysis of this effect requires a detailed knowledge of the exciting and absorption line shapes, but is much simplified when, as in the present experiment, atoms are being excited by radiation generated by identical atoms.

Kummler and McCarty assumed in their calculation a Gaussian shape of the incident line and a Doppler-broadened profile of the atomic absorption line. These assumptions are reasonable in the low pressure region of the present experiment where it may be shown that the deviation from the Maxwellian velocity distribution ranges from 0% for helium to 3% for xenon.

In considering the experimental results, the change of collision frequency with inert gas pressure is of particular interest. Kummler and McCarty's theory predicts that only a pressure shift of the absorption line would produce such an effect. (For example the pressure shift due to argon amounts to 0.15 cm^{-1} at 300 torr.[54]) However, the very rapid thermal relaxation of the system ensures that only the first inelastic collision experienced by an excited atom has any probability of occurring under non-equilibrium velocity distribution. It follows that the corrections for changes in the velocity distribution need be made only under single collision conditions (below one torr), where they amount to

less than 3%. It would, therefore, seem that the behaviour of the collision numbers at high pressures can not be explained on the basis of changes in the velocity distribution of the atoms in the mixture.

(d) A decrease in the lifetime of the ^2P states in potassium

There are two processes which can decrease the lifetimes of the resonance states in potassium: quenching by the inert gases and stimulation of emission by atomic collisions. A quenching of the resonance radiation may be accomplished by transferring excitation energy to the inert gas atoms with subsequent reradiation, or by total conversion of the excitation energy into kinetic energy of relative motion. Either of these mechanisms must involve a decrease in the total fluorescent intensity of the potassium doublet. Because of the large energy interval between the ^2P states in potassium and the nearest excited states in the inert gases, quenching is most likely to proceed by the inefficient kinetic energy conversion mechanism.[29] The cross sections for quenching are expected to be very much smaller than those for inelastic collisions.

The quenching process, if it were detectable, would compete with the pressure broadening and shift of the resonance lines; pressure broadening tends to increase the total intensity over a wide range of pressure (up to 10 or 20 torr) by increasing the ability of the potassium atoms to absorb the relatively broad (0.15 cm^{-1}) exciting lines. The total intensity reaches a maximum and then begins to decrease as

the centre of the absorption line is shifted farther away from the centre of the exciting line. The variation in the total fluorescent intensity with pressure in mixtures of potassium with helium, krypton and xenon is shown in figures 18, 19 and 20 respectively. Typically, the intensity begins to fall at about 20 torr. All the gases exhibit a maximum in total fluorescent intensity at about 5 torr; the very pronounced peak in the case of helium might be connected with the fact that helium produces a violet shift in the resonance lines, while the other inert gases produce a red shift.[40] If any quenching of fluorescence is taking place, the cross section for the process must be very much smaller than the optical cross sections for the inert gases since the pressure broadening effect appears to dominate the total intensity curve.

Demtroder[55] studied helium pressure-induced changes in the lifetimes of the 3^2P states of sodium. He interpreted the results of his experiment in terms of the quenching of resonance radiation by helium and calculated a quenching cross section of 0.34 $\mathring{A}^2$. Stamper[56] undertook a theoretical analysis of the Na-He system and concluded that as long as the atoms remained free and neutral, collisions would be sufficiently adiabatic to make quenching practically impossible. It is likely then that Demtroder actually observed stimulated emission of resonance radiation by a collision process.

If it is assumed that the behaviour of the Z-P curves may be accounted for by a decrease in the mean lifetime of the

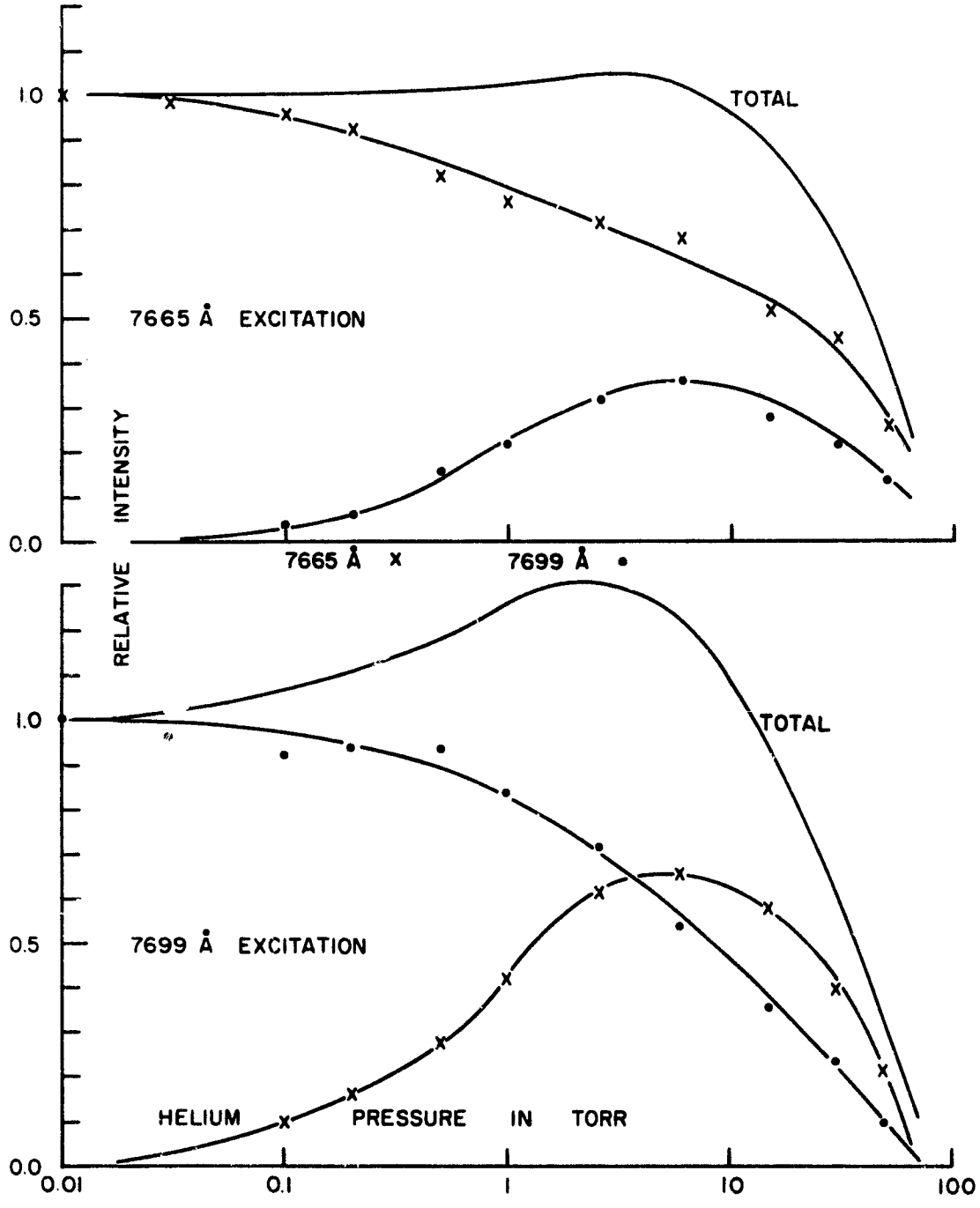

Fig. 18. Total Fluorescent Intensities in a Potassium-Helium Mixture

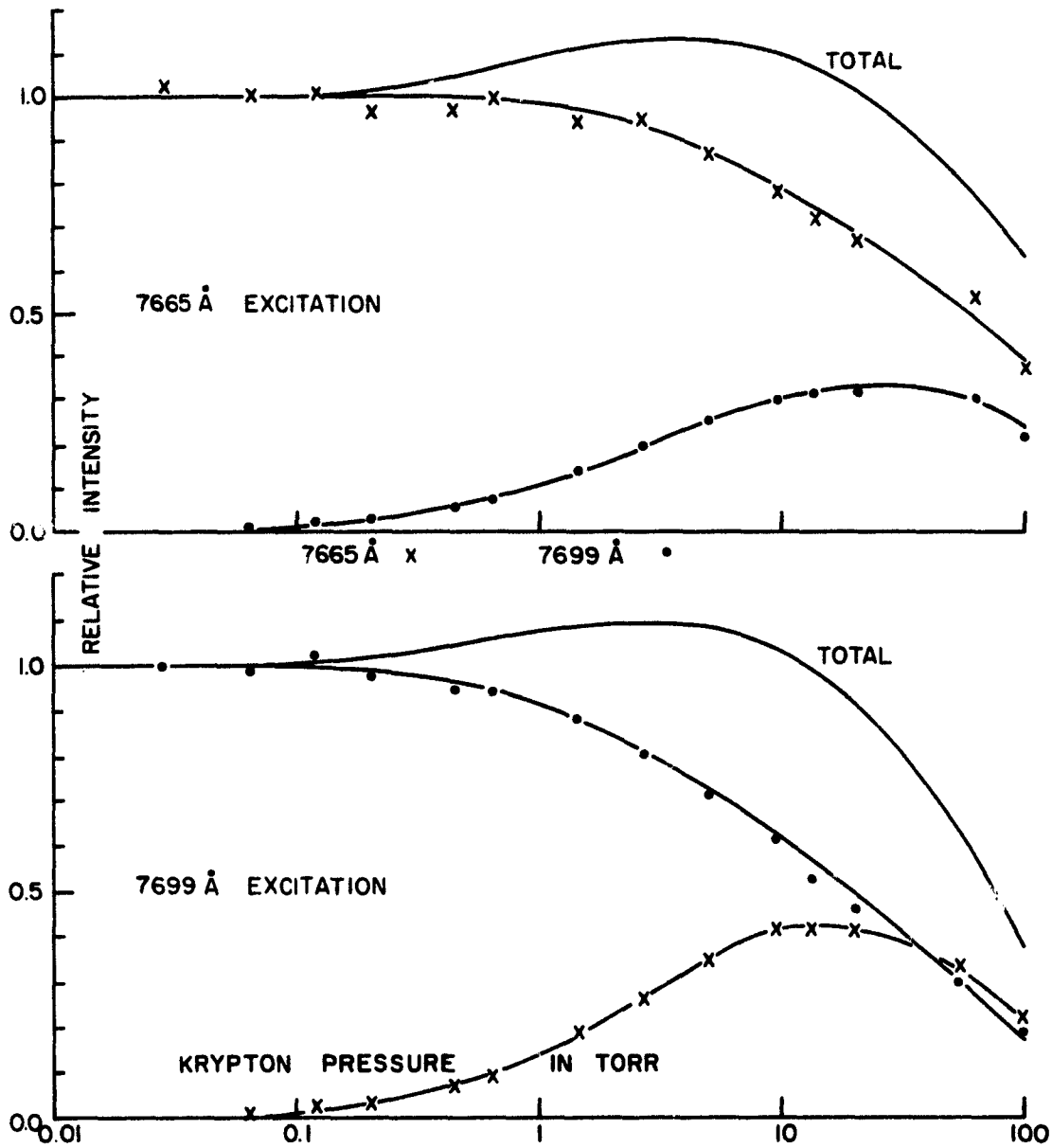

Fig. 19. Total Fluorescent Intensities in a Potassium-Krypton Mixture

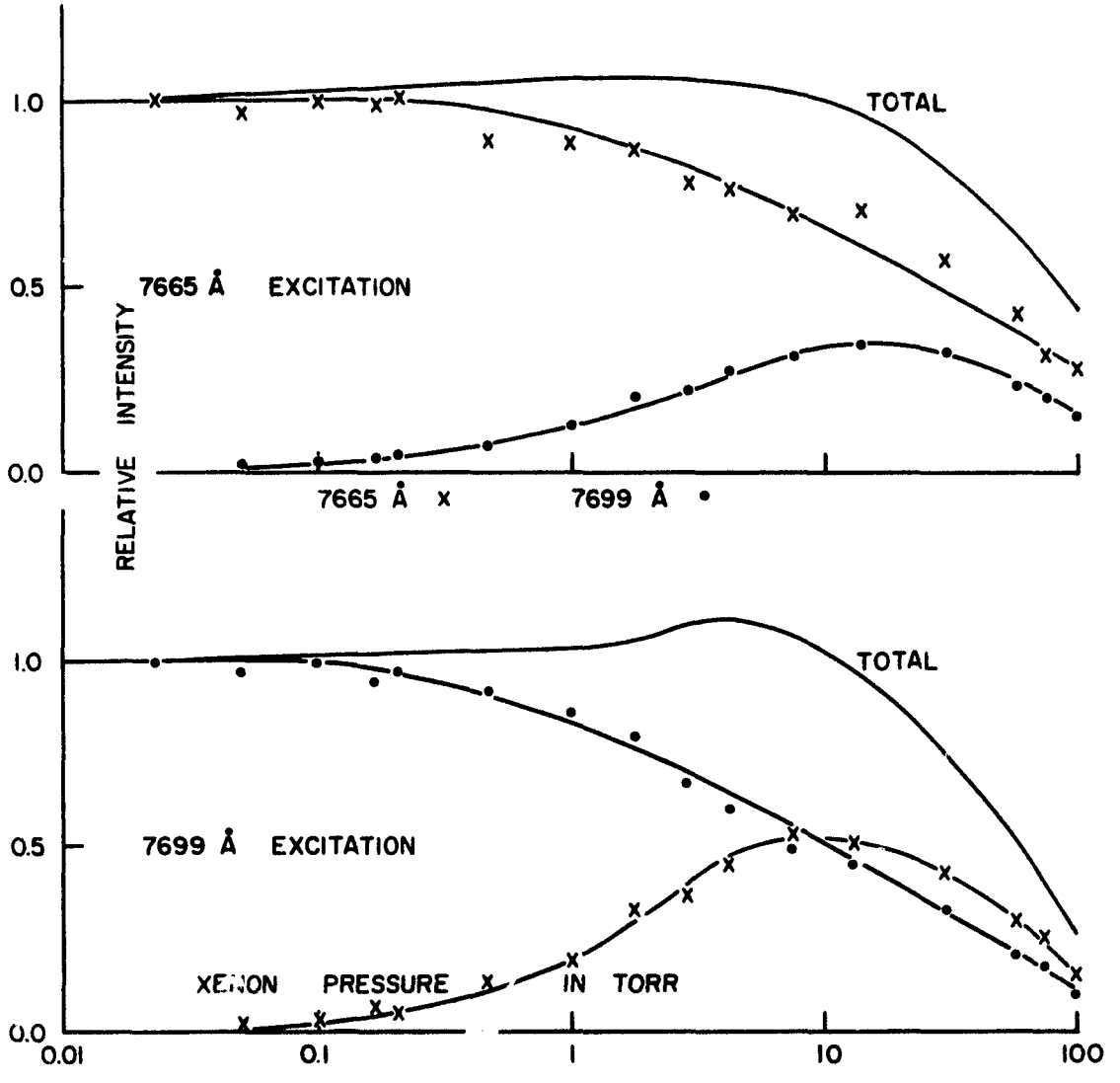

Fig. 20. Total Fluorescent Intensities in a Potassium-Xenon Mixture

^2P levels in potassium, then it is possible to calculate the effective lifetime τ' at any given inert gas pressure P. This calculation is based upon the collision numbers extrapolated from the low pressure (linear) region and the observed collision numbers at a given inert gas pressure. The ratio of the effective lifetime, τ', to the lifetime at zero inert gas pressure, τ, is shown as a function of inert gas pressure in figure 21. Results for all potassium-inert gas mixtures are shown along with the results of Demtroder's experiment.

There appears to be a general agreement between the shapes of the τ'/τ - P curves for potassium-inert gas mixtures and Demtroder's curve for Na-He. The flattened portions of the potassium curves correspond to the linear portions of the Z-P curves at high pressures. This overall agreement with Demtroder's results strongly suggests that the early saturation of the potassium-inert gas systems may be due to stimulated emission; the Z-P curves would become pressure independent because the lifetimes of the resonance states decrease with increasing inert gas pressure while the number of collisions per unit time increases.

By a process of elimination, it has become apparent that the behaviour of the Z-P curves probably depends on a pressure dependent change in the mechanism of the inelastic collisions and on collision-stimulated emission of the potassium resonance radiation.

Experiments designed to directly measure the lifetimes of the 4^2P levels in potassium under inert gas pressure

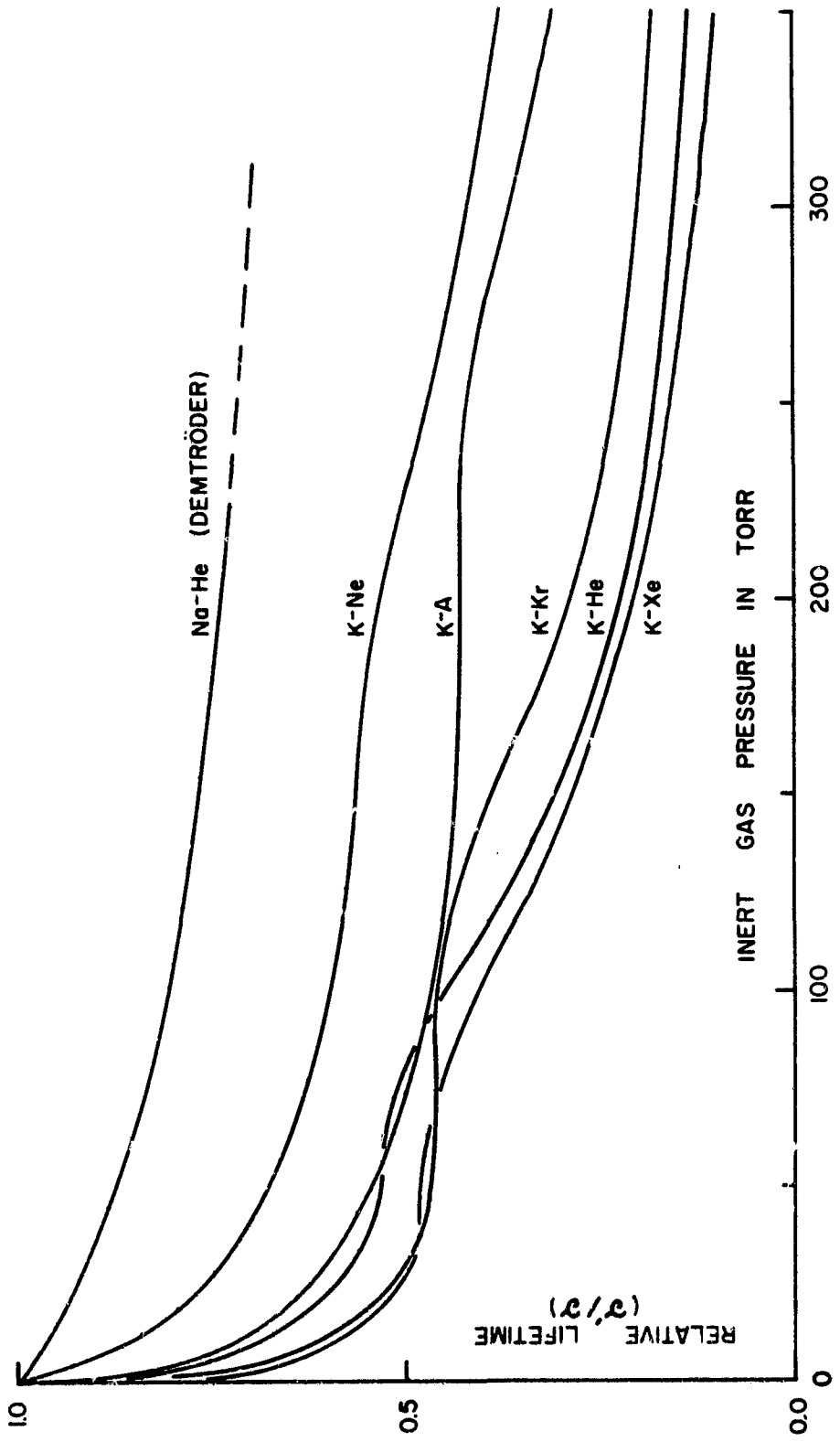

Fig. 21. A Plot of the Relative Lifetimes of the ^2P States in Potassium Against Inert Gas Pressure

are now in progress in this laboratory. The results of these experiments should indicate whether or not the above conclusions, reached by an indirect method, correspond to reality.

(iv) The Deviation of Q_{12}/Q_{21} for K-Xe Collisions from the Theoretically Predicted Value

It is only in the case of the K-Xe system that the theoretical value of Q_{12}/Q_{21} lies outside the range of error of the experimentally measured ratio. In the rubidium-inert gas systems[28], only the K-He and K-Ne cross sections conform to the theoretical Q_{12}/Q_{21} ratio and the remaining values fall below this ratio by progressively greater amounts, as the polarizabilities of the inert gases increase. In mixtures of cesium with the inert gases[26], only the Cs-He value agrees with the theoretical ratio; the remaining pairs show deviations which increase with the polarizability of the inert gases. The maximum observed deviation equals 82% for the Cs-Xe system.

The deviations in the cross section ratios with rubidium and cesium have been interpreted on the basis of a competing inelastic collision process involving van der Waals molecules[26], which includes exchanges between the kinetic energy continuum and the molecular bond energy. In view of the established gradation in the cross section ratio from cesium to rubidium, it may be that a similar mechanism is responsible for the small deviation of Q_{12}/Q_{21} in the K-Xe system from the theoretical value.

C. The Total Cross Sections for Inelastic Collisions between Potassium Atoms

The intensity ratios, η, were measured in the pure potassium vapour according to the technique outlined in section III,B. They are shown as functions of potassium vapour pressure in figure 22. As expected, the intensity ratios are linear at low vapour pressures. As radiation diffusion sets in, the observed η values increase rapidly and non-linearly. The intercepts of both curves on the η axis arise from the small transmission of the unwanted component of the fluorescence doublet through the analyzing interference filters. These intercepts, as well as the relationship between the observed η values and the η values corrected for the filter transmissions are explained below.

For either η value, let

β = transmission of the interference filters to sensitized fluorescence;

γ = transmission of the interference filters to resonance fluorescence;

δ = transmission of the neutral density filter to either component of the resonance doublet.

The intensities are represented by I and the superscripts R and S refer to resonance and sensitized fluorescence, respectively.

The observed fluorescent intensities are related to the true intensities by the following equations:

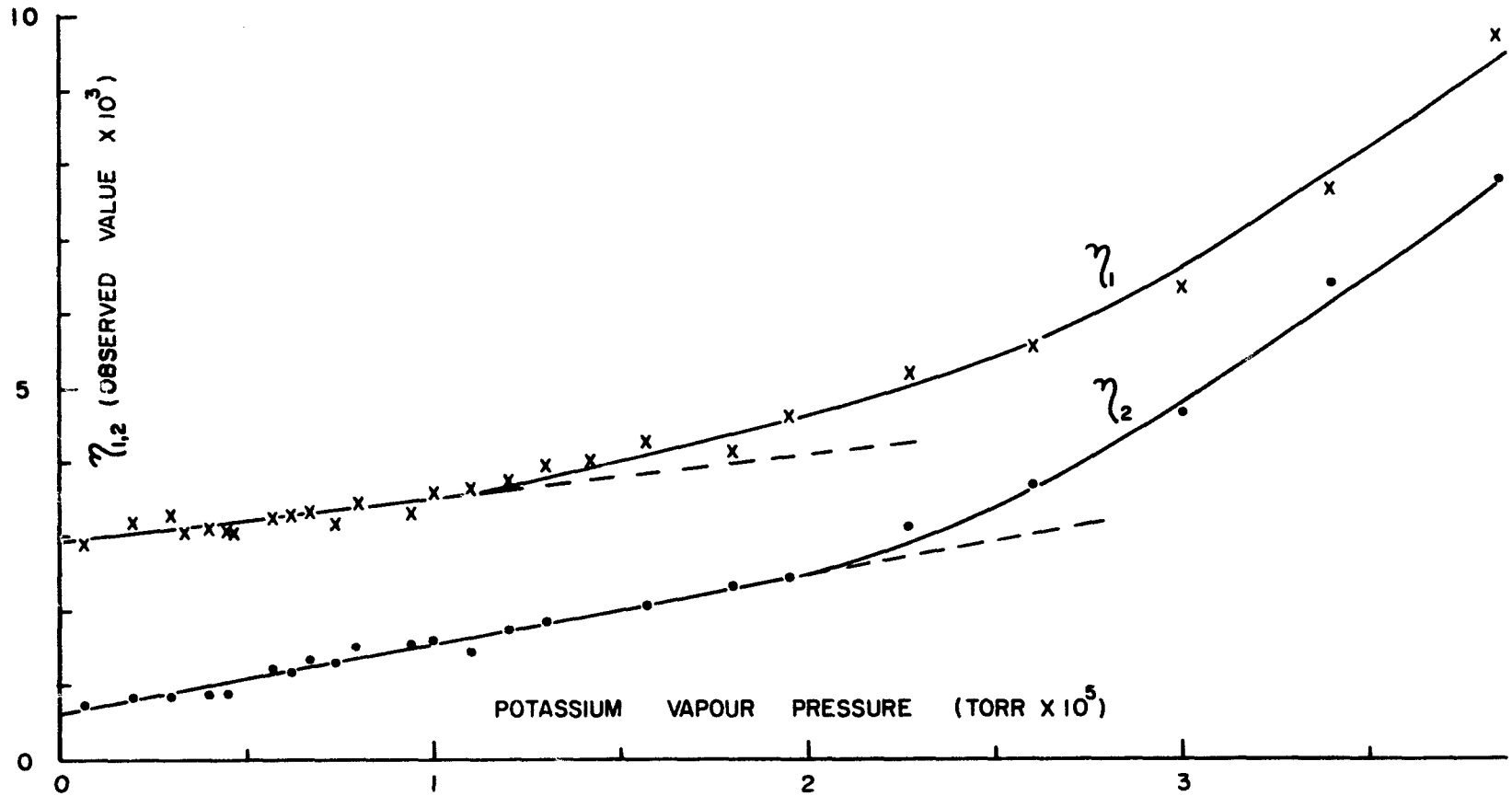

Fig. 22. The Observed Fluorescent Intensity Ratios in Potassium Vapour at Low Pressures

$$I^S_{obs} = \beta I^S + \gamma I^R \quad , \tag{38}$$

$$I^R_{obs} = \delta (I^R + I^S) \quad . \tag{39}$$

Dividing equation (38) by equation (39) and using the definitions

$$\eta_{obs} = \frac{I^S_{obs}}{I^R_{obs}} \quad \text{and} \quad \eta = \frac{I^S}{I^R} \quad ,$$

results in

$$\eta_{obs} = \frac{\beta\eta + \gamma}{(1 + \eta)} \quad . \tag{40}$$

Rearranging equation (40) gives

$$\eta_{obs}(1 + \eta) = \frac{\beta}{\delta}\eta + \frac{\gamma}{\delta} \quad . \tag{41}$$

It is clear from equation (41) that in the low vapour pressure limit, when $\eta \longrightarrow 0$,

$$\eta_{obs} = \frac{\gamma}{\delta} \quad . \tag{42}$$

γ/δ, the intercept of the η_{obs}-P curve on the ordinate axis will be designated as η^0_{obs}. If $\eta \ll 1$, equation (41) reduces to:

$$\eta = \frac{\delta}{\beta}(\eta_{obs} - \eta^0_{obs}) \quad . \tag{43}$$

The following equation is, however, correct for all values of η;

$$\eta = \left[\frac{\eta_{obs} - \eta^0_{obs}}{\beta/\delta - \eta_{obs}}\right] \quad . \tag{44}$$

The transmissions β and δ were measured in situ using potassium resonance fluorescence emitted from the cell

at a vapour pressure of about 10^{-5} torr; a DC recording method was employed to avoid overloading the scaler. The direct measurement of γ in situ is much more difficult. The intensity of the component in the fluorescent spectrum arising from sensitized fluorescence was expected to be comparable to that intensity of the component due to the resonance fluorescence at 10^{-5} torr, which would be transmitted through the interference filters. (The latter determines γ.) Since the relative intensity of the sensitized component as well as the total fluorescent intensity decrease linearly with vapour pressure, no advantage could be gained by lowering the vapour pressure in the cell. For this reason, the ratio γ/δ was obtained from a least squares analysis of the linear portions of the curves shown in figure 22. These intercepts, together with the directly measured values of δ yield the transmissions γ.

The pressure at which the η_2-P curve becomes non-linear (2×10^{-5} torr) is fairly obvious. However it is more difficult to select the point at which η_1 becomes non-linear and, therefore, the slope of this curve is more difficult to establish. It is expected from the discussion in section IV,A that η_1 will become non-linear at half the pressure at which η_2 becomes non-linear. This behaviour has been demonstrated in the cases of rubidium[27] and cesium[25], where the points of departure from linearity are much better defined than in the case of potassium. Because of these additional facts, the least squares analysis of η_1 was terminated at 1×10^{-5} torr.

The measured transmission parameters affecting the intensity ratios are listed in table 8.

TABLE 8

Properties of the Interference and Neutral Density Filters, Affecting the Values of η_1 and η_2

Parameter	Parameters Affecting η_1		Parameters Affecting η_2	
	Measured Value	Manufacturer's Specification	Measured Value	Manufacturer's Specification
β	0.343	0.42	0.352	0.41
δ	6.41×10^{-3}		5.91×10^{-3}	
η^0_{obs} (γ/δ)	2.92×10^{-3}		6.13×10^{-4}	
γ	1.87×10^{-5}	$\sim 2.0 \times 10^{-6}$	3.62×10^{-6}	$\sim 2 \times 10^{-6}$

The transmissions, β, measured for both fluorescent components, are about 10% smaller than the values specified by the manufacturer. This is due to the fact that the fluorescing region of the cell occupied a finite volume so that the emitted light could not be perfectly collimated. The value of γ taken from the intercept of the η_2 curve is in good agreement with the transmission supplied by the manufacturer; that taken from the η_1 curve is an order of magnitude higher than the manufacturer's value. This disparity probably reflects the greater sensitivity of the filters to non-parallel light of the long-wavelength component of the resonance doublet.

The values of the parameters listed in table 8, inserted in equations (43) and (44) together with the observed η values, yielded the true η values. Table 9 lists the observed η values as well as the true η values extracted from them for the full range of experimental vapour pressures.

TABLE 9

Fluorescent Intensity Ratios
Induced by Potassium-Potassium Collisions

Side Oven Temperature (°C)	Potassium Vapour Pressure (torr)	η_1^{obs} I_1/I_2	η_2^{obs} I_1/I_2	η_1 I_1/I_2	η_2 I_1/I_2
58.7	6.6×10^{-7}	2.89×10^{-3}	7.44×10^{-4}	0.00	2.20×10^{-6}
70.5	1.95×10^{-6}	3.18×10^{-3}	8.31×10^{-4}	4.86×10^{-6}	3.67×10^{-6}
75.8	3.0×10^{-6}	3.31×10^{-3}	8.50×10^{-4}	7.29×10^{-6}	3.98×10^{-6}
77.3	3.4×10^{-6}	3.07×10^{-3}		2.81×10^{-6}	
79.5	4.0×10^{-6}	3.10×10^{-3}	8.69×10^{-4}	3.37×10^{-6}	4.30×10^{-6}
81.0	4.5×10^{-6}	3.06×10^{-3}	8.81×10^{-4}	2.62×10^{-6}	4.50×10^{-6}
81.4	4.7×10^{-6}	3.03×10^{-3}		2.06×10^{-6}	
84.1	5.7×10^{-6}	3.25×10^{-3}	1.22×10^{-3}	6.17×10^{-6}	1.02×10^{-5}
85.0	6.2×10^{-6}	3.31×10^{-3}	1.16×10^{-3}	7.29×10^{-6}	9.24×10^{-6}
85.9	6.7×10^{-6}	3.33×10^{-3}	1.33×10^{-3}	7.67×10^{-6}	1.21×10^{-5}
87.0	7.4×10^{-6}	3.15×10^{-3}	1.28×10^{-3}	4.30×10^{-6}	1.13×10^{-5}
88.0	8.0×10^{-6}	3.45×10^{-3}	1.54×10^{-3}	9.91×10^{-6}	1.56×10^{-5}
90.0	9.4×10^{-6}	3.29×10^{-3}	1.55×10^{-3}	6.92×10^{-6}	1.58×10^{-5}
91.0	1.0×10^{-5}	3.61×10^{-3}	1.59×10^{-3}	1.29×10^{-5}	1.65×10^{-5}
91.8	1.1×10^{-5}	3.64×10^{-3}	1.44×10^{-3}	1.35×10^{-5}	1.39×10^{-5}
93.0	1.2×10^{-5}	3.73×10^{-3}	1.73×10^{-3}	1.51×10^{-5}	1.88×10^{-5}
94.0	1.3×10^{-5}	3.90×10^{-3}		1.83×10^{-5}	
94.1	1.3×10^{-5}	3.95×10^{-3}	1.86×10^{-3}	1.93×10^{-5}	2.10×10^{-5}
95.3	1.42×10^{-5}	3.98×10^{-3}		1.98×10^{-5}	
96.7	1.57×10^{-5}	4.29×10^{-3}	2.06×10^{-3}	2.56×10^{-5}	2.44×10^{-5}
97.8	1.80×10^{-5}	4.13×10^{-3}	2.34×10^{-3}	2.26×10^{-5}	2.91×10^{-5}
99.4	1.95×10^{-5}	4.58×10^{-3}	2.41×10^{-3}	3.10×10^{-5}	3.02×10^{-5}
101.7	2.27×10^{-5}	5.14×10^{-3}	3.13×10^{-3}	4.15×10^{-5}	4.23×10^{-5}

...continued

Table 9 - Fluorescent Intensity Ratios Induced by Potassium-Potassium Collisions (continued)

Side Oven Temperature (°C)	Potassium Vapour Pressure (torr)	η_1^{obs} I_1/I_2	η_2^{obs} I_1/I_2	η_1 I_1/I_2	η_2 I_1/I_2
103.5	2.60×10^{-5}	5.52×10^{-3}	3.69×10^{-3}	4.86×10^{-5}	5.17×10^{-5}
105.5	3.00×10^{-5}	6.30×10^{-3}	4.63×10^{-3}	6.32×10^{-5}	6.75×10^{-5}
107.3	3.40×10^{-5}	7.63×10^{-3}	6.38×10^{-3}	8.81×10^{-5}	9.69×10^{-5}
109.3	3.85×10^{-5}	9.71×10^{-3}	7.75×10^{-3}	1.27×10^{-4}	1.20×10^{-4}
111.2	4.40×10^{-5}	1.22×10^{-2}	1.06×10^{-2}	1.74×10^{-4}	1.68×10^{-4}
111.5	4.50×10^{-5}	1.41×10^{-2}	1.02×10^{-2}	2.09×10^{-4}	1.61×10^{-4}
112.9	4.95×10^{-5}	1.50×10^{-2}	1.29×10^{-2}	2.26×10^{-4}	2.07×10^{-4}
114.7	5.60×10^{-5}	2.01×10^{-2}	1.55×10^{-2}	3.22×10^{-4}	2.50×10^{-4}
114.8	5.70×10^{-5}	1.92×10^{-2}	1.56×10^{-2}	3.05×10^{-4}	2.52×10^{-4}
116.7	6.45×10^{-5}	2.37×10^{-2}	1.94×10^{-2}	3.89×10^{-4}	3.16×10^{-4}
118.3	7.20×10^{-5}	3.56×10^{-2}	2.83×10^{-2}	6.11×10^{-4}	4.65×10^{-4}
122.8	9.80×10^{-5}	6.19×10^{-2}	4.82×10^{-2}	1.10×10^{-3}	8.00×10^{-4}
129.4	1.5×10^{-4}	1.43×10^{-1}	1.22×10^{-1}	2.62×10^{-3}	2.05×10^{-3}
133.8	1.98×10^{-4}	2.64×10^{-1}	2.00×10^{-1}	4.94×10^{-3}	3.36×10^{-3}
139.8	2.90×10^{-4}	5.37×10^{-1}	4.51×10^{-1}	1.00×10^{-2}	7.58×10^{-3}
145.5	4.00×10^{-4}	1.14	9.13×10^{-1}	2.13×10^{-2}	1.53×10^{-2}
152.1	6.00×10^{-4}	2.35	2.05	4.60×10^{-2}	3.56×10^{-2}

The behaviour of the η values at high pressures has been investigated by Hoffmann and Seiwert[19] and by Chapman, Krause and Brockman[22]; the results of all these experiments are in substantial agreement with one another. In the present experiment it was found that η_1 and η_2 were in the theoretically predicted ratio ($\eta_2 = 1.60\,\eta_1$) at pressures below 2×10^{-5} torr. As the vapour pressure was increased, however, the ratio η_1/η_2 increased until a crossover of the two curves occurred at about 4×10^{-5} torr. Both η values then continued to rise with the square of the vapour pressure maintaining a constant ratio $\eta_2/\eta_1 = 0.77$. At about 2×10^{-3} torr the curves again crossed, and approached the values measured previously at higher vapour pressures.

This behaviour has been observed in cells both with and without an internal filter. The addition of 0 to 25 torr of krypton to the fluorescing vapour (vapour pressure 6×10^{-3} torr) did not appreciably alter this situation; η_1 was slightly larger than η_2. The addition of the buffer gas should have inhibited wall effects, if these had been the cause of the shift in the η_2/η_1 ratio.

The only essential difference between the cells now in use and those used previously[22] is that the exciting radiation passes through a vapour layer less than one millimeter in depth before reaching the region of observation. Formerly, this depth was 10-15 mm and the exciting lines reaching the region of observation in the vapour were strongly self-reversed. Most of the excitation under these conditions

would be accomplished by the wings of the line; when reemission occurred, reabsorption of fluorescent light would not be as extensive as it would have been for the line centre.

In the most recent cells the intensity of the fluorescent light is higher, but the effects of reabsorption are more apparent. Under these conditions, where the ratio of the oscillator strengths for the relevant transitions is 2.0 and the factor $\frac{g_1}{g_2} e^{-\Delta E/kT}$ is about 1.60, the ratio of η_2/η_1 is probably governed by the relative magnitudes of the two oscillator strengths, rather than by the collision cross sections.

It may be seen from equation (43) that the cross sections can be calculated from the slopes of the linear portions of the observed η curves; at the low vapour pressures involved, $\eta = \gamma Z$. The cross sections obtained in this way are listed in table 10 and are compared with cross sections from other sources. The quoted errors include those obtained from the least squares analysis (23% for η_1 and 3.5% for η_2) and the probable errors in the measurement of the transmission ratios δ/β (6%).

The relatively large error in Q_{21} is due to the fact that the linear section of the η_1-P curve does not extend to as high a vapour pressure as it does for η_2. Consequently, there are fewer experimental points which can be included in the analysis. Since the slope of the η_1 curve is not as steep as that for η_2, the experimental scatter of points contributes more noticeably to the experimental error. The calculated value of γ shown in table 8 indicates that the

TABLE 10

The Inelastic Cross Sections Q_{12} and Q_{21} for Potassium-Potassium Collisions

Source	Q_{12} (Å^2) $^2P_{1/2} \rightarrow {}^2P_{3/2}$	Q_{21} (Å^2) $^2P_{1/2} \leftarrow {}^2P_{3/2}$	Q_{12}/Q_{21} Experimental	Q_{12}/Q_{21} Theoretical
This investigation	370 ± 37	250 ± 75	1.48 ± 0.59	1.60
Chapman, Krause & Brockman[22]	6.6×10^4	6.6×10^4	1.0	1.60
Thangaraj[18]	330	165	2.0	1.70
Hoffmann & Seiwert[19]	120	60	2.0	

values of η_1 were obtained close to the limit imposed by the filter transmissions. It is, however, apparent from the agreement between the experimental and theoretical values of the ratio of Q_{12}/Q_{21} that the experimental value of Q_{21} is closer to the true value than the error of 30% might suggest.

There is a difference of about two orders of magnitude between the cross sections obtained in the present investigation and those given by Chapman, Krause and Brockman[22]. In the earlier experiment, it was thought that radiation diffusion would not persist below the vapour pressure of 3×10^{-4} torr and the cross sections were measured between 1×10^{-4} and 3×10^{-4} torr. It is now well known that diffusion of radiation is well established at these pressures not only in potassium but also in rubidium[27] and cesium[25] vapours. It has also been found that between the vapour pressures of 2×10^{-5} and 1×10^{-3} torr the η values increase with the square of the

potassium vapour pressure, as was the case with rubidium[27]. This strong pressure dependence leads to very large errors in cross sections measured in this pressure range.

The agreement between the results of the present investigation and those of Thangaraj[18] is remarkably good. If the errors inherent in Thangaraj's experiment are considered, the two sets of cross sections are virtually identical. Thangaraj used photographic techniques to study sensitized fluorescence under surface fluorescence conditions in potassium vapour, correcting for radiation diffusion by using Milne's[10] theory. The fact that two entirely different experimental techniques produced nearly the same cross sections is highly significant. The good correspondence which has also been obtained between the cross sections for rubidium-rubidium collisions determined by Thangaraj[18] and by Rae and Krause[27] indicates that the agreement in the case of potassium is not coincidental.

The values obtained by Hoffmann and Seiwert[19] are lower than those reported here by a factor of three. These authors corrected for imprisonment of radiation using an adaptation of Holstein's[11] theory. The generally better agreement of Thangaraj's values with those obtained here, under single collision conditions, suggests that Milne's theory might be more suitable for the correction of data obtained from sensitized fluorescence experiments, than had been thought previously.

V. CONCLUSIONS

(i) Transfer of Excitation in Potassium-Inert Gas Collisions

The cross sections for inelastic collisions between potassium and inert gas atoms, which lead to the mixing between the $4^2P_{1/2}$ and $4^2P_{3/2}$ states in potassium, were determined for the first time at very low potassium and inert gas pressures and under single collision conditions. Under these circumstances and in the absence of radiation trapping, the cross sections should not be affected by changes in the velocity distribution function, quenching of resonance radiation or changes in the life times of the resonance states. It appears that the cross sections $Q_{12}(^2P_{1/2} \rightarrow {}^2P_{3/2})$ and $Q_{21}(^2P_{1/2} \leftarrow {}^2P_{3/2})$ are in the ratio predicted by the principle of detailed balancing with the exception of the K-Xe cross sections where the ratio is slightly low, probably because of the formation of K-Xe van der Waals molecules. A similar but much more pronounced effect was observed with cesium-inert gas[26] and rubidium-inert gas[28] collisions.

Most theories postulated for these interactions assumed that the energy defect between the levels involved is small and that the interaction is non-adiabatic. It has been pointed out by Nikitin[3] that the potassium-inert gas collisions occur adiabatically. If one considers the Massey parameter[3], $\frac{a|\Delta E|}{hv_r}$, as a criterion for the adiabaticity of

a collision, the collision is assumed adiabatic if the parameter is much greater than unity. a is of the order of the gas-kinetic radius for the particular collision; its values were recalculated from Rothe and Bernstein's[52] cross sections for elastic collisions between potassium atoms and inert gas atoms. The resulting Massey parameters varied from 1.23 for collisions with helium to 6.19 for xenon, thus indicating that the potassium-inert gas collisions are just adiabatic and that the degree of adiabaticity varies over the range of inert gases. It is not very likely that any theory which assumes strict adiabatic or non-adiabatic conditions will fit the case of potassium-inert gas collisions.

It is also expected from the various theories which are based on models involving van der Waals or 'QID' interactions, that the collision cross sections should increase monotonically with the polarizabilities of the inert gases. The failure of this prediction in the case of potassium as well as rubidium[28] and cesium[26] may be explained on the basis of Jefimenko's[36] semi-classical model involving overlap forces which contribute significantly to the total interaction energy of the colliding systems.

The non-linearity of the collision numbers with inert gas pressure and the unexpected low saturation values of the collision numbers have been interpreted as arising from possible changes in the collision mechanism and from collision-stimulated emission. The present experiments were not designed for the explicit study of such effects but further investigations of quenching and collision-stimulated emission in

alkali metal-inert gas mixtures are now being carried out in this laboratory.

(ii) Transfer of Excitation in Potassium-Potassium Collisions

The cross sections $Q_{12}(4^2P_{1/2} \longrightarrow 4^2P_{3/2})$ and $Q_{21}(4^2P_{1/2} \longleftarrow 4^2P_{3/2})$ for potassium-potassium collisions were determined at much lower vapour pressures than could be reached previously. The values supersede those reported earlier[22] which, apparently, were subject to considerable influence from radiation trapping effects. Although one of these cross sections involves a larger experimental error than those for potassium-inert gas collisions, their ratio agrees quite well with that predicted by the principle of detailed balancing.

Seiwert[57] has shown that the experimentally measured inelastic cross sections for collisions in pure alkali metals are much larger than those calculated from Stueckelberg's[34] theory. The measured cross sections for potassium, rubidium[27] and cesium[25] are also larger than those predicted by Kallmann and London[31]. These results are not surprising since both of these theories make no provision for exchange forces between colliding atoms of the same species.

The cross section Q_{21} $(^2P_{1/2} \longleftarrow ^2P_{3/2})$ may be used, together with the corresponding cross sections for rubidium[27] and cesium[25], to test the dependence of the cross sections on the energy defect, ΔE. Figure 23 is a plot of Q_{21} against $(\Delta E)^{-1}$ for these three atoms. The cross sections appear to

vary as $(\Delta E)^{-1}$ in accordance with Franck's[5] rule; both Kallmann and London[31] and Stueckelberg[34] postulated a variation with $(\Delta E)^{-2/3}$.

If the $(\Delta E)^{-1}$ dependence included the interaction between sodium atoms, figure 23 would suggest an upper limit of 800 Å for the sodium-sodium cross section, Q_{21}. A study of these cross sections is now in progress in this laboratory.

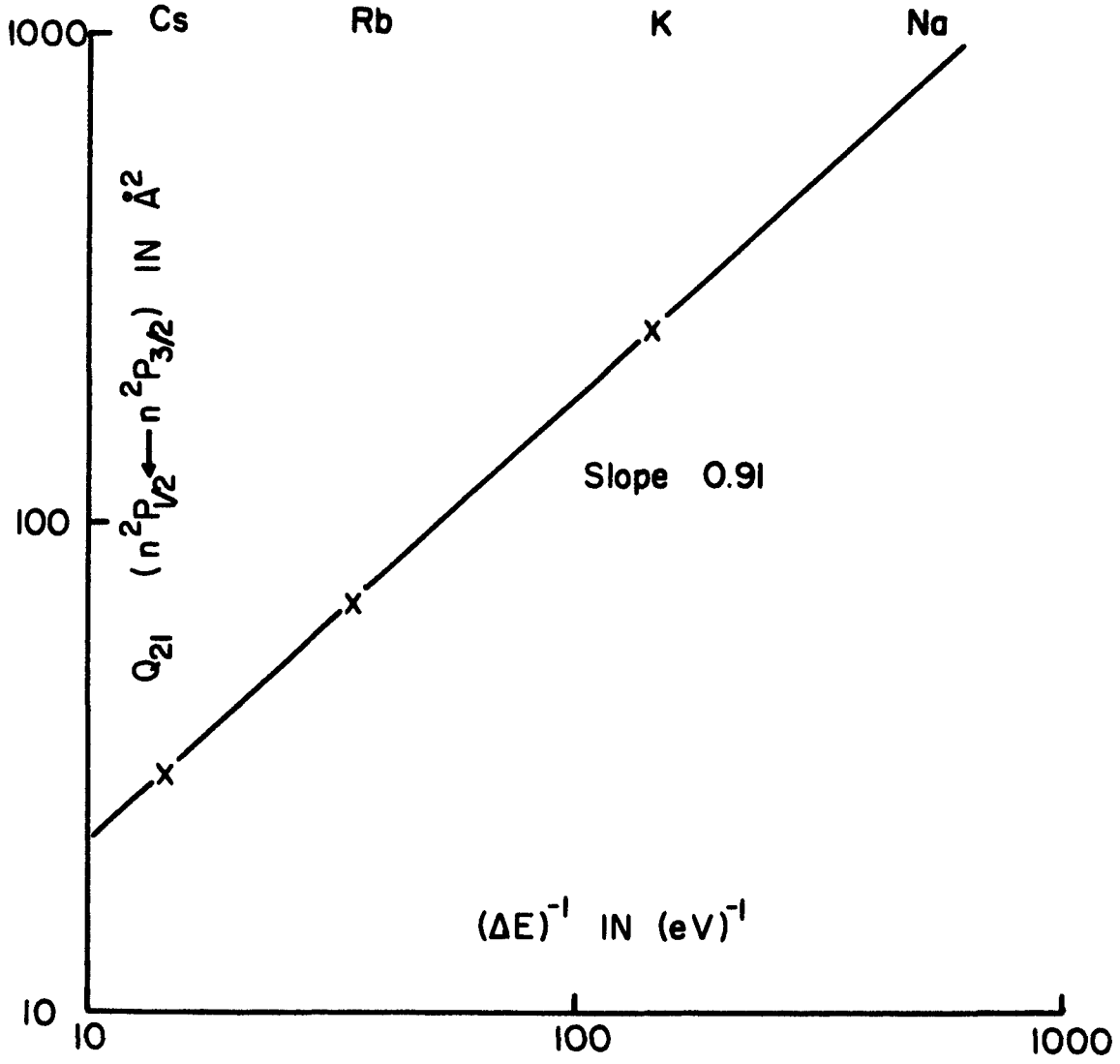

Fig. 23. The Relation Between the Cross Sections Q_{21} $(n^2P_{1/2} \leftarrow n^2P_{3/2})$ and the Energy Defect, ΔE

BIBLIOGRAPHY

1. J.A. Jordan, Ph.D. Thesis, University of Michigan, Ann Arbor, Michigan (1964).
2. J. Callaway and E. Bauer, Phys. Rev. (in print).
3. E.E. Nikitin, J. Chem. Phys. 43, 744 (1965).
4. G. Cario and J. Franck, Z. Physik 11, 161 (1922).
5. J. Franck, Naturwissenschaften 14, 211 (1929).
6. H. Beutler and B. Josephy, Z. Physik 53, 74 (1929).
7. O. Klein and S. Rosseland, Z. Physik 4, 46 (1921).
8. R.W. Wood, Phil. Mag. 10, 513 (1905).
9. K. Compton, Phil. Mag. 45, 752 (1923).
10. E. Milne, J. Lond. Math. Soc. 1, 1 (1926).
11. T. Holstein, Phys. Rev. 72, 1212 (1947).
12. J.P. Barrat, J. Phys. Radium 20, 42,633,541 (1959).
13. R.W. Wood, Z. Physik 13, 353 (1912).
14. R.W. Wood, Phil. Mag. 27, 1018 (1914).
15. R.W. Wood and F. Mohler, Phys. Rev. 11, 70 (1918).
16. W. Lochte-Holtgreven, Z. Physik 47, 362 (1928).
17. R. Seiwert, Ann. Physik 18, 54 (1956).
18. M.A. Thangaraj, Ph.D. Thesis, University of Toronto, Toronto, Ontario (1948).
19. K. Hoffmann and R. Seiwert, Ann. Physik 7, 71 (1961).
20. R. Seiwert, Ann. Physik 17, 371 (1956).
21. R. Seiwert, Ann. Physik 18, 35 (1956).
22. G.D. Chapman, L. Krause and I.H. Brockman, Can. J. Phys. 42, 535 (1964).

23. G.D. Chapman and L. Krause, Can. J. Phys. 43, 563 (1965).

24. H. Bunke and R. Seiwert, Optik und Spektroscopie aller Wellenlängen (Akademie Verlag) (1962).

25. M. Czajkowski and L. Krause, Can. J. Phys. 43, 1259 (1965).

26. M. Czajkowski, D. McGillis and L. Krause, Can. J. Phys. (in print).

27. A.G.A. Rae and L. Krause, Can. J. Phys. 43, 1574 (1965).

28. B. Pitre, A.G.A. Rae and L. Krause, Can. J. Phys. (in print).

29. E.E. Nikitin and V.K. Bykhovskii, Opt. Spectry. 17, 444 (1965).

30. L.I. Schiff, Quantum Mechanics (Second Edition, McGraw-Hill Book Company, Inc., New York, 1955).

31. H. Kallmann and F. London, Z. Physik Chem. (Leipzig) B2, 220 (1929).

32. C. Zener, Phys. Rev. 38, 277 (1931).

33. O.K. Rice, Proc. Nat. Acad. 17, 34 (1931).

34. E.C.G. Stueckelberg, Helv. Phys. Acta, 5, 369 (1932).

35. D.R. Bates, Discussions Faraday Soc. 33, 7 (1962).

36. O. Jefimenko, J. Chem. Phys. 37, 2125 (1962).

37. E. Fermi, Nuovo Cimento 11, 157 (1934).

38. O. Jefimenko, J. Chem. Phys. 39, 2457 (1963).

39. O. Jefimenko, J. Chem. Phys. 42, 205 (1965).

40. O. Jefimenko and M.G. Williams, J. Chem. Phys. 42, 207 (1965).

41. P. Bender, Ph.D. Thesis, Princeton University, Princeton, New Jersey (1956).

42. W.R. Thorson, J. Chem. Phys. 42, 3878 (1965).

43. R. Atkinson, G.D. Chapman and L. Krause, J. Opt. Soc. Amer. 55, 1269 (1965).

44. K. Hoffmann, Expt'l Tech. Phys. 39, 217 (1962).

45. L. Krause and R. Neville, J. Sci. Inst. 34, 698 (1963).

46. R.W. Ditchburn and J.C. Gilmour, Rev. Mod. Phys. 131, 310 (1941).

47. Landolt-Bornstein, Zahlwerte und Funktionen (Springer Verlag, 1950).

48. E. Whalley and W.G. Schneider, J. Chem. Phys. 23, 1644 (1955).

49. H.S.W. Massey and E.H.S. Burhop, Electronic and Ionic Impact Phenomena (Oxford University Press, 1952).

50. A. Dalgarno, Private Communication.

51. W.R. Thorson, Private Communication.

52. E.W. Rothe and R.B. Bernstein, J. Chem. Phys. 31, 1619 (1959).

53. R.H. Kummler and M. McCarty, J. Chem. Phys. 42, 2587 (1965).

54. S. Ch'en and M. Takeo, Rev. Mod. Phys. 29, 20 (1957).

55. W. Demtroder, Z. Physik 166, 42 (1962).

56. J.H. Stamper, J. Chem. Phys. 43, 759 (1965).

57. R. Seiwert, Unelastische Stose Zwischen Angeregten und Unangeregten Atomen (in print).

VITA AUCTORIS

The author was born in Windsor, Ontario, in 1940, where he received his early education. In 1958 he joined the Royal Canadian Air Force as a technical list officer and entered the Honours Chemistry and Physics programme at Assumption University of Windsor under Air Force sponsorship. Released from the R.C.A.F. in 1961, the author continued his studies under an in-course scholarship, obtaining the B.Sc. degree in 1962. In the same year, he won the Society of Chemical Industry Merit Award Key in Chemistry and a National Research Council of Canada graduate bursary.

In 1963, the author obtained the M.Sc. degree in Physics and won an N.R.C. graduate studentship for the years 1963-1966.

APPENDIX A

Reprinted from JOURNAL OF THE OPTICAL SOCIETY OF AMERICA, Vol. 55, No. 10, 1269-1274, October 1965
Printed in U. S. A.

Light Sources for the Excitation of Atomic Resonance Fluorescence in Potassium and Rubidium*

R. J. ATKINSON,† G. D. CHAPMAN,‡ AND L. KRAUSE
Department of Physics, University of Windsor, Canada

(Received 22 April 1965)

A description is given of radio frequency light sources which produce potassium and rubidium resonance radiation of high intensity. The properties of the spectral lamps have been systematically investigated in relation to their operating parameters. The rf lamps emit resonance lines of much higher peak intensities, smaller halfwidths and smaller degrees of self-reversal than do commercially available lamps. Typical halfwidths of the resonance lines of potassium and rubidium produced by the rf sources were found to be 0.15 cm^{-1} and 0.37 cm^{-1}, respectively, compared with the corresponding widths of 0.34 cm^{-1} and 1.5 cm^{-1}, respectively, emitted by Osram spectral lamps operated at low currents.

1. INTRODUCTION

THE investigation of excitation transfer in atomic collisions by methods involving sensitized fluorescence requires appropriate sources of resonance radiation. An ideal source should emit resonance lines of high intensity, small halfwidth and no self-reversal. These criteria are particularly important when the fluorescence experiments must be performed at low alkali-vapor pressures, at which there is no trapping of resonance radiation and where the atomic absorption lines are quite sharp for lack of pressure broadening.

Although some lamps produce resonance lines of high integrated intensities, the intensities at the line centers may be weakened because of pressure broadening or self-reversal. While Doppler broadening is not usually a serious problem, broadening by collisions with like atoms or with atoms of other gases is responsible for most of the observed linewidths. In discharges where ions are present in large concentrations, Stark effect further increases the widths of the emitted lines. Self-reversal is caused by the absorption of the centers of the spectral lines emitted by the vapor lamp, if the light has to pass through a cooler layer of unexcited atoms before emerging to the outside.

In one common type of lamp used for the production of atomic spectra, an ionic discharge is passed between two electrodes. Osram lamps utilize an ac discharge, contained in a vacuum envelope to reduce conduction of heat and thus self-reversal. Houtermans[1] designed a lamp with a flattened discharge section, the purpose of which was to further reduce self-reversal. This lamp was recently tried by Ermisch and Seiwert[2] but without success because of thermal strains in the alkali-resistant glass. Hoffmann and Seiwert[3] also investigated the Cario–Lochte-Holtgreven[4] lamp and the Druyvesteyn[5] lamp, both of which exhibited special features whose purpose was to decrease the browning of the glass by the corrosive action of the alkali metal and to reduce the amount of self-reversal. While these attempts met, on the whole, with reasonable success, the resulting alkali resonance lines were of rather low intensity.

Jackson used electrodeless discharges to study hfs in cesium[6] and in rubidium.[7] With the advent of optical pumping techniques a new demand arose for high intensity sources of unreversed alkali resonance lines. Bell, Bloom, and Lynch[8] developed the Varian rf lamp and Gerard[9] suggested a design of a lamp which lent itself to further modification and which formed the basis for the development of the lamp used in this investigation. Rf lamps, in which the power input and temperature can be accurately controlled, are now being used in this laboratory for the excitation of sensitized fluorescence in the vapors of potassium,[10] cesium,[11] and rubidium[12] at vapor pressures below 10^{-4} Torr, at which commercially available light sources cannot be used because of inadequate intensities at the centers of the resonance lines. The following is a description of the lamp in its various forms as it is now being used in this laboratory and a report on its evaluation as to intensities, halfwidths and self-reversal of the emitted resonance lines. Where possible a comparison has been made with the performance of the commercially available lamps manufactured by the Osram and Varian companies.

2. DESCRIPTION OF THE LIGHT SOURCES

The resonance radiation was produced in a radio frequency electrodeless discharge contained in a cylindrical glass tube. The tube was mounted in a coil which formed part of a tank circuit in an rf power oscillator. The base of the tube, which acted as a reservoir for the alkali

* Supported by the U. S. Air Force Office of Scientific Research under Grant AFOSR 361-63.
† Holder of N.R.C. Bursary 1963-64.
‡ Holder of N.R.C. Studentship 1963-65.
[1] F. G. Houtermans, Z. Physik **76**, 474 (1932).
[2] W. Ermisch and R. Seiwert, Ann. Physik **2**, 393 (1959).
[3] K. Hoffmann and R. Seiwert, Exp. Tech. Physik **8**, 161 (1960).
[4] G. Cario and W. Lochte-Holtgreven, Z. Physik **42**, 22 (1927).
[5] M. J. Druyvesteyn, Physica **2**, 255 (1935).
[6] D. A. Jackson, Proc. Roy. Soc. (London) **A121**, 432 (1928).
[7] D. A. Jackson, Proc. Roy. Soc. (London) **A139**, 673 (1933).
[8] W. E. Bell, A. L. Bloom, and J. Lynch, Rev. Sci. Instr. **32**, 688 (1961).
[9] V. B. Gerard, J. Sci. Instr. **39**, 217 (1962).
[10] G. D. Chapman, L. Krause, and I. H. Brockman, Can. J. Phys. **42**, 535 (1964).
[11] M. Czajkowski and L. Krause, Can. J. Phys. **43**, 1259 (1965).
[12] A. G. A. Rae and L. Krause, Can. J. Phys. (to be published).

metal, rested in a heater used to control the vapor pressure.

The rf discharge was maintained in a Pyrex cylinder 6 cm long and about 2 cm in diameter, which contained about 0.5 g of the alkali metal. Potassium and rubidium metals, which had been obtained from the A. D. McKay Company of New York, were purified by a multi-stage vacuum distillation, of which the lamp bulbs formed the final stage. It was found that the discharge was most stable in the presence of argon at a pressure of 2 torr. The character of the emitted resonance lines depended radically on the operating temperature of the lamp. The heater, which was designed to regulate the temperature and the vapor pressure of the alkali metal, consisted of a small coil wrapped around the base of the discharge tube and inserted in an asbestos block. The coil was made of No. 26 Chromel A heating wire, and had a resistance of about 3 Ω. The heater current was regulated by a transistorized controller employing a thermistor as a sensing element. The temperature of the lamp, which was measured by means of an Alumel–Chromel thermocouple placed in contact with the glass reservoir, could be varied from 70° to 200°C. A minimal lamp base temperature of just less than 70°C was obtained with the heater turned off and was produced by the dielectric heating effect which raised the temperature of the glass envelope within the rf coil to well over 200°C. While in most applications the discharge section and its coil were mounted vertically, a horizontal lamp had to be produced for use in a strong magnetic field.[13] The horizontal discharge tube was provided with two heaters, one at each end, of which one had a greater heating capacity. Normally, after several hours of operation a strong browning would appear on the Pyrex envelope. The formation of this deposit, arising from the corrosive action of the hot alkali vapor, could be inhibited by washing the bulbs thoroughly with 10% solution of HF.[11]

The diagram of the lamp oscillator circuit is shown in Fig. 1. The oscillator was of a push-pull type and was operated in class C. Its frequency was determined by the resonant frequency of the plate tank circuit, which consisted of a 15-turn coil, and by the associated stray capacitance. A typical coil inductance of 20–30 μH and a capacitance of about 1 μF would be appropriate to operation at 40 Mc/sec. Ordinarily the plate voltage was 325 V and the plate current was in the range 100–150 mA per tube. The screen-grid currents were about 25 mA and could be varied by means of a 10-K potentiometer to control the power dissipated in the plate circuit. They were equalized by means of the 100-Ω potentiometer and were held constant by the GE 46 tungsten lamps which have positive temperature coefficients of resistance. The 2-μF capacitors on the screen grids were essential for reliable operation; they maintained the grids at rf ground, limiting the currents to very low values and inhibiting spurious oscillations of frequencies other than that of the push–pull circuit. Such spurious, electron-coupled oscillations produced discharge patterns in the lamp which did not result in emission of resonance radiation or in dielectric heating of the Pyrex envelope.[14] Six such nonproductive modes were observed, all of which were characterized by very high grid currents. The circuit was connected to the high-voltage power supply through an inductive input L-section filter which had two advantages over the capacitive input π-section filter suggested by Gerard.[9] It allowed the center of the coil to float above rf ground and tended to eliminate a cold spot which otherwise occurred in the corresponding region of the discharge tube. Connecting a capacitor to the center of the coil, as had been suggested by Gerard, also altered the resonant frequency of the tank circuit and made the circuit unstable over long periods of operation. With the circuit elements shown in Fig. 1, the lamp operated at about 40 Mc/sec. The oscillator produced a clean, sinusoidal wave form over all values of current with no complications due to spurious oscillations. As a result, a skin discharge was established in the lamp, resulting in a very strong emission of the alkali resonance doublet.

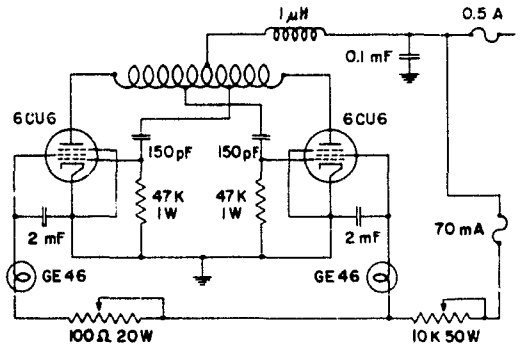

FIG. 1. The rf oscillator circuit.

3. EXPERIMENTAL PROCEDURE

The experimental investigation of the resonance lines emitted by the rf lamps involved the determination of integrated intensities, peak intensities at the line centers, and line shapes, as functions of the operating temperatures of the lamps. Whenever feasible, an equivalent series of experiments was carried out with the Osram and Varian spectral lamps. The apparatus used to study the spectral line shapes consisted of the appropriate light source, a monochromator, a Fabry–Perot interferometer, and a camera. For purposes of determining the relative intensities of the spectral lines, a photomultiplier tube assembly replaced the interferometer following the exit slit of the monochromator.

The monochromator was a Bausch & Lomb grating instrument employing a 1200 line/mm replica grating blazed at 7500 Å in the first order. Its reciprocal dis-

[13] R. Seiwert (private communication).
[14] A. G. A. Rae (private communication).

persion was 16 Å/mm and, with a slitwidth of 1.75 mm, the potassium resonance doublet was resolved with a spectral purity of at least 1 part in 2000. The Hilger and Watts model N200 Fabry–Perot interferometer utilized aluminized mirrors 2.5 cm in diameter; a D72 spectrometer camera was matched to the interferometer and was used to photograph the fringes.

The relative intensities of the spectral lines were measured with a Dumont 6911 11-stage photomultiplier tube which has an S-1 photocathode with a peak sensitivity in the region 7000–9000 Å. The photomultiplier, mounted in a light-tight jacket, was placed against the exit slit of the monochromator. The output of the tube was recorded with a Leeds and Northrup micro-microampere strip-chart recorder which continuously monitored variations in lamp intensity. The intensity of the rf lamp was determined as a function of the temperature at the base of the lamp. In the case of the Osram lamp the intensity was determined as a function of the lamp current but no changes in operating conditions of the Varian lamp were possible.

The intensity of a Fabry–Perot fringe at its peak is proportional to the peak intensity of the spectral line producing it whereas, with wide monochromator slits, the signal recorded with a photomultiplier tube is proportional to the integrated intensity of the spectral line. Using the interferometer at a theoretical resolving power of 5×10^5, we were able to determine the halfwidths of the spectral lines for a variety of operating conditions.

The interferometer was adjusted for parallelism of the light beam and of the mirrors, and was covered to exclude stray light. The fringes were photographed using Kodak Type 1N Spectroscopic Plates which have a peak sensitivity in the range 7700–8400 Å. Exposures were of five-second duration; compensation for varying source intensities was made by adjusting the variable apertures. The resulting fringes were of roughly equal peak intensities throughout the range of light sources and operating conditions. The photographic emulsion was calibrated separately for each spectral line by taking five-second exposures of the parallel monochromatic beam passing through a series of apertures of known areas.

Traces of the interference fringes were obtained by scanning the plates with a Jarrell-Ash Model 2310 recording microphotometer which was also used to obtain the calibration curves for the photographic emulsion. In this way it was possible to obtain the intensity profiles of the Fabry–Perot fringes and hence of the spectral lines. The half-intensity points were determined for all the fringes and, in the case of self-reversed lines, the ratios of the intensities at the peaks to those at the central minima (degrees of self-reversal) were also found. The halfwidths of the resonance lines were obtained by measuring the diameters of up to five Fabry–Perot fringes in each exposure and substituting their squares in a rectangular array.[15] This procedure, carried out for each spectral line over a range of operating conditions of the sources, required the scanning and measurement of about 250 interferograms.

4. DISCUSSION OF THE RESULTS

(a) Potassium Lamps

The integrated intensities of the resonance lines emitted by the rf lamp and by the Osram lamp are plotted in Fig. 2 which, in the case of the Osram lamp, shows the variation of intensity with operating current and, in the case of the rf lamp, with temperature. The slight minimum in the emission from the Osram lamp may be attributed to the rapid rise in self-absorption with vapor pressure. The rf lamp, which produces resonance radiation of greater intensity, exhibits a maximum in the total intensity of emission at 180°C which corresponds to a vapor pressure of 2.6×10^{-3} torr. The intensities of the two components (7665 Å, 7699 Å) are not in the ratio of the statistical weights of the excited states, $^2P_{\frac{3}{2}}:{}^2P_{\frac{1}{2}}=4:2$. This indicates the presence of self-absorption, as the absorption coefficient of the 7665-Å component is twice as large as that of the 7699-Å component.

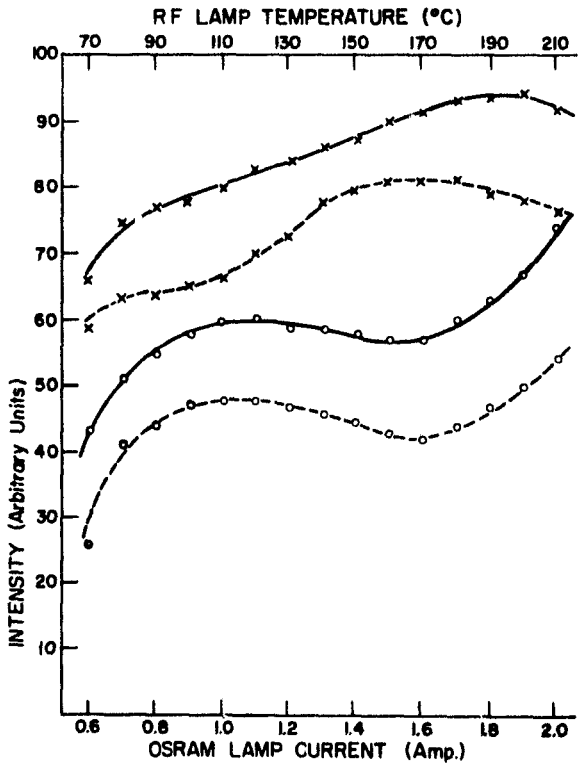

FIG. 2. Integrated relative intensities of the potassium resonance lines emitted by the rf and Osram lamps. ×, rf lamp; ○, Osram lamp; ——, 7665-Å line; – – –, 7699-Å line.

[15] S. Tolansky, J. Sci. Instr. 8, 223 (1931).

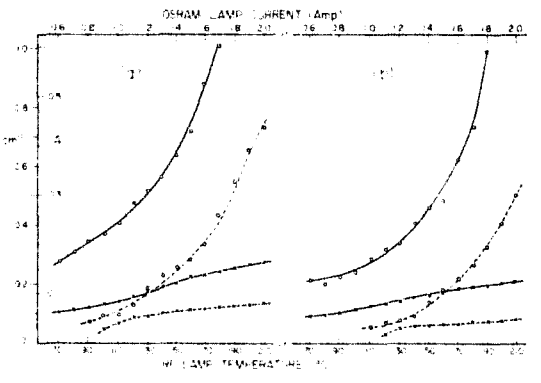

FIG. 3. The halfwidths $\Delta\nu$, and separations of self-reversal peaks $\delta\nu$, of the potassium resonance lines emitted by the rf and Osram lamps: (a), the 7665-Å component; (b), the 7699-Å component. ×, rf lamp; ○, Osram lamp; ——, $\Delta\nu$; – – – –, $\delta\nu$.

The average values of the halfwidths of the resonance lines, the separations between their self-reversal maxima and the degrees of self-reversal were obtained from the Fabry–Perot fringes, of which three exposures were made for each lamp, spectral line, and operating condition. The halfwidths and separations between the self-reversal maxima are plotted in Fig. 3 as functions of the operating parameters of the lamps. It may be seen that the halfwidths of the resonance lines emitted by the rf lamp are much smaller and increase nearly linearly with temperature over the whole temperature range 70°–210°C. The ratios $I_{max}/I(\nu_0)$ of the intensities at the self-reversal peaks to those at the centers of the lines, are plotted in Fig. 4 against the operating parameters of the Osram and rf lamps. Self-reversal does not appear in Osram lamps at operating currents below 1 A or, in rf lamps, at operating temperatures below 120°C. The effect occurs in the Osram lamp because in it the discharge is concentrated near the axis of the discharge tube. In the rf discharge, on the other hand, the skin effect tends to restrict the excitation to a thin layer near the walls of the tube. There is still some self-absorption, though, of the radiation coming from the rear wall of the discharge tube and passing through the central column of unexcited vapor.

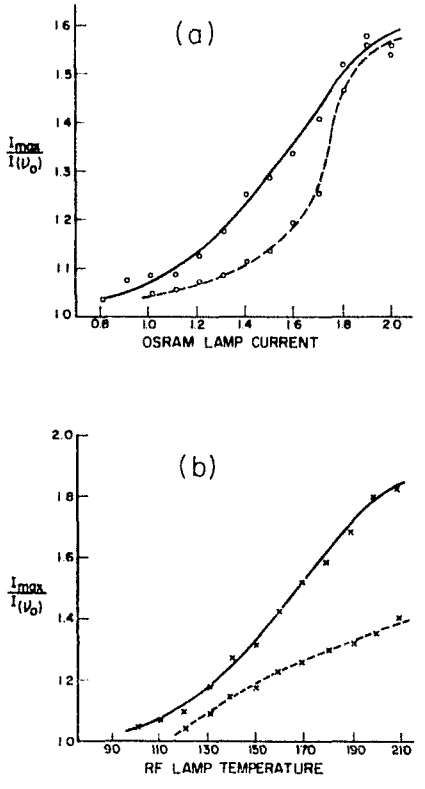

FIG. 4. The degrees of self-reversal in the potassium resonance lines: (a), emission from the Osram lamp; (b), emission from the rf lamp. ——, 7665-Å line; – – – –, 7669-Å line.

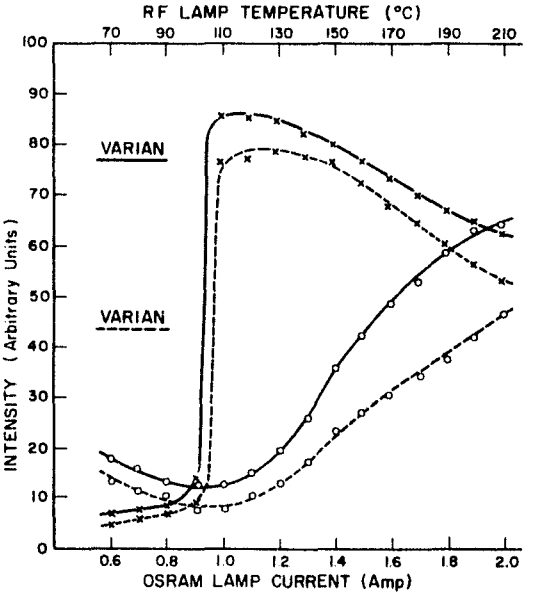

FIG. 5. Integrated relative intensities of the rubidium resonance lines emitted by the rf, Osram and Varian lamps. The levels for the Varian source are constant and may not be varied with operating conditions. ×, rf lamp; ○, Osram lamp; ——, 7800-Å line; – – – –, 7948-Å line.

It was also possible to determine the approximate ratios of the peak intensities of corresponding resonance lines produced by the two lamps under normal operating conditions. These ratios are the reciprocals of the ratios of the amounts of light allowed to enter the camera when photographing the interference fringes. This method yielded a value of 3.6 for the ratio of the peak intensity of a line emitted by the rf lamp to that emitted by the Osram lamp; the ratio of the integrated intensities is approximately 1.6. Assuming, for the sake of implicity, rectangular shapes, the above values lead tosa ratio of 0.44 for the linewidths (rf: Osram). With the rf lamp operated at 130°C and the Osram lamp at 1 A, the direct determination gave an average ratio of 0.48.

(b) Rubidium Lamps

The integrated intensities of the resonance lines emitted by the rf, Osram, and Varian lamps are plotted in Fig. 5 against their appropriate operating parameters which, in the case of the Varian lamp, are fixed. The intensity of the emission from the rf lamp is several times greater than from the Osram lamp. The combined intensity of the two resonance lines shows a maximum at a temperature of 130°, corresponding to a vapor pressure of 1.2×10^{-3} torr, which is of the same order of magnitude as with potassium. The pronounced peak at 110°C is attributed by Bell, Bloom, and Lynch[8] to a competition between argon and rubidium discharges near this critical temperature.

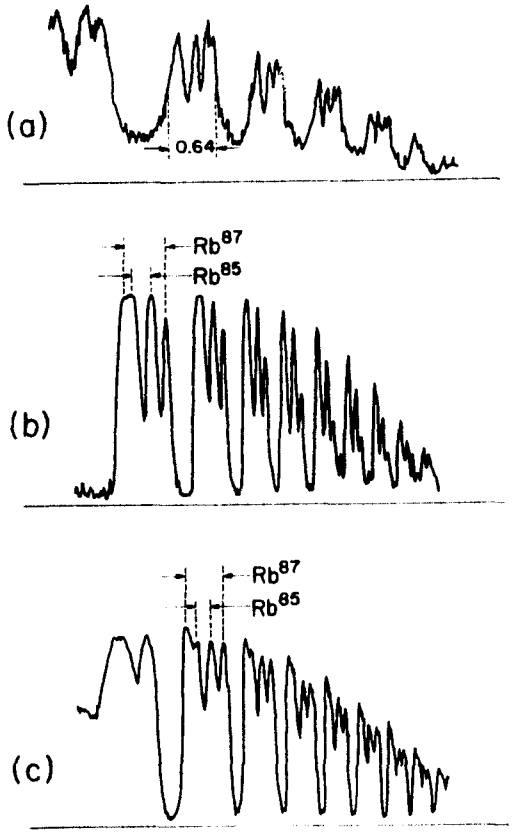

FIG. 6. The hyperfine structure of the 7948-Å rubidium resonance line showing the hfs splitting of the ground state which equals 0.1011 cm^{-1} in ^{85}Rb and 0.2278 cm^{-1} in ^{87}Rb. (a), Emission from the Osram lamp operated at 0.9 A, showing halfwidth in cm^{-1}; (b), emission from the Varian lamp; (c), emission from the rf lamp at 110°C.

Ordinary rubidium, which was used in all three lamps, consists of two isotopes: ^{85}Rb and ^{87}Rb in their natural abundance ratio of 3:1. Thus each resonance line includes a contribution from the two isotopes. The hfs splitting of the ground states equals 0.1011 cm^{-1} and 0.2278 cm^{-1}, respectively,[16] and causes each resonance line to consist of four hfs components: the outer two due to ^{87}Rb and the inner two due to ^{85}Rb. This structure was partially resolved using a spacing of 12.00 mm between the Fabry–Perot mirrors and is shown for the 7948-Å line in Fig. 6. The hfs splittings of the ^2P levels are smaller by at least one order of magnitude and cannot be seen in the exposures. The traces of the interference fringes indicate that a partial resolution of the hfs has been achieved with all three lamps. However, while in the case of the rf lamp it was possible to see it at the usual operating temperatures and highest intensities, the Osram lamp showed it only at very low currents, at which the intensities were extremely feeble.

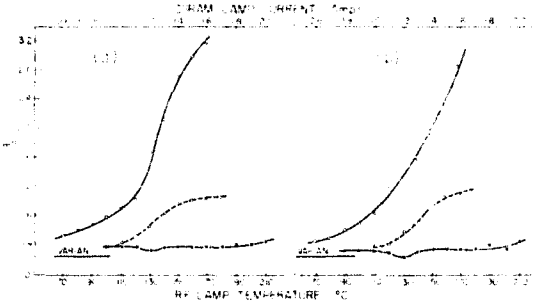

FIG. 7. The halfwidths $\Delta\nu$, and separations of the self-reversal peaks $\delta\nu$, of the rubidium resonance lines emitted by the rf, Osram, and Varian lamps. (a), The 7800-Å component; (b), the 7948-Å component. ×, rf lamp; ○, Osram lamp; ——, $\Delta\nu$; – – – –, $\delta\nu$.

The half-widths and, in the case of the Osram lamp, the separations of the self-reversal peaks were obtained from the Fabry–Perot patterns by means of the same procedures as were followed with the potassium doublet. The results are plotted in Fig. 7 against the appropriate operating parameters. It may be seen that the half-widths of the lines emitted by the rf lamp are much smaller than those due to the Osram lamp operating at currents above 1 A, where useful intensities are produced. The decrease of approximately 15% in the half-width of the lines produced by the rf discharge occurred consistently at 130°C and coincided with the condition for maximal integrated intensity. The Varian rubidium lamp produced somewhat narrower though less intense resonance lines than our rf discharge. This might well be due to the presence of krypton as carrier gas, which permits a stable discharge at the low operating temperature of 90°C. The ^{87}Rb hfs components, which are at the edges of the resonance lines, also appear less intense in relation to the central ^{85}Rb components than they do in our discharge, indicating a difference in the relative abundances of the rubidium isotopes in the two lamps. However, the hfs components were not well enough resolved to permit measurements of their intensities. The two rf lamps did not exhibit self-reversal in the resonance lines but each hfs component showed slight self-reversal when the lamp was operated at higher temperatures. In the Osram lamp, self-reversal appeared when the lamp current was increased to 1.0A

[16] S. A. Ochs and P. Kusch, Phys. Rev. 85, 145 (1952).

and the degree of self-reversal increased rapidly with current; at 1.4 A the central minima were only two thirds the intensity of the side maxima.

The ratios of the peak intensities of the corresponding resonance lines produced by the rf and Osram lamps were determined, as in the case of the potassium doublet, from the ratios of the apertures in the light beam used to photograph the fringes. It was found that the peak intensities of the lines emitted by the rf discharge were greater by a factor of eight than those produced by the Osram lamp operated at a current of 1.5 A, at which the lines were very broad. In this case, however, the peak intensity of lines emitted by the Osram lamp refers to the intensity of the self-reversal peaks; the intensity at the center of the resonance line is only about two thirds of that.

5. CONCLUSIONS

The new radio frequency lamps emit resonance lines whose integrated intensities, in the case of potassium, are about twice as great and, in the case of rubidium, about four times as great as those produced by the Osram lamps at their recommended operating currents. The intensities at the centers of the resonance lines are four times greater for potassium and eleven times greater for rubidium. The latter property is particularly important for purposes of exciting resonance fluorescence in alkali vapors at very low densities. At extremely low vapor pressures the absorption lines are very narrow and only a narrow frequency band at the center of the exciting lines is absorbed by the atoms and either re-radiated as resonance fluorescence or, after a transfer of excitation, re-radiated as sensitized fluorescence.[10] Thus, at very low vapor pressures or very low pressures of inert gases which may also be used to induce transfer of excitation,[17] the low halfwidths and high peak intensities of the exciting lines are very useful. At higher vapor pressures or inert gas pressures, the contours of the exciting lines may be matched quite closely with those of the absorption lines in the alkali vapor to produce optimal conditions at all times. Figure 8 shows the variation of the total fluorescent intensity in pure potassium vapor with potassium vapor pressure, with both the rf and the Osram lamps used for excitation.[10] At vapor pressures below 10^{-2} torr the Osram lamp is completely inefficient and produces no significant fluorescence whereas the rf discharge is most effective at low vapor pressures. The 7665-Å component is broadened more than the 7699-Å component in the rf discharge and, at low vapor pressures of the irradiated sample, the 7665-Å absorption line is narrower than the incident exciting line. As the vapor pressure increases and the contour of the absorption line becomes broadened and matched to that of the exciting line, a small maximum is produced in the intensity curve. The resonance lines in the absorbing vapor then become further broadened with increasing vapor pressures and the efficiency of the process decreases. The maxima at 10^{-2} torr and those at 10^{-1} torr, corresponding to excitation with the Osram lamp, are due to the phenomenon of volume fluorescence caused by the diffusion of the resonance radiation throughout the volume of the vapor. At still higher densities surface fluorescence assumes a dominant role and no exciting radiation penetrates beyond the surface layer.

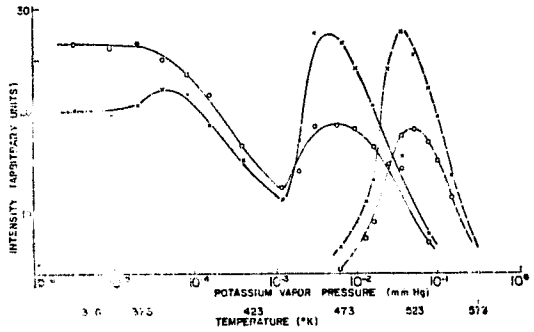

FIG. 8. Variation of the fluorescent intensity in potassium with vapor pressure, showing excitation with rf and Osram lamps. ×, 7665-Å incident; ○, 7699-Å incident; ——, rf lamp; – – – –, Osram lamp. Curves are normalized to show equal peak intensities.

Radiofrequency discharge lamps of this type are now being used in investigations of sensitized fluorescence in potassium,[17] cesium,[11] and rubidium[12] vapors at vapor pressures as low as 10^{-6} torr, which could not be reached previously for lack of suitable light sources. Only at these low densities can fluorescence phenomena be investigated in the virtual absence of radiation trapping effects.

ACKNOWLEDGMENT

The authors are indebted to Dr. D. S. Russell of the Division of Applied Chemistry, National Research Laboratories in Ottawa, for the chemical analysis of the brown deposit formed in the lamp.

[17] G. D. Chapman and L. Krause, Can. J. Phys. 43, 563 (1965).